IN THE UNITED STATES PATENT AND TRADEMARK OFFICE

In re application of: Chopp, et al.

Serial No.   10/075,715   Group Art Unit: 1614

Filed: 02/13/2002   Examiner: GEMBEH, Shirley V.

For: NITRIC OXIDE DONORS FOR INDUCING NEUROGENESIS

Attorney Docket No. 1059.00073

Assistant Commissioner for Patents
Washington, D.C. 20231

DECLARATION

I, Dr. Michael Chopp, being duly sworn, do hereby state that:

1.   I am a co-inventor of the above-captioned application.

2.   I am skilled in the art and have worked extensively in the field of neurogenesis.

3.   The Office Action holds that only PDE5 inhibitors are shown to work with the present invention. As is evidenced in the journal articles provided, other PDE inhibitors also work with the present invention because they elevate cGMP levels. For example, rat brain expresses PDE2, 5, and 9 genes (Van Staveren, et al. 2003). PDE2 regulates the basal cGMP concentration in thalamic neurons (Hepp, et al. 2007). A selective PDE2 inhibitor (Bay60-7550), a selective PDE5 inhibitor (sildenafil), and a selective PDE9 inhibitor (Sch51866) increase cGMP levels in cultured human retinal pigment epithelium (Diederen, et al. 2007) and regulate cGMP levels in rat spinal cord (de Vente, et al. 2006). Thus, all PDE inhibitors increase cGMP, not just PDE5, and the claims comply with the written description requirement.
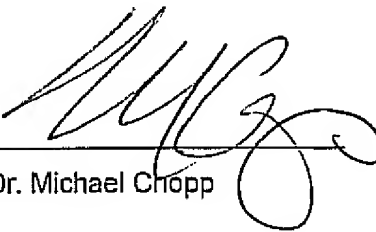
References

1.   Van Staveren WC, Steinbusch HW, Markerink-Van Ittersum M, Repaske DR, Goy MF, Kotera J, Omori K, Beavo JA, De Vente J. Mrna expression patterns of the cgmp-hydrolyzing phosphodiesterases types 2, 5, and 9 during development of the rat brain. J Comp Neurol. 2003;467:566-580.

2.   Hepp R, Tricoire L, Hu E, Gervasi N, Paupardin-Tritsch D, Lambolez B, Vincent P. Phosphodiesterase type 2 and the homeostasis of cyclic gmp in living thalamic neurons. J Neurochem. 2007;102:1875-1886.

3.   Diederen RM, La Heij EC, Markerink-van Ittersum M, Kijlstra A, Hendrikse F, de Vente J. Selective blockade of phosphodiesterase types 2, 5 and 9 results in cyclic 3'5' guanosine monophosphate accumulation in retinal pigment epithelium cells. Br J Ophthalmol. 2007;91:379-384.

4.   de Vente J, Markerink-van Ittersum M, Vles JS. The role of phosphodiesterase isoforms 2, 5, and 9 in the regulation of no-dependent and no-independent cgmp production in the rat cervical spinal cord. J Chem Neuroanat. 2006;31:275-303.

The undersigned declares further all statements made herein of his knowledge are true and that all statements made upon information and belief are believed to be true, and further that the statements were made with the knowledge that willful and false statements and the like so made are punishable by fine or imprisonment, or both, under Section 1001 of Title 18 of the United States Code and that such willful false statements may jeopardize the validity of the application or any patent issuing thereon.

Date: 6/18, 2008

Dr. Michael Chopp

mRNA Expression Patterns of the cGMP-Hydrolyzing Phosphodiesterases Types 2, 5, and 9 during Development of the Rat Brain

WILMA C.G. VAN STAVEREN,[1]* HARRY W.M. STEINBUSCH,[1]
MARJANNE MARKERINK-VAN ITTERSUM,[1] DAVID R. REPASKE,[2]
MICHAEL F. GOY,[3] JUN KOTERA,[4] KENJI OMORI,[4] JOSEPH A. BEAVO,[5]
AND JAN DE VENTE[1]

[1]Department of Psychiatry and Neuropsychology, Division Cellular Neuroscience,
Maastricht University, European Graduate School of Neuroscience (EURON),
6200 MD Maastricht, The Netherlands
[2]Division of Endocrinology, Children's Hospital Medical Center, Cincinnati, Ohio, USA
[3]Department of Cell and Molecular Physiology, University of North Carolina,
Chapel Hill, North Carolina, USA
[4]Discovery Research Laboratory, Tanabe Seiyaku Co. Ltd, Saitama, Japan
[5]Department of Pharmacology, University of Washington, Seattle, Washington, USA

ABSTRACT

Recent evidence indicates that cGMP plays an important role in neural development and neurotransmission. Since cGMP levels depend critically on the activities of phosphodiesterase (PDE) enzymes, mRNA expression patterns were examined for several key cGMP-hydrolyzing PDEs (type 2 [PDE2], 5 [PDE5], and 9 [PDE9]) in rat brain at defined developmental stages. Riboprobes were used for nonradioactive in situ hybridization on sections derived from embryonic animals at 15 days gestation (E15) and several postnatal stages (P0, P5, P10, P21) until adulthood (3 months). At all stages PDE9 mRNA was present throughout the whole central nervous system, with highest levels observed in cerebellar Purkinje cells, whereas PDE2 and PDE5 mRNA expression was more restricted. Like PDE9, PDE5 mRNA was abundant in cerebellar Purkinje cells, although it was observed only on and after postnatal day 10 in these cells. In other brain regions, PDE5 mRNA expression was minimal, detected in olfactory bulb, cortical layers, and in hippocampus. PDE2 mRNA was distributed more widely, with highest levels in medial habenula, and abundant expression in olfactory bulb, olfactory tubercle, cortex, amygdala, striatum, and hippocampus. Double immunostaining of PDE2, PDE5, or PDE9 mRNAs with the neuronal marker NeuN and the glial cell marker glial fibrillary acidic protein revealed that these mRNAs were predominantly expressed in neuronal cell bodies. Our data indicate that three cGMP-hydrolyzing PDE families have distinct expression patterns, although specific cell types coexpress mRNAs for all three enzymes. Thus, it appears that differential expression of PDE isoforms may provide a mechanism to match cGMP hydrolysis to the functional demands of individual brain regions. J. Comp. Neurol. 467:566–580, 2003. © 2003 Wiley-Liss, Inc.

Indexing terms: in situ hybridization; cyclic nucleotides; PDEs

The second messengers adenosine 3',5'-cyclic monophosphate (cAMP) and guanosine 3',5'-cyclic monophosphate (cGMP) help to regulate a number of important biological processes, including phototransduction, olfaction (Broillet and Firestein, 1999), smooth muscle contraction and relaxation (Carvajal et al., 2000), neurotransmission (Garthwaite, 1991; Kind and Neumann, 2001), and neural development (Truman et al., 1996; Gibbs and Truman, 1998; Schachtner et al., 1999; Van Wagenen and Rehder, 1999; Gibbs et al., 2001; Simpson et al., 2002).

Intracellular levels of cAMP and cGMP are controlled by their rate of synthesis via adenylyl and guanylyl cyclases, respectively (Lucas et al., 2000; Wedel and Garbers, 2001; Watts, 2002), and by their rate of degradation via 3',5'-cyclic nucleotide phosphodiesterases (PDEs) (Beavo, 1995; Houslay, 1998; Conti and Jin, 1999; Dousa, 1999; Francis et al., 2001). PDEs are comprised of a large group of enzymes that hydrolyze cAMP and cGMP to their inactive 5'-derivates. To date, numerous PDE genes have been cloned, representing 11 different PDE families (PDE1-PDE11). Many of these genes are expressed in several alternately spliced forms, indicating the existence of a large number of PDE isoforms, which are expressed with distinct localization patterns in the brain (Repaske et al., 1993; Furuyama et al., 1994; Yan et al., 1994; Beavo, 1995; Kotera et al., 1997; Fujishige et al., 1999; Fawcett et al., 2000; Soderling and Beavo, 2000; Andreeva et al., 2001; Francis et al., 2001). Three PDE families specifically use cGMP as a substrate: PDE5 (Thomas et al., 1990; Kotera et al., 1997; Loughney et al., 1998), PDE9 (Fisher et al., 1998; Guipponi et al., 1998; Soderling et al., 1998), and the photoreceptor-specific PDE6 (Gillespie and Beavo, 1988). Furthermore, cGMP can be degraded by dual-substrate PDEs: PDE1 (Furuyama et al., 1994; Yan et al., 1994), PDE2 (Sonnenburg et al., 1991; Repaske et al., 1993; Yang et al., 1994; Rosman et al., 1997; Juilfs et al., 1999), PDE10 (Fujishige et al., 1999; Kotera et al., 1999b; Soderling et al., 1999), and PDE11 (Fawcett et al., 2000; Hetman et al., 2000).

At present, the functions of cGMP in the central nervous system (CNS) are slowly emerging. A role for cGMP during development of the CNS has been proposed (Truman et al., 1996; Markerink-Van Ittersum et al., 1997; Bicker, 1998, 2001; Gibbs and Truman, 1998; Schachtner et al., 1999; Van Wagenen and Rehder, 1999; Gibbs et al., 2001; Simpson et al., 2002). cGMP is involved in network formation during neuronal maturation (Scholz and Truman, 2000; Bicker, 2001; Scholz et al., 2001) and can regulate directional guidance of growth cones (Song et al., 1998; Song and Poo, 1999). Furthermore, it has been demonstrated that cGMP is involved in the directional outgrowth of cortical neurons during maturation (Polleux et al., 2000).

Evidence from several in vivo models has been presented which suggest that cGMP is implicated in processes of learning and memory in the adult. Inhibition of cGMP synthesis impaired performance in a number of learning and memory behavioral tasks (Kendrick et al., 1997; Bernabeu et al., 1997; Izquierdo et al., 2000; Edwards et al., 2002). In contrast, administration of the cGMP analog 8-Br-cGMP (Bernabeu et al., 1996) or application of the PDE5 inhibitor sildenafil (Baratti and Boccia, 1999) enhanced retention in an inhibitory avoidance learning paradigm. Recently, several selective PDE5 inhibitors (Prickaerts et al., 1997, 2002b), or a cGMP analog (Prickaerts et al., 2002a) have been shown to enhance retention in a rat object recognition task. In addition, it has been recently reported that application of a selective PDE2 inhibitor can also enhance retention in this task (Boess et al., 2003). This suggests a role for both PDE2 and PDE5 in object memory formation. An association of PDE2 with the limbic system has been described (Repaske et al., 1993), however, according to the literature, localization of PDE5 was restricted mainly to the cerebellum (Kotera et al., 1997, 2000; Juilfs et al., 1999; Giordano et al., 2001).

The above findings suggest the involvement of cGMP in synaptic plasticity both during neural development and in learning and memory processes. Therefore, the mRNA expression patterns of PDE5 during brain development were compared to the cellular localization of PDE2 at similar stages. Finally, as PDE9 has a broad distribution

Abbreviations

Ca	cortical area	IGr	internal granular layer
cAMP	adenosine 3'5'-cyclic monophosphate	In	intestine
Cb	cerebellum	LHb	lateral habenula
cc	corpus callosum	LV	lateral ventricle
cGMP	guanosine 3'5'-cyclic monophosphate	M	molecular layer
Chp	choroid plexus	Met	metencephalon
CNS	central nervous system	MHb	medial habenula
CPu	caudate putamen	Mi	mitral cell layer
Cx	cortex	NO	nitric oxide
DG	dentate gyrus	Ob	olfactory bulb
DIG	digoxigenin	OT	olfactory tubercle
E	external granule cell layer	PBS	phosphate-buffered saline
EDTA	ethylenediaminetetra-acetate	PC	Purkinje cell layer
EHNA	erythro-9-(2-hydroxy-3-nonyl)adenine	PCR	polymerase chain reaction
EPl	external plexiform layer	PDE	3'5'-cyclic nucleotide phosphodiesterase
G	granule cell layer	RT	room temperature
GFAP	glial fibrillary acidic protein	SNC	substantia nigra pars compacta
GL	glomerular layer	SNR	substantia nigra pars reticulata
H	hippocampus	TBS	Tris-buffered saline
Hip	hippocampal area	Th	thalamus
I	internal granule cell layer	Tha	thalamic area
IBMX	3-isobutyl-1-methylxanthine	VTA	ventral tegmental area

throughout the brain (Andreeva et al., 2001), this enzyme was also included in our study. Since PDE9 has the highest affinity for cGMP of all the PDE families known to date, this enzyme could play a fundamental role in keeping cGMP at low basal levels (Fisher et al., 1998; Soderling et al., 1998), thus having an important role in directing outgrowth and directional guidance of neurons.

Here we show that distinct expression patterns for PDE2, PDE5, and PDE9 mRNA are already established at early stages of brain development and maintained into adulthood, suggesting a role for these PDE families in neural development and neurotransmission. Moreover, it is shown for the first time that besides the PDE5 mRNA expression in Purkinje cells, as reported earlier (Kotera et al., 1997), PDE5 is also present in other brain areas, such as the hippocampus, cortex, and olfactory bulb. In addition, expression of the three cGMP-hydrolyzing PDEs is observed mainly in neuronal cell bodies.

MATERIALS AND METHODS
Animals

Lewis rats were obtained from the local animal facility at Maastricht University. Experiments were approved by the committee on animal welfare according to Dutch governmental rules. In order to study mRNA expression of the different cGMP-hydrolyzing PDEs during development, animals were used at the age of embryonic day 15 (E15), postnatal day 0 (P0, day of birth), day 5 (P5), day 10 (P10), day 21 (P21), and adult rats (3 months).

Riboprobe synthesis

For the in situ hybridization of PDE2, a pBS+ vector containing a part of rat PDE2 (nt 1964–2314, GenBank accession no. NM_031079) was used. This construct (GenBank accession no. M94540) and the specificity of the probe has been previously described (Repaske et al., 1993). The construct was linearized using EcoRI or HindIII, to generate antisense or sense probes with T3 or T7 polymerase, respectively.

The expression of PDE5 was studied by cloning a part of the rat PDE5 sequence (nt 2206–2580, GenBank accession no. D89093) into the SacI and EcoRI sites of a pCRII-TOPO vector (Invitrogen, La Jolla, CA). A probe comprising this part of PDE5 has been described previously (Kotera et al., 1997). Sense probes were made after BstXI digestion by Sp6 RNA polymerase and antisense probes after linearization with HindIII and T7 RNA polymerase.

PDE9 riboprobes were constructed from the mouse PDE9A1 as a template. Primer wvsforw1 (5'-ACG CTT GGA TCC ATG GGG GCC GGC TCC TCA-3') containing a BamHI site and primer wvsrev1 (5'-GCT TGT ATG CGG CCG CCT GGA GGC CAC AGA GCC AGA CCA T-3') containing a NotI site were used for PCR (nucleotides 10–828 from mouse PDE9A1, AF031147). The PCR product was digested with both restriction enzymes and then the product was ligated into the BamHI and NotI site of a pCRII TOPO vector (Invitrogen). Antisense PDE9 probes were made with T7 polymerase from the pCRIITOPO plasmid linearized with BamHI, while sense probes were produced by Sp6 RNA polymerase after linearization of pCRIITOPO vector with XhoI.

All constructs were analyzed by DNA sequencing before probe synthesis. After restriction digestion of each con-

struct, as described above, antisense and sense riboprobes were made from a 5 μg DNA template by in vitro transcription with digoxigenin (DIG)-labeled UTP using a DIG RNA labeling kit (Roche, Nutley, NJ) according to the manufacturer's instructions.

In situ hybridization

Animals were decapitated and their brains were dissected, frozen in CO_2, and stored at −80°C until sectioning. Animals aged E15 were frozen as a whole. Frozen serial sagittal sections (14 μm) were cut and thawed onto SuperFrost Plus slides (Menzel-Glaser, Germany) and stored at −80°C until use. From each age group, three animals were studied and from each animal consecutive sections were used for hybridization of PDE2, PDE5, and PDE9 with sense and antisense probes. In addition, coronal sections from adult rats were cut at different levels related to bregma: 1.60/1.20, −0.40/−0.80, −3.14/−3.30, −4.52/−4.80, and −7.30/−7.64, according to Paxinos and Watson (1986). Sections were thawed for 10 minutes at 50°C and thereafter postfixed with 4% paraformaldehyde in 0.1 M phosphate-buffered saline (PBS, pH 7.4) for 20 minutes at room temperature (RT), followed by three short washes with PBS. Then sections were incubated for 10 minutes at RT with 0.1 M triethanolamine containing 0.25% (v/v) acetic anhydride. Slides were washed two times with 2× SSC for 5 minutes and thereafter washed at 37°C with 2× SSC containing 50% (v/v) formamide before the start of the hybridization.

Hybridization was performed overnight in a humid chamber at 55°C under coverslips in 100–200 μl hybridization mix (50% (v/v) deionized formamide, 250 μg/ml salmon sperm DNA, 1 mg/ml tRNA, 10% dextran sulfate, 2× SSC, 1× Denhardt's solution and 200–400 ng/ml DIG-labeled RNA probe). After the hybridization, sections were washed in 2× SSC, 1× SSC and 0.1× SSC, all solutions containing 50% formamide. Each wash step was performed at 55°C and lasted 20 minutes. Next, to eliminate single-stranded (unhybridized) probe, the sections were treated with RNAse T1 (2 U/ml, Roche) in 2× SSC containing 1 mM ethylenediaminetetra-acetate (EDTA) for 15 minutes at 37°C followed by a 20-minute wash with 1× SSC at 55°C. After washing for 10 minutes with 2× SSC at RT, sections were incubated for 5 minutes with buffer 1 (150 mM NaCl and 100 mM maleic acid (pH 7.5)) followed by blocking for 2–3 hours at RT with buffer 2 (150 mM NaCl, 100 mM maleic acid (pH 7.5), and 1% blocking reagent (Roche, #1096176)) containing 5% sheep serum. Next, slides were incubated overnight at 4°C with a 1:2,000 dilution of anti-DIG-alkaline phosphatase in buffer 2 containing 1% sheep serum. Thereafter, slides were washed three times with buffer 1 followed by washing for 10 minutes with Tris-buffered saline (TBS, pH 7.6) containing 0.025% Tween 20 and, thereafter, three times 5 minutes with TBS. After two washes of 5 minutes in buffer 3 (100 mM Tris-HCl (pH 9.5), 0.1 M NaCl, and 0.05 M $MgCl_2$), the sections were incubated with freshly prepared nitro-blue tetrazolium and 5-bromo-4-chloro-3-indolyl-phosphate in buffer 4 (50 mM Tris (pH 9.5), 100 mM NaCl, 50 mM $MgCl_2$, 1 mM levamisole) and stained for 1–2 days in the dark at RT. The buffer was replaced by fresh buffer after the first day. The color reaction was stopped with 10 mM Tris-HCl and 1 mM EDTA (pH 8.0). After washing in TBS, sections were mounted with TBS-glycerol. For the developmental studies, the samples from

the different stages were prepared identically, using the same batch of probe and identical washing and staining procedures.

Double immunostaining

After the development of the in situ hybridization, some sections derived from adult rats were counterstained with two cellular markers. Neurons were visualized with mouse anti-neuronal nuclei (NeuN) (Chemicon International, Temecula, CA) diluted 1:50 with TBS containing 0.3% Triton (TBS-T). Astrocytes were stained by using a polyclonal antibody directed against glial fibrillary acidic protein (GFAP) diluted 1:25, kindly donated by Dr. F. Ramaekers (Maastricht, The Netherlands). Sections were incubated overnight with the primary antibodies at 4°C and thereafter washed with TBS-T, TBS, and TBS-T; each step lasted 10 minutes. For visualization of the primary antibodies, sections were incubated with 1:800 Cy3-conjugated affinity pure donkey antimouse IgG (Jackson, West Grove, PA) or 1:100 Alexa fluor 488 goat antirabbit IgG conjugate (Molecular Probes, Leiden, The Netherlands) for 90 minutes at RT. After being washed in TBS-T and TBS, sections were mounted with TBS-glycerol.

Microscopical evaluation

Sections were examined using an Olympus AX70 microscope equipped with a cooled CCD Olympus Digital video camera F-view. Images were stored digitally using the computer program Analysis (Soft Imaging System, Münster, Germany), then arranged and adjusted to match for contrast with Adobe PhotoShop 5.5 (San Jose, CA). For each PDE family the mRNA expression was scored separately, varying from absent (–) to strong expression (+++), by comparing the relative intensity of the staining in the different brain areas according to Paxinos and Watson (1986) and Paxinos et al. (1994).

RESULTS

Nonradioactive in situ hybridization was used to study the mRNA expression patterns of PDE2, PDE5, and PDE9 during the development of the rat brain from E15 to adulthood. Serial sagittal sections were hybridized with antisense and sense probes from the three different PDE families. In Figure 1 the expression of the three cGMP-hydrolyzing PDE families is shown for three developmental stages. Control sections hybridized with sense probes (Fig. 1J–L) or processed without probe (not shown), did not show specific staining. In addition, sections pretreated with RNase (not shown) were devoid of staining, indicating that the probes bound specifically to RNA.

Comparison of the six developmental stages and the different PDE families, demonstrated that PDE9 mRNA had the widest distribution, followed by PDE2 and PDE5 mRNAs (Fig. 1, Tables 1–4). A more detailed description of the expression of these PDE families in the different brain areas is given below.

Olfactory bulb

In the olfactory bulb, PDE2, PDE5, and PDE9 mRNAs were detected at all stages investigated (Fig. 1, Tables 1–4). At age E15, PDE9 had the widest distribution and densest expression throughout the olfactory area compared to PDE2 and PDE5 (Fig. 1A–C) and was present in a population of closely packed cells in which only a small rim of cytoplasm stained strongly (Fig. 2F). After birth into adulthood, PDE2, PDE5, and PDE9 mRNAs were present throughout the layers in the olfactory bulb, with the strongest expression in the mitral cell layer (Table 1, Fig. 2A–C). All three PDE families were also expressed in scattered cells throughout the external plexiform layer. In addition, PDE2 and PDE9 were expressed in the internal granular layer, which did not contain PDE5 mRNA. Furthermore, PDE9 mRNA expression was observed in the glomerular layer, which also contained PDE5 mRNA but did not show PDE2 mRNA expression. Overall, these expression patterns were maintained during maturation and into adulthood (Fig. 2A–C, Tables 1–4).

Cortex

At E15, neither PDE2 (Fig. 3A, upper panel) nor PDE5 (Fig. 3A, middle panel) mRNA was detected in the cortical area, in contrast to PDE9 mRNA, which was present in many densely packed cells (Fig. 3A, lower panel). After birth, PDE2, PDE5, and PDE9 expressing cells were present in the cortex in increasingly more sharply defined patterns (Fig. 3), paralleling the progressive organization of the different cortical layers during maturation. PDE5 mRNA was detected in scattered cell bodies at stage P5 and retained during maturation (Fig. 3, middle panel). At stages P0 and P5 the strongest PDE5 mRNA staining was observed in what appears to be neuroepithelium. In the adult, high expression of PDE2 and PDE9 mRNAs was detected in all cortical layers (Fig. 4, Table 1). In contrast, PDE5 mRNA was observed in cell bodies that were stained with varying intensity throughout the different cortical layers (Fig. 4B, Table 1). Moreover, at early postnatal stages PDE9 mRNA expression could be detected in the corpus callosum, which was absent in adult animals. No PDE2 or PDE5 mRNAs were observed in the corpus callosum at all ages investigated (Tables 1–4).

Basal forebrain and striatum

During development of the brain, PDE2 and PDE9 mRNAs were expressed strongly in the caudate putamen (Fig. 1), whereas PDE5 mRNA expression in this area was not detected or expressed at low levels in scattered cells at the stages investigated (Tables 1–4). mRNA expression of all three PDE families was present in cell bodies and not in white matter tracts (Fig. 2G–I). Furthermore, during development, PDE2 and PDE9 mRNA were detected in the olfactory tubercle (Fig. 1), the islands of Calleja, the nucleus accumbens, and the amygdala (Table 1). In these regions PDE5 expression was low to hardly detectable at all developmental stages (Fig. 1, Table 1).

Hippocampus

In the hippocampal area both PDE2 and PDE9 mRNAs were expressed at stage E15, whereas no PDE5 expression was observed at this time point (Fig. 5). After birth, PDE2, PDE5, and PDE9 mRNAs were present in pyramidal cells of the CA1–CA3 and in the granule cells of the dentate gyrus, and some scattered cell bodies outside these layers (Figs. 5, 2J–L, Tables 1–4). At all stages PDE2 expression was stronger in pyramidal cells compared to the granule cells in the dentate gyrus (Fig. 5, upper panel), whereas PDE9 mRNA was strongly expressed in both cell types (Fig. 5, lower panel). In contrast, PDE5 mRNA expression in the hippocampus was weakly detected and from P5 onwards (Fig. 5, middle panel) pyramidal cells and gran-

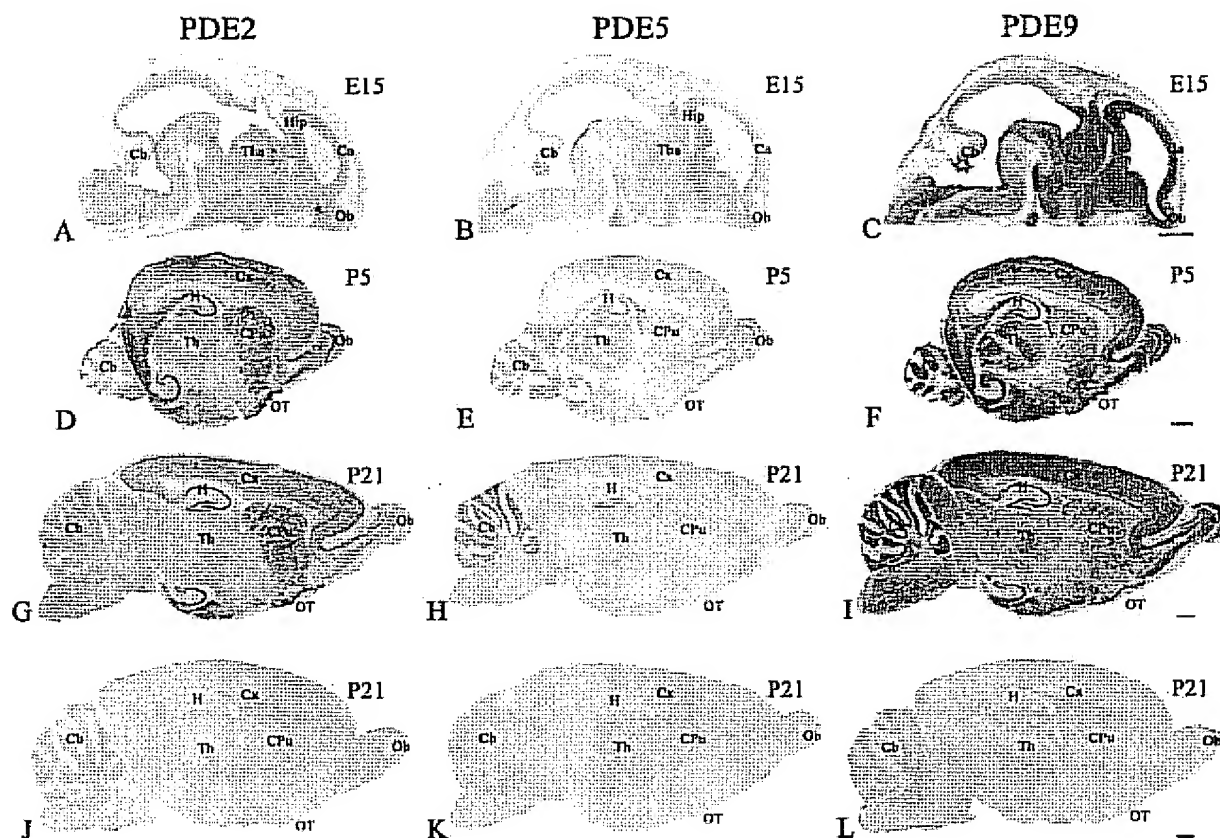PDE2   PDE5   PDE9

Fig. 1. Localization of PDE2, PDE5, and PDE9 mRNA during development of the rat brain at ages E15, P5, and P21 by nonradioactive in situ hybridization. For each time point, consecutive sagittal sections were hybridized with PDE2 (A,D,G), PDE5 (B,E,H) and PDE9 (C,F,I) antisense probes or sense probes derived from PDE2 (J), PDE5 (K) and PDE9 (L). Sagittal sections were photographed using a 2× objective and pictures were assembled with Adobe PhotoShop.

Recording conditions were kept constant for each PDE riboprobe. Ca, cortical area; Cb, cerebellum; CPu, caudate putamen; Cx, cortex; H, hippocampus; Hip, hippocampal area; Ob, olfactory bulb; OT, olfactory tubercle; Th, thalamus; Tha, thalamic area. Scale bar = 1,000 μm in C (applies to A–C), F (applies to D–F), I (applies to G–I), L (applies to J–L).

ule cells were moderately stained with some dispersed cells inside these layers, which were stained more robustly (Fig. 2K).

Thalamus and hypothalamus

At E15, PDE2 and PDE9 mRNA expression was detected in the thalamic area, whereas no PDE5 was present (Fig. 1). In addition, at this stage PDE9 mRNA expression was also observed in the hypothalamic area, which did not show PDE2 or PDE5 mRNA expression. From P0 into adulthood, PDE2 and PDE5 mRNA expression levels were low to hardly detectable in the thalamus and hypothalamus (Fig. 1). However, in coronal sections from adult rats very strong PDE2 expression was observed in the medial habenula, whereas PDE9 showed a moderate level of expression and PDE5 mRNA was undetectable (Fig. 2D–E, Table 4). Furthermore, PDE2 mRNA was detected in hypothalamic subnuclei (Table 4), such as in the histaminergic cell group in the tubero mammillary area (Fig. 2O). In addition, moderate PDE2 and PDE5 mRNA expression was observed in the supraoptic nucleus (Table 4).

PDE9 mRNA was moderate to strongly present in thalamus and hypothalamus throughout development of the

TABLE 1. Comparison of PDE2 mRNA Expression Patterns During Development of the Rat Brain From Embryonic Stage E15 Until Postnatal day 21 (P21)

Brain area	E15	P0	P5	P10	P21
Olfactory bulb	+				
Glomerular layer		−	−	−	−
Mitral cell layer		++	+++	+++	++
Granule cell layer		+	+	+	+
Cortical neuroepithelium					
Preplate zone	−				
Ventricular zone	−				
Marginal zone		+			
Cortical plate		++			
Subcortical plate		+			
Neocortex					
Layer I			−	−	−
Layer II–III			++	+++	+++
Layer IV			++	+++	+++
Layer V–VI		++	++	+++	+++
Corpus callosum		−	−	−	−
Caudate putamen	+	++	+++	+++	+++
Hippocampal formation	+				
Pyramidal cells		+++	+++	+++	+++
Granule cell layer		+	++	++	++
Cerebellum	−				
Molecular layer		−	−	−	+
Purkinje cell layer		−	−	+	+
External granule cell layer			−	−	
Internal granule cell layer			−	−	+

−, absent; +, weak; ++, moderate; +++, strong.

TABLE 2. Comparison of PDE5 mRNA Expression Patterns During Development of the Rat Brain From Embryonic Stage E15 Until Postnatal day 21 (P21)

Brain area	E15	P0	P5	P10	P21
Olfactory bulb	+				
Glomerular layer		−	+	+	+
Mitral cell layer		+	+	+	+
Granule cell layer		−	−	−	−
Cortical neuroepithelium					
Preplate zone	−				
Ventricular zone	−				
Marginal zone		−			
Cortical plate	−				
Subcortical plate	−				
Neocortex					
Layer I			−	−	−
Layer II–III			+	+	+
Layer IV			+	+	+
Layer V–VI		−	+	+	+
Corpus callosum		−	−	−	−
Caudate putamen	−	−	+	+	+
Hippocampal formation	−				
Pyramidal cells		−	+	++	++
Granule cell layer		−	+	++	++
Cerebellum	−				
Molecular layer		−	−	−	+
Purkinje cell layer		−	+++	+++	
External granule cell layer		+	+		
Internal granule cell layer		+	+	++	

−, absent; +, weak; ++, moderate; +++, strong.

TABLE 3. Comparison of PDE9 mRNA Expression Patterns During Development of the Rat Brain From Embryonic Stage E15 Until Postnatal day 21 (P21)

Brain area	E15	P0	P5	P10	P21
Olfactory bulb	++				
Glomerular layer		+	+	+	+
Mitral cell layer		++	++	++	++
Granule cell layer		+	+	+	+
Cortical neuroepithelium					
Preplate zone	+				
Ventricular zone	+				
Marginal zone		++			
Cortical plate		++			
Subcortical plate		++			
Neocortex					
Layer I			−	−	−
Layer II–III			+++	+++	+++
Layer IV			+++	+++	+++
Layer V–VI		++	+++	+++	+++
Corpus callosum		+	+	+	−
Caudate putamen		++	++	++	++
Hippocampal formation	++				
Pyramidal cells		++	++	+++	+++
Granule cell layer		++	++	+++	+++
Cerebellum	+				
Molecular layer		+	−	−	+
Purkinje cell layer		+++	+++	+++	+++
External granule cell layer			++	++	
Internal granule cell layer			++	++	++

−, absent; +, weak; ++, moderate; +++, strong.

brain (Fig. 1, Table 4). In the thalamus from the adult, PDE9 mRNA expression was detected in the medial habenula and the lateral habenula (Fig. 2E) with the strongest expression in the reticular thalamic nucleus (Table 4). The expression of PDE9 mRNA in the hypothalamus was strongest in the supraoptic nucleus (Table 4).

Midbrain

PDE2 and PDE5 mRNAs were hardly detectable in the superior or inferior colliculus at all stages investigated. PDE2 mRNA was observed in the substantia nigra pars compacta (Fig. 2M) and raphe nuclei (Table 4). PDE5 mRNA was not detected in the midbrain, with the exception of weak expression in the pontine nuclei (Table 4).

The expression of PDE9 mRNA was observed in several midbrain areas, including superior and inferior colliculus and substantia nigra (Fig. 2N).

Cerebellum

At E15, neither PDE2 (Fig. 6A, upper panel) nor PDE5 (Fig. 6A, middle panel) mRNA was detected in the cerebellum, in contrast to PDE9 mRNA, which was weakly expressed and exhibited a rather diffuse appearance (Fig. 6A, lower panel). Low PDE2 expression was found in Purkinje cells, first observed at P10 (Fig. 6D, upper panel) and maintained into adulthood (Fig. 6, upper panel, Fig. 2P, Table 1). PDE5 and PDE9 mRNAs were also detected in Purkinje cells; however, at relatively higher levels of expression than PDE2 mRNA (Figs. 6, 2P–R). The expression of PDE5 in Purkinje cells was first seen at P10 and maintained into adulthood (Fig. 6, middle panel), whereas PDE9 mRNA was detected from P0 onwards (Fig. 6, lower panel, Tables 1–4).

Furthermore, PDE2 and PDE9 mRNAs, and to some extent PDE5 mRNA, were observed in isolated cells in the molecular layer (Figs. 6, 2P–R). In addition, PDE2, PDE5, and PDE9 mRNAs were present in the granule cell layer. PDE2 mRNA was present in cells that have the characteristics of Golgi cells (Fig. 2P), which apparently also express PDE9 mRNA (Fig. 2R) but not PDE5 mRNA (Fig. 2Q). PDE5 and PDE9 mRNAs were also detected in the internal and external granule cell layer at P5 and P10 (Fig. 6).

Brain stem

In the brain stem, no PDE2 mRNA expression was detected in sagittal sections at any stage. PDE5 mRNA was present in the metencephalon at E15 (Fig. 6A, middle panel) and was detected in some nuclei of the reticular formation during maturation (not shown). PDE9 mRNA expression was also observed in subnuclei of the reticular formation (not shown).

Double immunostaining

To investigate in which cell types the cGMP-hydrolyzing PDEs were expressed, brain sections from adult rats were double-labeled with the neuronal marker NeuN or the glial cell marker GFAP (Fig. 7). Throughout the brain, PDE2, PDE5, and PDE9 mRNAs colocalized predominantly with NeuN, as demonstrated for the cortex in Figure 7.

DISCUSSION

In this study, we have shown that the mRNAs encoding three cGMP-hydrolyzing PDEs have distinct localization patterns, both in the mature rat brain and at embryonic and postnatal stages when significant developmental and maturational events are in progress. Earlier studies have indicated changes in PDE1 and PDE3 mRNA and protein expression or PDE activity during development of the brain (Billingsley et al., 1990; Reinhardt and Bondy, 1996). An increase in PDE activity was reported during development of the brain from fetus to adulthood (Smoake et al., 1974; Davis and Kuo, 1976). Furthermore, lower basal cGMP levels in aged brain areas compared to adult have been reported as a consequence of a more active degradation of cGMP by PDEs (Chalimoniuk and Strosznajder, 1998).

TABLE 4. PDE2, PDE5, and PDE9 mRNA expression in the Adult Rat Brain by Nonradioactive In Situ Hybridization

Brain area	PDE2	PDE5	PDE9	Brain area	PDE2	PDE5	PDE9
Forebrain				Hypothalamus			
Olfactory bulb				Supra optic nucleus	++	++	+++
Glomerular layer	−	+*	+	Medial preoptic area	+	−	+−
External plexiform layer	÷	−	++	Lateral preoptic area	−	+	+−
Mitral cell layer	++	++	++	Median eminence	+	−	+−
Internal plexiform layer	−	−	−	Arcuate hypothalamic nucleus	+	−	++
Internal granular layer	+	−	+	Ventromedial hypothalamic nucleus	+	−	++
Anterior olfactory nucleus	+++	+	+++	Dorsomedial hypothalamic nucleus	−	−	++
				Medial mammillary nucleus	−	−	++
Caudate putamen	+++	+*	+++	Lateral mammillary nucleus	++	−	++
Accumbens nucleus	+++	−	+++				
Septal nuclei	++	+	+++	Midbrain			
Nuclei of the diagonal band	+	−	+++	Superior colliculus	−	−	+
Olfactory tubercle	+++	−	+++	Inferior colliculus	−	−	+
Islands of Calleja	++	−	++	Substantia nigra, pars compacta	++	−	++
Bed nucleus of stria terminalis	+	+	++	Substantia nigra, pars reticulata	−	−	++
Ventral pallidum	+	−	+	Ventral tegmental area	−	−	++
Globus pallidus	−	−	+	Retrorubral field and nucleus	−	−	+
Amygdala	+++	−	+++	Raphe nuclei	++	−	+
Indusium griseum	+++	+	++	Central grey	−	−	+
Fornix	−	−	−	Pontine nuclei	−	+	++
Cortex				Cerebellum			
Layer I	−	−	−	Molecular layer	+*	+*	+*
Layer II	+++	+*	+++	Purkinje cell layer	+	++++	++++
Layer III	+++	+*	+++	Granule cell layer	+*	++	+−
Layer IV	+++	+*	+++	Cerebellar nuclei	−	+	+−
Layer V	+++	+*	+++				
Layer VI	+++	+*	+++	Brainstem			
				Reticular formation	−	+	+++
Piriform cortex	+++	++	+++				
Cingulate cortex	+++	+	+++	Circumventricular organs			
Entorhinal cortex	+++	+	+++	Choroid plexus	−	+	++
				Ependymal cells	−	−	+
Hippocampus				Subcommissural organ	++	−	+
Pyramidal cells in CA1	+++	++*	+++				
Pyramidal cells in CA2	+++	++*	+++				
Pyramidal cells in CA3	+++	++*	+++				
Non-pyramidal cells	+++	++*	+++				
Dentate gyrus	++	++*	+++				
Subiculum	++	+*	+++				
Thalamus							
Medial habenula	++++	−	++				
Lateral habenula	−	−	+				
Paraventricular thalamic nucleus	−	−	++				
Intermediodorsal thalamic nucleus	−	−	++				
Central medial thalamic nucleus	−	−	++				
Parafascicular thalamic nucleus	−	−	++				
Lateral posterior thalamic nucleus	−	−	++				
Mediodorsal thalamic nucleus	−	−	++				
Laterodorsal thalamic nucleus	−	−	++				
Ventral posteromedial thalamic nucleus	−	−	++				
Ventral posterolateral thalamic nucleus	−	−	++				
Ventromedial thalamic nucleus	−	−	++				
Reticular thalamic nucleus	+	−	+++				
Posterior thalamic nuclear group	−	−	++				
Anterior pretectal nucleus	−	−	++				
Medial geniculate nucleus	−	−	++				
Dorsolateral geniculate nucleus	−	−	++				
Ventrolateral geniculate nucleus	−	−	++				
Zona incerta	−	−	++				

−, absent; +, weak; ++, moderate; +++, strong; ++++, strongest signal detected; *, strong staining in scattered cells.

Previous studies have shown that nitric oxide (NO) synthase and the NO-mediated cGMP-producing enzyme soluble guanylyl cyclase are expressed with distinct localization patterns during brain development and are widely distributed throughout the adult CNS (Bredt and Snyder, 1994; Burgunder and Cheung, 1994; Giuili et al., 1994). Furthermore, targets of cGMP like cGMP-dependent protein kinases (El-Husseini et al., 1999; De Vente et al., 2001) and cyclic nucleotide-gated channels (Wei et al., 1998; Kingston et al., 1999) are also widely expressed in the adult rat brain. The broad distribution of cGMP-hydrolyzing PDEs throughout the CNS, as reported here, is in accordance with the wide distribution of other elements that are involved in the cGMP-signaling pathway, supporting the hypothesis that cGMP-signal transduction has widespread physiological roles, both in the mature and the developing brain. Recently, our group presented evidence that application of selective PDE2 or PDE5 inhibitors can lead to an improved retention for object memory (Prickaerts et al., 1997, 2002b; Boess et al., 2003). Moreover, it was shown that in vitro incubation of hippocampal slices with selective PDE2 or PDE5 inhibitors in combination with an NO donor resulted in distinct cGMP accumulation patterns (Van Staveren et al., 2001; Prickaerts et al., 2002b; Boess et al., 2003). These findings suggest that augmentation of cGMP levels during training, through inhibition of PDE2 or PDE5, might cause the improved performance, although inhibition of other PDE families cannot be excluded. Therefore, we wanted
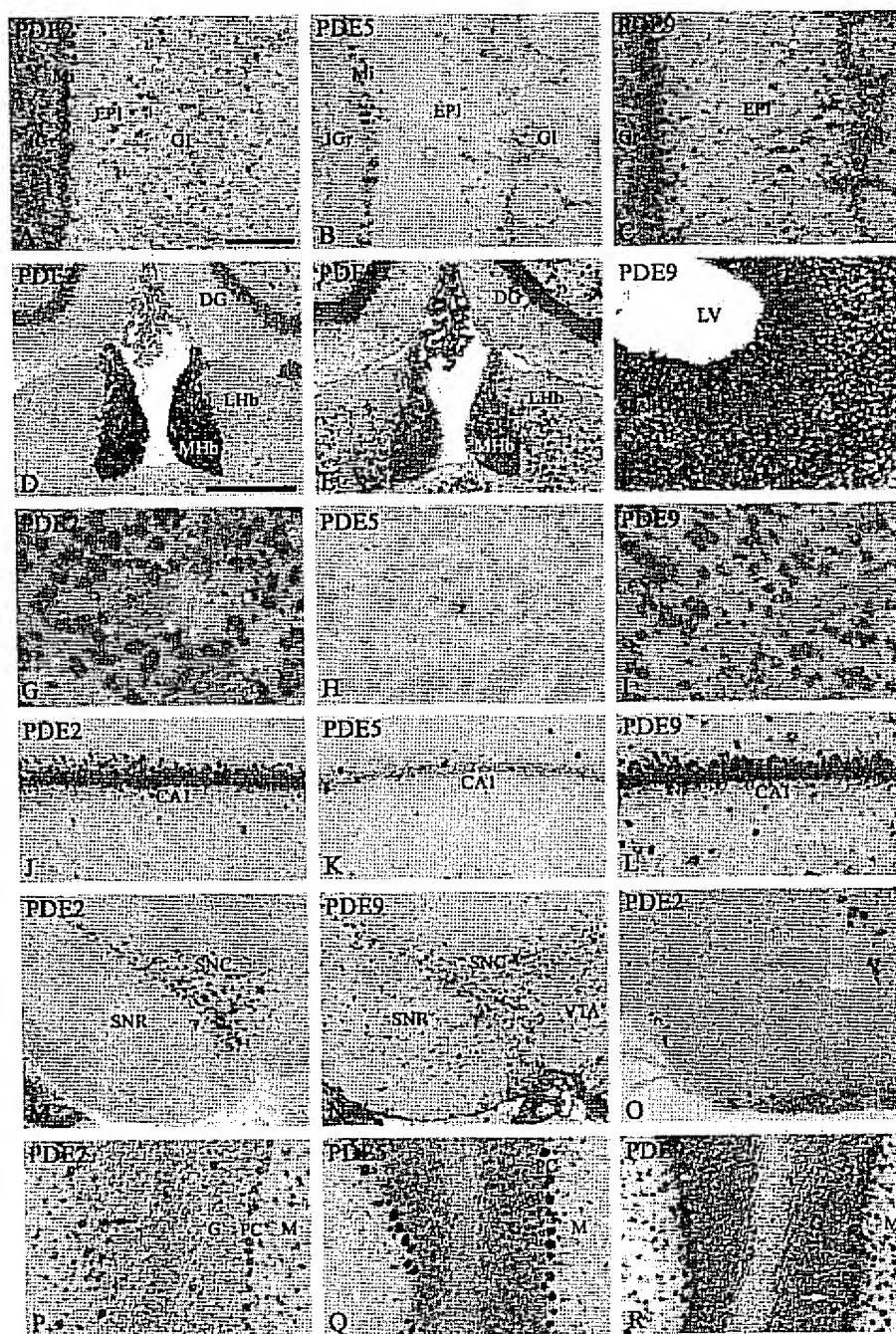
Fig. 2. mRNA expression of cGMP-hydrolyzing PDEs in rat brain areas by nonradioactive in situ hybridization. The antisense probes used are indicated in the left upper corner. Olfactory bulb from adult animal (A–C) and at E15 (F); habenula and choroid plexus (D,E); caudate putamen (G–I); hippocampus (J–L); substantia nigra (M,N); mammillary area with magnification of the histaminergic cell group (inset) (O) and cerebellum (P–R). DG, dentate gyrus; EPl, external plexiform layer; G, granule cell layer; GL, glomerular layer; IGr, internal granular layer; LHb, lateral habenula; LV, lateral ventricle; M, molecular layer; MHb, medial habenula; Mi, mitral cell layer; PC, Purkinje cell layer; SNC, substantia nigra pars compacta; SNR, substantia nigra pars reticulata; VTA, ventral tegmental area. Arrow indicates possible Golgi cell. Scale bar = 200 μm in A (applies to A–C, inset O); 500 μm for M,N,O; J–L, P–R; 100 μm for F–L; 500 μm in D (applies to D and E).

to study the cellular localization of both PDE2 and PDE5 in greater detail.

The expression patterns of the three cGMP-hydrolyzing PDE families studied are not identical, although they overlap to some extent (see below), indicating diversity in the involvement of cGMP-mediated signal transduction pathways. Of the three different families investigated, PDE9 mRNA expression is most abundant throughout the brain, followed by PDE2, and then PDE5. This pattern is consistent during maturation, although not always present at younger stages, as shown for instance for PDE2 and PDE5 in Purkinje cells.

PDE2 mRNA expression was strong in structures that belong to the limbic system, i.e., olfactory cortex, amygdala, and hippocampus, in agreement with our previous study involving adult animals (Repaske et al., 1993). PDE2 protein has been described in similar areas in cell bodies from neurons and in axons and dendrites (Juilfs et
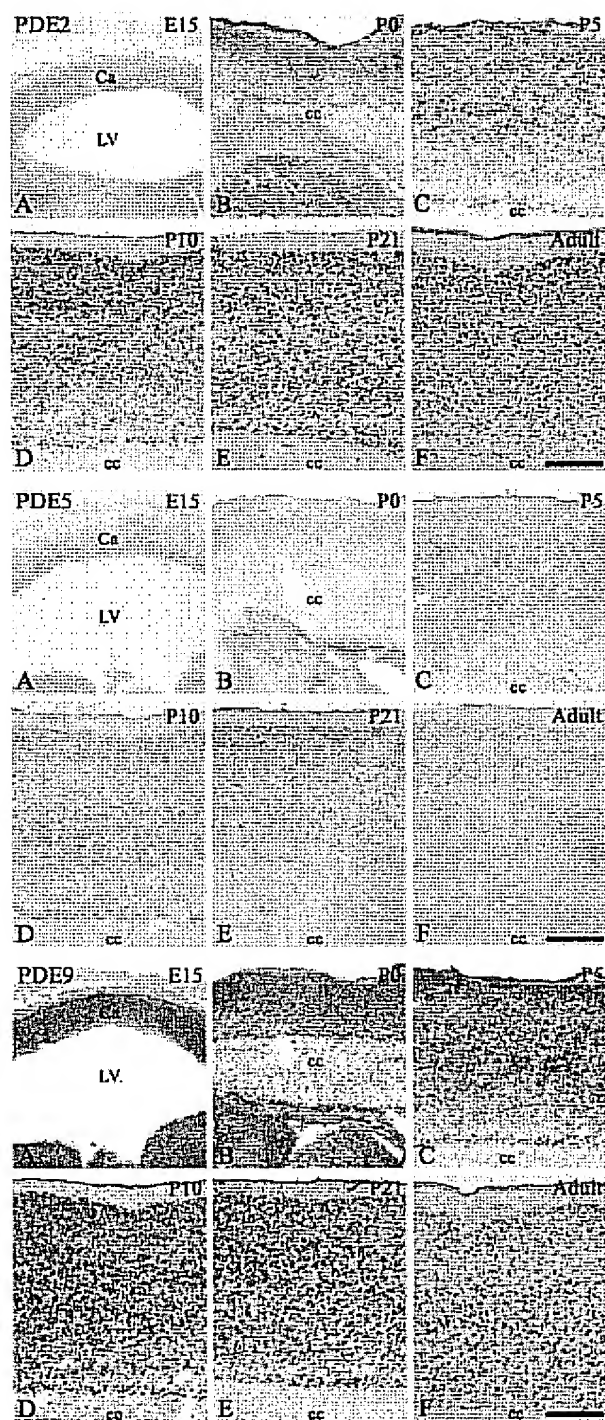
Fig. 3. Localization of PDE2, PDE5, and PDE9 mRNA in the cortex during development of the rat brain by nonradioactive in situ hybridization. The different ages, labeled A–F in each panel, are indicated in the upper right corner. Recording conditions were kept constant for each PDE riboprobe. Ca, cortical area; cc, corpus callosum; LV, lateral ventricle. Scale bars = 500 μm (applies to all parts).

al., 1999). This places PDE2 in an appropriate location for a role in learning, memory, emotion, and synaptic plasticity. In addition, we have observed PDE2 mRNA in the substantia nigra pars compacta, dorsal raphe nucleus, and histaminergic cell groups of the tubero mammillary region. This could point to a role for PDE2 in dopaminergic, serotonergic, and histaminergic neurotransmission. Surprisingly, when NO is applied in combination with a PDE inhibitor (either a nonselective inhibitor, such as 3-isobutyl-1-methylxanthine (IBMX) or a selective PDE2 inhibitor, such as erythro-9-(2-hydroxy-3-nonyl)adenine (EHNA)) to brain slices incubated in vitro, somata in these regions were not cGMP-immunoreactive (De Vente et al., 1998). Indeed, we have never observed colocalization of cGMP-immunoreactivity in dopaminergic, serotonergic, or histaminergic fibers in any region of the rat brain (De Vente et al., 2000; Steinbusch et al., 2001). This suggests either that, although sGC is demonstrably present in many of these regions (Schmidt et al., 1992; De Vente et al., 1998), basal and NO-stimulated cGMP synthesis must be very low in these cell bodies, or that the activity of an IBMX-resistant PDE (such as PDE9) may be dominant in this cellular region.

In contrast to PDE2 and PDE9, PDE5 mRNA expression is very limited. The highest expression is observed in Purkinje cells, and PDE5 expression in these cells is visualized for the first time at P10. These results are in agreement with Northern blot analysis during development of the rat cerebellum (Kotera et al., 1997) and with immunocytochemical studies showing PDE5 protein expression in cell bodies from Purkinje cells and in the major branches of their extensive dendritic tree (Juilfs et al., 1999; Kotera et al., 2000; Giordano et al., 2001). Additionally, we detected PDE5 mRNA expression in cells throughout the cortical areas, in the hippocampus, and the olfactory bulb, a finding that has not been mentioned in previous PDE5 expression studies (Kotera et al., 1997, 2000; Juilfs et al., 1999; Giordano et al., 2001). The PDE5 expression found in hippocampus suggests that it potentially might function in learning and memory processes. In this regard, the presence of PDE5 mRNA in hippocampus and entorhinal cortex supports the concept that PDE5 is involved in object recognition (Prickaerts et al., 1997, 2002b).

It is unlikely that our current observations are the result of artifactual localization of PDE5 mRNA. First, hybridization with sense probes or pretreatment with RNase did not result in any staining. Second, Northern blot analysis in different brain areas from rat, human, and canine indicate that while highest expression is found in the cerebellum, lower levels are also present in other brain areas, such as hippocampus, cortex, and olfactory bulb (Kotera et al., 1997, 1999a; Loughney et al., 1998). Finally, in agreement with previous studies (Kotera et al., 1997, 1999a; Hanson et al., 1998), we found high PDE5 expression in lung, aorta, and intestine (not shown), providing further support for the reliability of the PDE5 riboprobe used.

In agreement with a previous study (Andreeva et al., 2001), PDE9 mRNA is the most widely distributed of the PDEs that we analyzed. Our data closely match the data of this previous study of PDE9 localization. Comparison of PDE9 mRNA expression with published data for other cGMP-hydrolyzing PDE family members, such as PDE1 (Furuyama et al., 1994; Yan et al., 1994), PDE10 (Fujish-
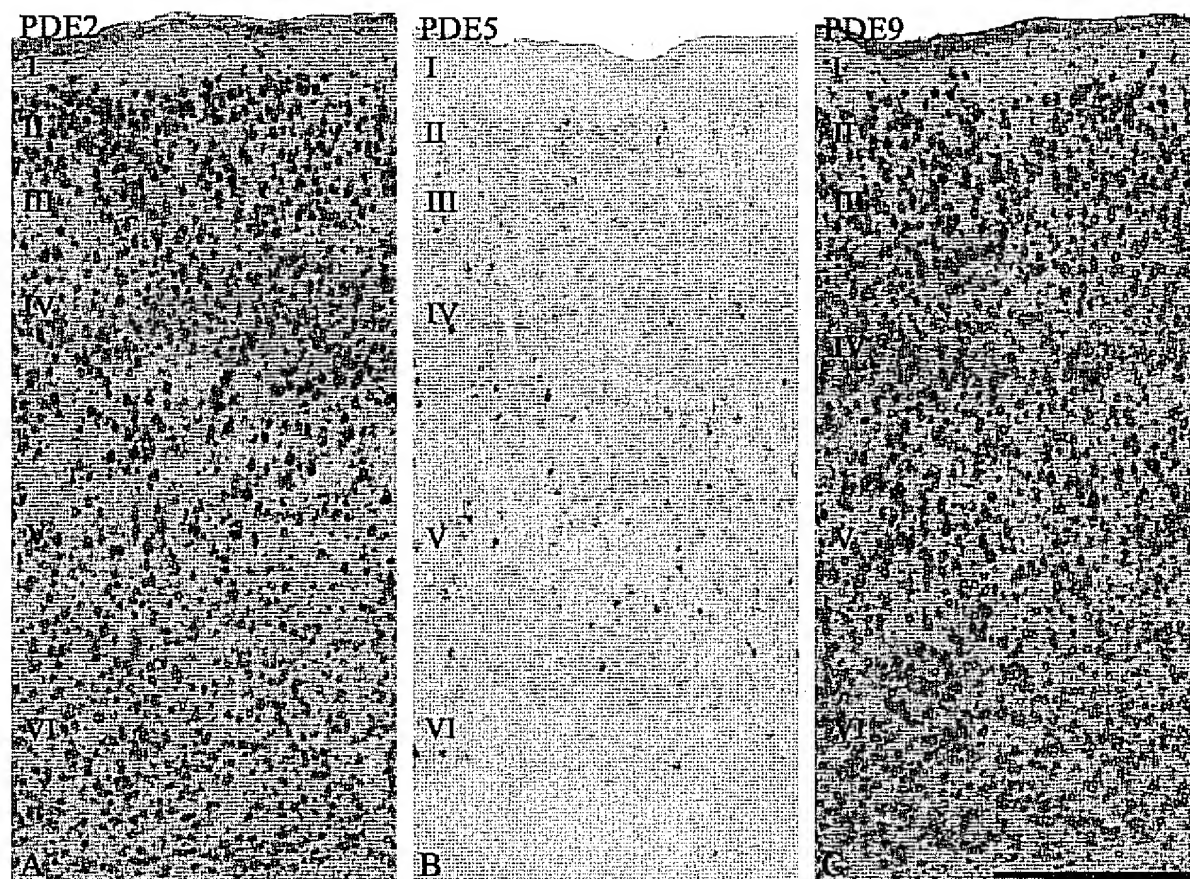
PDE2   PDE5   PDE9

Fig. 4. Localization of PDE2, PDE5, and PDE9 mRNA in the frontal cortex of an adult rat by nonradioactive in situ hybridization. Scale bar = 500 μm in C (applies to A–C).

ige et al., 1999), and PDE11 (Fawcett et al., 2000), indicates that PDE9 has the broadest CNS distribution of all known PDEs. Our present study, in conjunction with previous work (Repaske et al., 1993; Kotera et al., 1997), indicates that some cell types such as Purkinje cells and hippocampal pyramidal cells express the mRNA of all three cGMP-hydrolyzing PDEs. Although no localization studies of these three PDE families could be performed on the same tissue sections, other studies have shown that both pyramidal and Purkinje cells also express PDE1 (Kincaid et al., 1987; Furuyama et al., 1994), PDE3 (Reinhardt and Bondy, 1996), PDE4 (Iwahashi et al., 1996; McPhee et al., 2001), and PDE7 (Miro et al., 2001). This suggests that cells can express multiple PDE families. However, it is important to note several caveats. First, our studies have focused on mRNA expression, and do not necessarily provide an accurate index of protein expression. Second, a variety of splice variants have been described for PDE2, PDE5, and PDE9 in such species as bovine, canine, rat, mouse, and human (Sonnenburg et al., 1991; Yang et al., 1994; Rosman et al., 1997; Guipponi et al., 1998; Kotera et al., 1998, 1999a; Loughney et al., 1998; Soderling et al., 1998). With the probes used in our study, we cannot distinguish among the splice variants in each family.

Comparison of the K_m values for cGMP of PDE1 (1.1–5.0 μM), PDE2 (15–30 μM), PDE5 (1–5 μM), PDE9 (70–170 nM), PDE10 (3 μM), and PDE11 (1 μM) (values obtained from Francis et al., 2001), indicates that PDE9 has the highest affinity for cGMP. In this respect it seems actually striking that, besides PDE9 expression, other cGMP-hydrolyzing PDE families are expressed in the same cell type. The broad expression pattern of PDE9 and its low K_m value for cGMP suggest that PDE9 could function as a "housekeeping" PDE that keeps levels of cGMP low in most cells. In this respect, it should be noted that in most tissues intracellular levels of cGMP compared to cAMP are usually 10–50 times lower (Ferrendelli, 1978). The restricted distribution of other PDEs suggests that they could be involved in more specific signaling pathways. Specific antibodies directed against the different PDE families and their representation in multiple variants might give more insight into the localization of PDEs in cellular compartments, as has been demonstrated for olfactory neurons (Juilfs et al., 1997).

In adult rat brain slices it has been a common observation that, irrespective of the PDE inhibitor or the NO donor used, neuronal fibers and/or astrocytes can be cGMP-immunoreactive, whereas in neuronal cell bodies in the cortex and hippocampus, almost without exception, no cGMP is
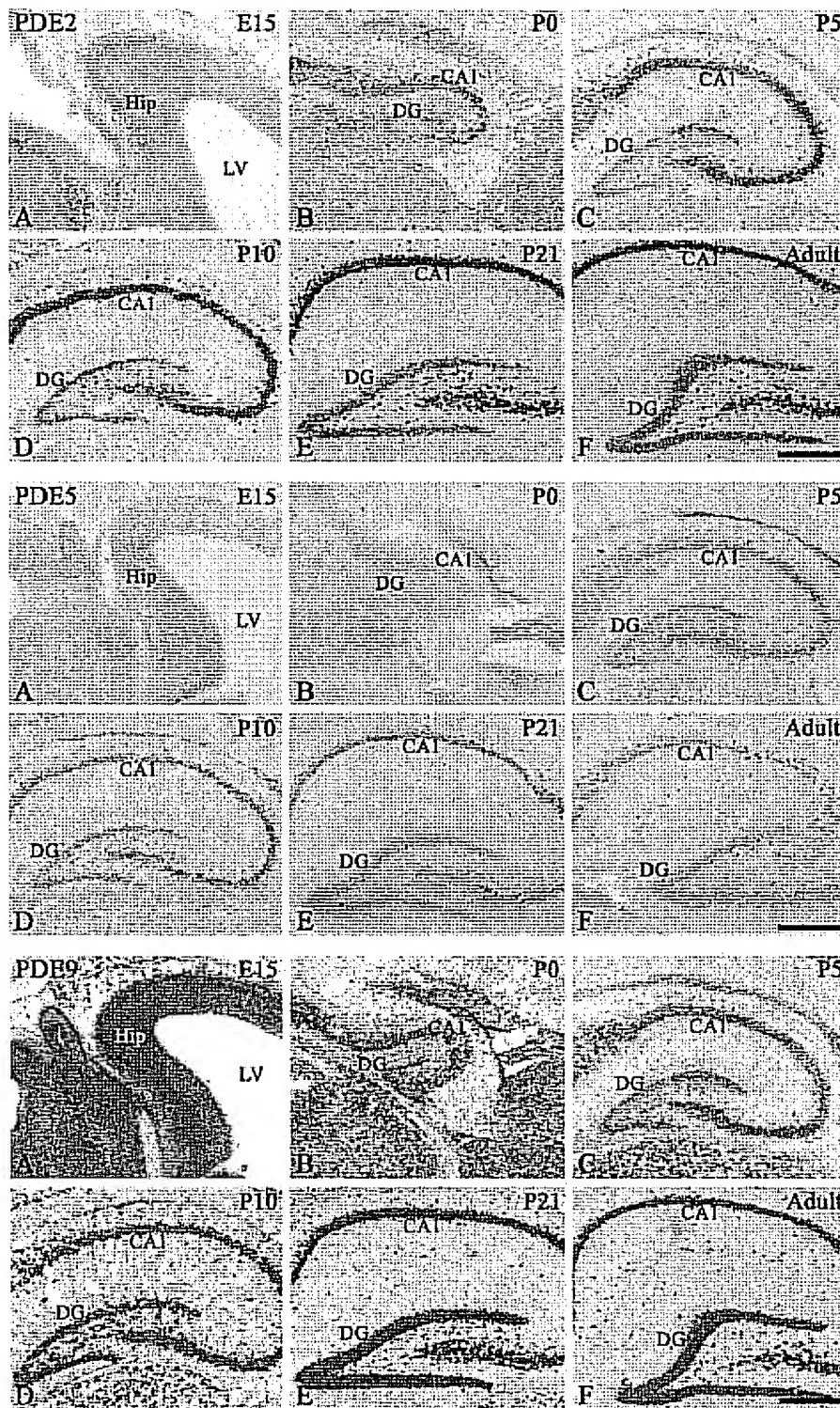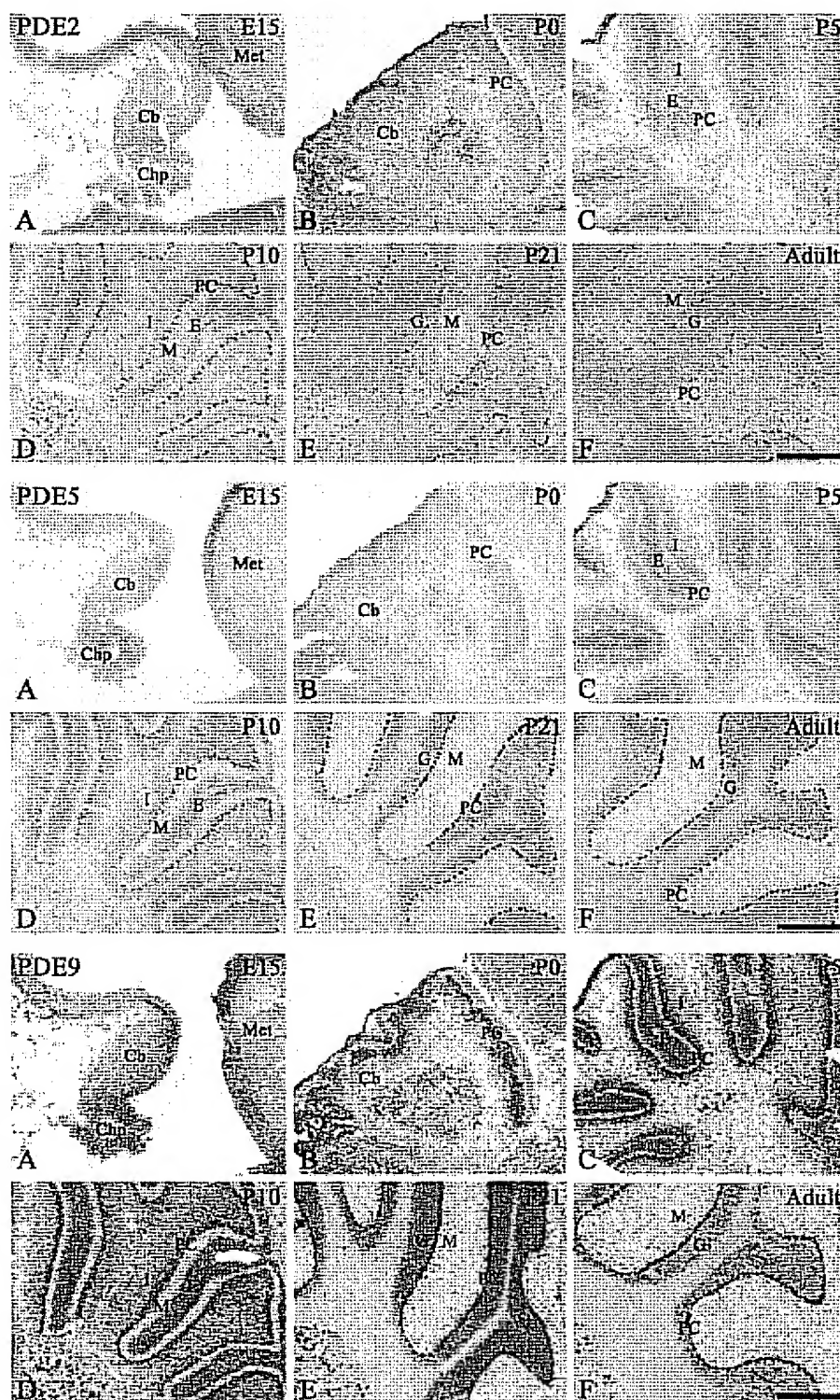
Fig. 5. Localization of PDE2, PDE5, and PDE9 mRNA in the hippocampus during development of the rat brain by nonradioactive in situ hybridization. The different ages, labeled A–F in each panel, are indicated in the upper right corner. Recording conditions were kept constant for each PDE ribo-probe. DG, dentate gyrus; Hip, hippocampal area; LV, lateral ventricle. Scale bars = 500 μm (applies to all parts).

visualized (De Vente et al., 1998; Van Staveren et al., 2001). In particular, cGMP-immunoreactivity has not been observed in hippocampal pyramidal cell bodies or cerebellar Purkinje cell bodies, although these cells are known to express sGC (Burgunder and Cheung, 1994; Giuili et al., 1994). It was observed that PDE2, PDE5, and PDE9 mRNAs are

Fig. 6. Localization of PDE2, PDE5, and PDE9 mRNA in the cerebellum during development of the rat brain by nonradioactive in situ hybridization. The different ages, labeled A–F in each panel, are indicated in the upper right corner. Recording conditions were kept constant for each PDE ribo-probe. Cb, cerebellum; Chp, choroid plexus; E, external granule cell layer; G, granule cell layer; I, internal granule cell layer; M, molecular layer; Met, metencephalon; PC, Purkinje cell layer. Scale bars = 500 μm (applies to all parts).

mainly expressed in neurons throughout the brain. Abundant somatic expression of multiple PDE family members could provide an explanation for the absence of cGMP-immunoreactivity in the cell bodies of many neurons.

To summarize, our results show that PDE2, PDE5, and PDE9 mRNAs are present throughout the developing CNS, and that each PDE family has a distinct localization pattern. The expression patterns are by and large main-
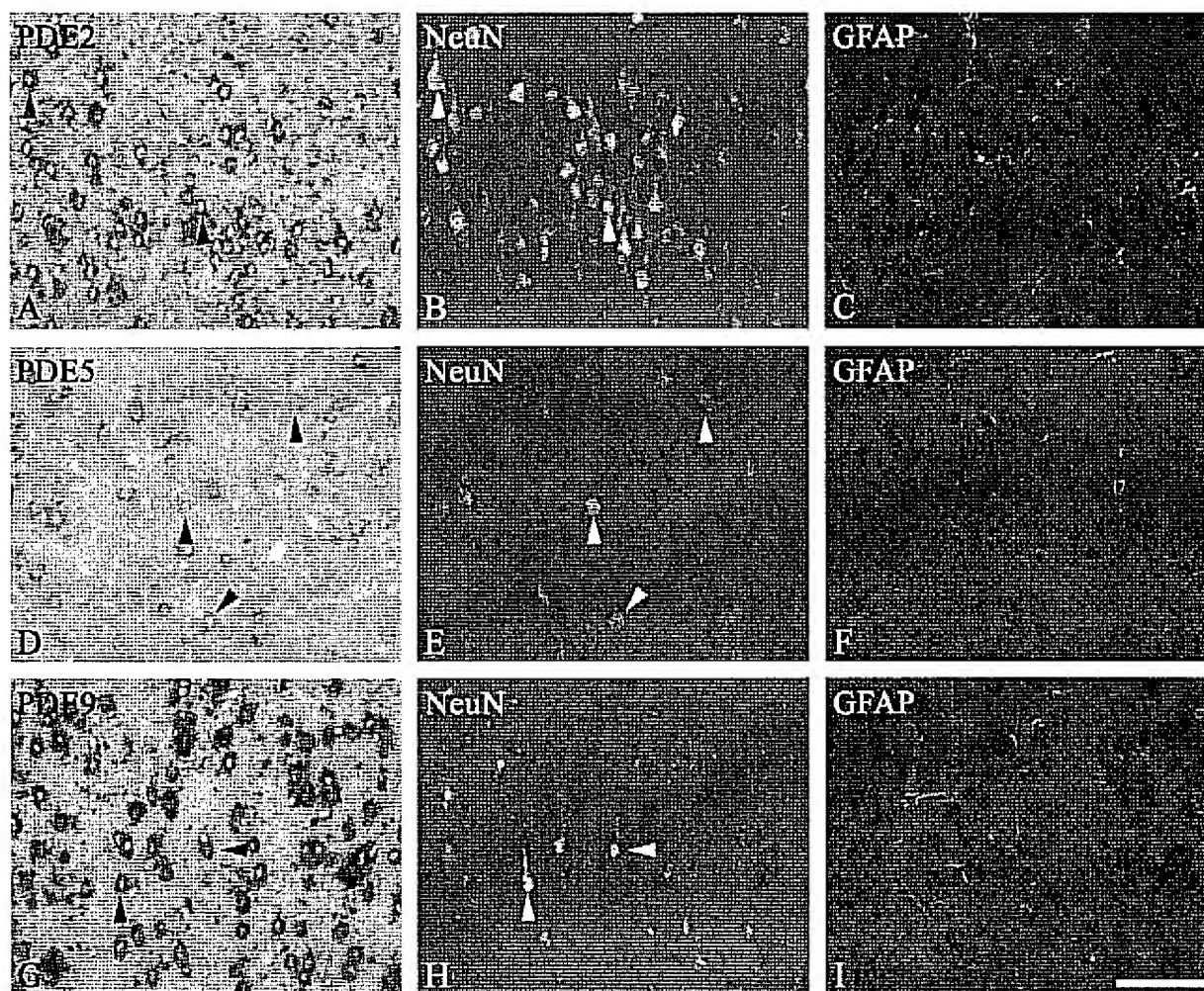
Fig. 7. Double staining of PDE2, PDE5, and PDE9 mRNAs with NeuN or GFAP in adult rat cortical layer V. Sections hybridized with PDE2 (A–C), PDE5 (D–F), or PDE9 (G–I) antisense probes were double labeled for NeuN (B,E,H) or GFAP (C,F,I). Pictures from the antisense probes were taken using brightfield illumination, whereas NeuN and GFAP were photographed using a single fluorescence filter. Arrowheads indicate neurons. Scale bar = 100 μm in I (applies to A–I).

tained during brain development. PDE9 mRNA has the widest distribution and could function in cells to maintain low basal cGMP levels. PDE2 mRNA is strongly expressed in structures of the limbic system. PDE5 mRNA expression is the most limited, being highly expressed only in cerebellar Purkinje cells, and to a lesser extent in cortex, hippocampus, and olfactory bulb. In addition, some cell types, such as Purkinje cells, pyramidal cells, mitral cells, and possibly some cortical neurons, express all three PDE families. The mRNA localization patterns suggest involvement of these cGMP-hydrolyzing PDE families in many different brain functions, including learning and memory processes and motor behavior.

ACKNOWLEDGMENTS

LITERATURE CITED

Andreeva SG, Dikkes P, Epstein PM, Rosenberg PA. 2001. Expression of cGMP specific phosphodiesterase 9A mRNA in the rat brain. J Neurosci 21:9068–9076.

Baratti CM, Boccia MM. 1999. Effects of sildenafil on long-term retention of an inhibitory avoidance response in mice. Behav Pharmacol 10:731–737.

Beavo JA. 1995. Cyclic nucleotide phosphodiesterases: functional implications of multiple isoforms. Physiol Rev 75:725–748.

Bernabeu R, Schmitz P, Faillace MP, Izquierdo I, Medina JH. 1996. Hippocampal cGMP and cAMP are differentially involved in memory processing of inhibitory avoidance learning. Neuroreport 7:585–588.

Bernabeu R, Schroder N, Quevedo J, Cammarota M, Izquierdo I, Medina JH. 1997. Further evidence for the involvement of a hippocampal cGMP/cGMP-dependent protein kinase cascade in memory consolidation. Neuroreport 8:2221–2224.

Bicker G. 1998. NO news from insect brains. Trends Neurosci 21:349–355.

Bicker G. 2001. Sources and targets of nitric oxide signalling in insect nervous systems. Cell Tissue Res 303:137–146.

Billingsley ML, Polli JW, Balaban CD, Kincaid RL. 1990. Developmental

expression of calmodulin-dependent cyclic nucleotide phosphodiesterase in rat brain. Brain Res Dev Brain Res 53:253–263.

Boess FG, Hendrix M, Van Der Stany FJ, Van Staveren W, De Vente J, Sik A, Prickaerts J, Blokland A, Koenig G. 2003. Inhibition of PDE2 — a novel mechanism for the treatment of memory disorders. Book of Abstracts, 6th International Conference AD/PD 2003, May 8–12, 2003, Seville, Spain. p 18.

Bredt DS, Snyder SH. 1994. Transient nitric oxide synthase neurons in embryonic cerebral cortical plate, sensory ganglia, and olfactory epithelium. Neuron 13:301–313.

Broillet MC, Firestein S. 1999. Cyclic nucleotide-gated channels. Molecular mechanisms of activation. Ann NY Acad Sci 868:730–740.

Burgunder JM, Cheung PT. 1994. Expression of soluble guanylyl cyclase gene in adult rat brain. Eur J Neurosci 6:211–217.

Carvajal JA, Germain AM, Huidobro-Toro JP, Weiner CP. 2000. Molecular mechanism of cGMP-mediated smooth muscle relaxation. J Cell Physiol 184:409–420.

Chalimoniuk M, Strosznajder JB. 1998. Aging modulates nitric oxide synthesis and cGMP levels in hippocampus and cerebellum. Effects of amyloid beta peptide. Mol Chem Neuropathol 35:77–95.

Conti M, Jin SL. 1999. The molecular biology of cyclic nucleotide phosphodiesterases. Prog Nucleic Acid Res Mol Biol 63:1–38.

Davis CW, Kuo JF. 1976. Ontogenetic changes in levels of phosphodiesterase for adenosine 3':5'-monophosphate and guanosine 3':5'-monophosphate in the lung, brain and heart from guinea pigs. Biochim Biophys Acta 444:554–562.

De Vente J, Hopkins DA, Markerink-van Ittersum M, Emson PC, Schmidt HHH, Steinbusch HWM. 1998. Distribution of nitric oxide synthase and nitric oxide-receptive, cyclic GMP-producing structures in the rat brain. Neuroscience 87:207–241.

De Vente J, Markerink-van Ittersum M, Van Abeelen J, Emson PC, Axer H, Steinbusch HWM. 2000. NO-mediated cGMP synthesis in cholinergic neurons in the rat forebrain: effects of lesioning dopaminergic or serotonergic pathways on nNOS and cGMP synthesis. Eur J Neurosci 12:507–519.

De Vente J, Asan E, Gambaryan S, Markerink-van Ittersum M, Axer H, Gallatz K, Lohmann SM, Palkovits M. 2001. Localization of cGMP-dependent protein kinase type II in rat brain. Neuroscience 108:27–49.

Dousa TP. 1999. Cyclic-3',5'-nucleotide phosphodiesterase isozymes in cell biology and pathophysiology of the kidney. Kidney Int 55:29–62.

Edwards TM, Rickard NS, Ng KT. 2002. Inhibition of guanylate cyclase and protein kinase G impairs retention for the passive avoidance task in the day-old chick. Neurobiol Learn Mem 77:313–326.

El-Husseini AE, Williams J, Reiner PB, Pelech S, Vincent SR. 1999. Localization of the cGMP-dependent protein kinases in relation to nitric oxide synthase in the brain. J Chem Neuroanat 17:45–55.

Fawcett L, Baxendale R, Stacey P, McGrouther C, Harrow I, Soderling S, Hetman J, Beavo JA, Phillips SC. 2000. Molecular cloning and characterization of a distinct human phosphodiesterase gene family: PDE11A. Proc Natl Acad Sci USA 97:3702–3707.

Ferrendelli JA. 1978. Distribution and regulation of cyclic GMP in the central nervous system. Adv Cyclic Nucleotide Res 9:453–464.

Fisher DA, Smith JF, Pillar JS, St Denis SH, Cheng JB. 1998. Isolation and characterization of PDE9A, a novel human cGMP-specific phosphodiesterase. J Biol Chem 273:15559–15564.

Francis SH, Turko IV, Corbin JD. 2001. Cyclic nucleotide phosphodiesterases: relating structure and function. Prog Nucleic Acid Res Mol Biol 65:1–52.

Fujishige K, Kotera J, Omori K. 1999. Striatum- and testis-specific phosphodiesterase PDE10A isolation and characterization of a rat PDE10A. Eur J Biochem 266:1118–1127.

Furuyama T, Iwahashi J, Tano Y, Takagi H, Inagaki S. 1994. Localization of 63-kDa calmodulin-stimulated phosphodiesterase mRNA in the rat brain by in situ hybridization histochemistry. Brain Res Mol Brain Res 26:331–336.

Garthwaite J. 1991. Glutamate, nitric oxide and cell-cell signalling in the nervous system. Trends Neurosci 14:60–67.

Gibbs SM, Truman JW. 1998. Nitric oxide and cyclic GMP regulate retinal patterning in the optic lobe of Drosophila. Neuron 20:83–93.

Gibbs SM, Becker A, Hardy RW, Truman JW. 2001. Soluble guanylate cyclase is required during development for visual system function in Drosophila. J Neurosci 21:7705–7714.

Gillespie PG, Beavo JA. 1988. Characterization of a bovine cone photoreceptor phosphodiesterase purified by cyclic GMP-sepharose chromatography. J Biol Chem 263:8133–8141.

Giordano D, De Stefano ME, Citro G, Modica A, Giorgi M. 2001. Expression of cGMP-binding cGMP-specific phosphodiesterase (PDE5) in mouse tissues and cell lines using an antibody against the enzyme amino-terminal domain. Biochim Biophys Acta 1539:16–27.

Giuili G, Luzi A, Poyard M, Guellaen G. 1994. Expression of mouse brain soluble guanylyl cyclase and NO synthase during ontogeny. Brain Res Dev Brain Res 81:269–283.

Guipponi M, Scott HS, Kudoh J, Kawasaki K, Shibuya K, Shintani A, Asakawa S, Chen H, Lalioti MD, Rossier C, Minoshima S, Shimizu N, Antonarakis SE. 1998. Identification and characterization of a novel cyclic nucleotide phosphodiesterase gene (PDE9A) that maps to 21q22.3: alternative splicing of mRNA transcripts, genomic structure and sequence. Hum Genet 103:386–392.

Hanson KA, Burns F, Rybalkin SD, Wager Miller J, Beavo J, Clarke WR. 1998. Developmental changes in lung cGMP phosphodiesterase-5 activity, protein, and message. Am J Respir Crit Care Med 158:279–288.

Hetman JM, Robas N, Baxendale R, Fidock M, Phillips SC, Soderling SH, Beavo JA. 2000. Cloning and characterization of two splice variants of human phosphodiesterase 11A. Proc Natl Acad Sci USA 97:12891–12895.

Houslay MD. 1998. Adaptation in cyclic AMP signalling processes: a central role for cyclic AMP phosphodiesterases. Semin Cell Dev Biol 9:161–167.

Iwahashi Y, Furuyama T, Tano Y, Ishimoto I, Shimomura Y, Inagaki S. 1996. Differential distribution of mRNA encoding cAMP-specific phosphodiesterase isoforms in the rat brain. Brain Res Mol Brain Res 38:14–24.

Izquierdo LA, Vianna M, Barros DM, Mello e Souza T, Ardenghi P, Sant' Anna MK, Rodrigues C, Medinam JH, Izquierdo I. 2000. Short- and long-term memory are differentially affected by metabolic inhibitors given into hippocampus and entorhinal cortex. Neurobiol Learn Mem 73:141–149.

Juilfs DM, Fulle HJ, Zhao AZ, Houslay MD, Garbers DL, Beavo JA. 1997. A subset of olfactory neurons that selectively express cGMP-stimulated phosphodiesterase (PDE2) and guanylyl cyclase-D define a unique olfactory signal transduction pathway. Proc Natl Acad Sci USA 94:3388–3395.

Juilfs DM, Soderling S, Burns F, Beavo JA. 1999. Cyclic GMP as substrate and regulator of cyclic nucleotide phosphodiesterases (PDEs). Rev Physiol Biochem Pharmacol 135:67–104.

Kendrick KM, Guevara-Guzman R, Zorrilla J, Hinton MR, Broad KD, Mimmack M, Ohkura S. 1997. Formation of olfactory memories mediated by nitric oxide. Nature 388:670–674.

Kincaid RL, Balaban CD, Billingsley ML. 1987. Differential localization of calmodulin-dependent enzymes in rat brain: evidence for selective expression of cyclic nucleotide phosphodiesterase in specific neurons. Proc Natl Acad Sci USA 84:1118–1122.

Kind PC, Neumann PE. 2001. Plasticity: downstream of glutamate. Trends Neurosci 24:553–555.

Kingston PA, Zufall F, Barnstable CJ. 1999. Widespread expression of olfactory cyclic nucleotide-gated channel genes in rat brain: implications for neuronal signalling. Synapse 32:1–12.

Kotera J, Yanaka N, Fujishige K, Imai Y, Akatsuka H, Ishizuka T, Kawashima K, Omori K. 1997. Expression of rat cGMP-binding cGMP-specific phosphodiesterase mRNA in Purkinje cell layers during postnatal neuronal development. Eur J Biochem 249:434–442.

Kotera J, Fujishige K, Akatsuka H, Imai Y, Yanaka N, Omori K. 1998. Novel alternative splice variants of cGMP-binding cGMP-specific phosphodiesterase. J Biol Chem 273:26982–26990.

Kotera J, Fujishige K, Imai Y, Kawai E, Michibata H, Akatsuka H, Yanaka N, Omori K. 1999a. Genomic origin and transcriptional regulation of two variants of cGMP-binding cGMP-specific phosphodiesterases. Eur J Biochem 262:866–873.

Kotera J, Fujishige K, Yuasa K, Omori K. 1999b. Characterization and phosphorylation of PDE10A2, a novel alternative splice variant of human phosphodiesterase that hydrolyzes cAMP and cGMP. Biochem Biophys Res Commun 261:551–557.

Kotera J, Fujishige K, Omori K. 2000. Immunohistochemical localization of cGMP-binding cGMP-specific phosphodiesterase (PDE5) in rat tissues. J Histochem Cytochem 48:685–693.

Loughney K, Hill TR, Florio VA, Uher L, Rosman GJ, Wolda SL, Jones BA, Howard ML, McAllister-Lucas LM, Sonnenburg WK, Francis SH, Corbin JD, Beavo JA, Ferguson K. 1998. Isolation and characterization of cDNAs encoding PDE5A, a human cGMP-binding, cGMP-specific 3',5'-cyclic nucleotide phosphodiesterase. Gene 216:139–147.

Lucas KA, Pitari GM, Kazerounian S, Ruiz-Stewart I, Park J, Schulz S, Chepenik KP, Waldman SA. 2000. Guanylyl cyclases and signaling by cyclic GMP. Pharmacol Rev 52:375–414.

Markerink-Van Ittersum M, Steinbusch HWM, De Vente J. 1997. Region-specific developmental patterns of atrial natriuretic factor- and nitric oxide-activated guanylyl cyclases in the postnatal frontal rat brain. Neuroscience 78:571–587.

McPhee I, Cochran S, Houslay MD. 2001. The novel long PDE4A10 cyclic AMP phosphodiesterase shows a pattern of expression within brain that is distinct from the long PDE4A5 and short PDE4A1 isoforms. Cell Signal 13:911–918.

Miro X, Perez-Torres S, Palacios JM, Puigdomenech P, Mengod G. 2001. Differential distribution of cAMP-specific phosphodiesterase 7A mRNA in rat brain and peripheral organs. Synapse 40:201–214.

Paxinos G, Watson C. 1986. The rat brain in stereotaxic coordinates. New York: Academic Press.

Paxinos G, Ashwell KWS, Törk I. 1994. Atlas of the developing rat nervous system. New York: Academic Press.

Polleux F, Morrow T, Ghosh A. 2000. Semaphorin 3A is a chemoattractant for cortical apical dendrites. Nature 404:567–573.

Prickaerts J, Steinbusch HWM, Smits JF, De Vente J. 1997. Possible role of nitric oxide-cyclic GMP pathway in object recognition memory: effects of 7-nitroindazole and zaprinast. Eur J Pharmacol 337:125–136.

Prickaerts J, de Vente J, Honig W, Steinbusch HWM, Blokland A. 2002a. cGMP, but not cAMP, in rat hippocampus is involved in early stages of object memory consolidation. Eur J Pharmacol 436:83–87.

Prickaerts J, Van Staveren WCG, Sik A, Markerink-van Ittersum M, Niewöhner U, Van der Staay FJ, Blokland A, De Vente J. 2002b. Effects of two selective phosphodiesterase type 5 inhibitors, sildenafil and vardenafil, on object recognition memory and hippocampal cyclic GMP levels in the rat. Neuroscience 113:351–361.

Reinhardt RR, Bondy CA. 1996. Differential cellular pattern of gene expression for two distinct cGMP-inhibited cyclic nucleotide phosphodiesterases in developing and mature rat brain. Neuroscience 72:567–578.

Repaske DR, Corbin JG, Conti M, Goy MF. 1993. A cyclic GMP-stimulated cyclic nucleotide phosphodiesterase gene is highly expressed in the limbic system of the rat brain. Neuroscience 56:673–686.

Rosman GJ, Martins TJ, Sonnenburg WK, Beavo JA, Ferguson K, Loughney K. 1997. Isolation and characterization of human cDNAs encoding a cGMP-stimulated 3',5'-cyclic nucleotide phosphodiesterase. Gene 191:89–95.

Schachtner J, Homberg U, Truman JW. 1999. Regulation of cyclic GMP elevation in the developing antennal lobe of the Sphinx moth, Manduca sexta. J Neurobiol 41:359–375.

Schmidt HH, Gagne GD, Nakane M, Pollock JS, Miller MF, Murad F. 1992. Mapping of neural nitric oxide synthase in the rat suggests frequent co-localization with NADPH diaphorase but not with soluble guanylyl cyclase, and novel paraneural functions for nitrinergic signal transduction. J Histochem Cytochem 40:1439–1456.

Scholz NL, Truman JW. 2000. Invertebrate models for studying NO-mediated signaling. In: Steinbusch HWM, De Vente J, Vincent SR, editors. Functional neuroanatomy of the nitric oxide system. Amsterdam: Elsevier. p 417–441.

Scholz NL, De Vente J, Truman JW, Graubard K. 2001. Neural network partitioning by NO and cGMP. J Neurosci 21:1610–1618.

Simpson PJ, Miller I, Moon C, Hanlon AL, Liebl DJ, Ronnett GV. 2002. Atrial natriuretic peptide type C induces a cell-cycle switch from proliferation to differentiation in brain-derived neurotrophic factor- or nerve growth factor-primed olfactory receptor neurons. J Neurosci 22:5536–5551.

Smoake JA, Song SY, Cheung WY. 1974. Cyclic 3',5'-nucleotide phosphodiesterase. Distribution and developmental changes of the enzyme and its protein activator in mammalian tissues and cells. Biochim Biophys Acta 341:402–411.

Soderling SH, Beavo JA. 2000. Regulation of cAMP and cGMP signaling: new phosphodiesterases and new functions. Curr Opin Cell Biol 12: 174–179.

Soderling SH, Bayuga SJ, Beavo JA. 1998. Identification and characterization of a novel family of cyclic nucleotide phosphodiesterases. J Biol Chem 273:15553–15558.

Soderling SH, Bayuga SJ, Beavo JA. 1999. Isolation and characterization of a dual-substrate phosphodiesterase gene family: PDE10A. Proc Natl Acad Sci USA 96:7071–7076.

Song HJ, Poo MM. 1999. Signal transduction underlying growth cone guidance by diffusible factors. Curr Opin Neurobiol 9:355–363.

Song H, Ming G, He Z, Lehmann M, McKerracher L, Tessier-Lavigne M, Poo M. 1998. Conversion of neuronal growth cone responses from repulsion to attraction by cyclic nucleotides. Science 281:1515–1518.

Sonnenburg WK, Mullaney PJ, Beavo JA. 1991. Molecular cloning of a cyclic GMP-stimulated cyclic nucleotide phosphodiesterase cDNA. Identification and distribution of isozyme variants. J Biol Chem 266: 17655–17661.

Steinbusch HWM, Allen GV, De Vente J, Hopkins DA. 2001. The interaction between the histaminergic system and the NO-cGMP pathway: a functional neuroanatomical study in the mammillary region and cerebral cortex of the rat. In: Watanabe T, Timmerman H, Yanai K, editors. Histaminergic research in the new millenium. Amsterdam: Elsevier. p 51–59.

Thomas MK, Francis SH, Corbin JD. 1990. Characterization of a purified bovine lung cGMP-binding cGMP phosphodiesterase. J Biol Chem 265: 14964–14970.

Truman JW, De Vente J, Ball EE. 1996. Nitric oxide-sensitive guanylate cyclase activity is associated with the maturational phase of neuronal development in insects. Development 122:3949–3958.

Van Staveren WCG, Markerink-van Ittersum M, Steinbusch HWM, De Vente J. 2001. The effects of phosphodiesterase inhibition on cyclic GMP and cyclic AMP accumulation in the hippocampus of the rat. Brain Res 888:275–286.

Van Wagenen S, Rehder V. 1999. Regulation of neuronal growth cone filopodia by nitric oxide. J Neurobiol 39:168–185.

Watts VJ. 2002. Molecular mechanisms for heterologous sensitization of adenylate cyclase. J Pharmacol Exp Ther 302:1–7.

Wedel BJ, Garbers DL. 2001. The guanylyl cyclase family at Y2K. Annu Rev Physiol 63:215–233.

Wei JY, Roy DS, Leconte L, Barnstable CJ. 1998. Molecular and pharmacological analysis of cyclic nucleotide-gated channel function in the central nervous system. Prog Neurobiol 56:37–64.

Yan C, Bentley JK, Sonnenburg WK, Beavo JA. 1994. Differential expression of the 61 kDa and 63 kDa calmodulin-dependent phosphodiesterases in the mouse brain. J Neurosci 14:973–984.

Yang Q, Paskind M, Bolger G, Thompson WJ, Repaske DR, Cutler LS, Epstein PM. 1994. A novel cyclic GMP stimulated phosphodiesterase from rat brain. Biochem Biophys Res Commun 205:1850–1858.

MGet It

Phosphodiesterase type 2 and the homeostasis of cyclic GMP in living thalamic neurons.

Hepp R, Tricoire L, Hu E, Gervasi N, Paupardin-Tritsch D, Lambolez B, Vincent P.

Université Pierre et Marie Curie-Paris 6, CNRS, UMR 7102, Paris, France. regine.hepp@snv.jussieu.fr

The ubiquitous second messenger cyclic GMP (cGMP) is synthesized by soluble guanylate cyclases in response to nitric oxide (NO) and degraded by phosphodiesterases (PDE). We studied the homeostasis of cGMP in living thalamic neurons by using the genetically encoded fluorescence resonance energy transfer sensor Cygnet, expressed in brain slices through viral gene transfer. Natriuretic peptides had no effect on cGMP. Basal cGMP levels decreased upon inhibition of NO synthases or soluble guanylate cyclases and increased when PDEs were inhibited. Single cell RT-PCR analysis showed that thalamic neurons express PDE1, PDE2, PDE9, and PDE10. Basal cGMP levels were increased by the PDE2 inhibitors erythro-9-(2-hydroxy-3-nonyl) adenine (EHNA) and BAY60-7550 but were unaffected by PDE1 or PDE10 inhibitors. We conclude that PDE2 regulates the basal cGMP concentration in thalamic neurons. In addition, in the presence of 3-isobutyl-1-methylxanthine (IBMX), cGMP still decreased after application of a NO donor. Probenecid, a blocker of cGMP transporters, had no effect on this decrease, leaving PDE9 as a possible candidate for decreasing cGMP concentration. Basal cGMP level is poised at an intermediate level from which it can be up or down-regulated according to the cyclase and PDE activities.

Selective blockade of phosphodiesterase types 2, 5 and 9 results in cyclic 3'5' guanosine monophosphate accumulation in retinal pigment epithelium cells

R M H Diederen, E C La Heij, M Markerink-van Ittersum, A Kijlstra, F Hendrikse and J de Vente

Updated information and services can be found at:
http://bjo.bmj.com/cgi/content/full/91/3/379

These include:

References	This article cites 23 articles, 13 of which can be accessed free at: http://bjo.bmj.com/cgi/content/full/91/3/379#BIBL
Rapid responses	You can respond to this article at: http://bjo.bmj.com/cgi/eletter-submit/91/3/379
Email alerting service	Receive free email alerts when new articles cite this article - sign up in the box at the top right corner of the article

Notes

To order reprints of this article go to:
http://journals.bmj.com/cgi/reprintform

To subscribe to *British Journal of Ophthalmology* go to:
http://journals.bmj.com/subscriptions/

EXTENDED REPORT

Selective blockade of phosphodiesterase types 2, 5 and 9 results in cyclic 3'5' guanosine monophosphate accumulation in retinal pigment epithelium cells

R M H Diederen, E C La Heij, M Markerink-van Ittersum, A Kijlstra, F Hendrikse, J de Vente

See end of article for
authors' affiliations
....

Correspondence to:
R Diederen, Department of
Ophthalmology, University
Hospital Maastricht, PO Box
5800, P Debyelaan 25,
6202 AZ Maastricht, The
Netherlands; r.diederen@
NP.unimaas.nl

Accepted 6 August 2006
Published Online First
30 August 2006
....

Aim: To investigate which phosphodiesterase (PDE) is involved in regulating cyclic 3'5' guanosine monophosphate breakdown in retinal pigment epithelium (RPE) cells.

Methods: cGMP content in the cultured RPE cells (D407 cell line) was evaluated by immunocytochemistry in the presence of non-selective or isoform-selective PDE inhibitors in combination with the particulate guanylyl cyclase stimulator atrial natriuretic peptide (ANP) or the soluble guanylyl cyclase stimulator sodium nitroprusside (SNP). mRNA expression of PDE2, PDE5 and PDE9 was studied in cultured human RPE cells and rat RPE cell layers using non-radioactive in situ hybridisation.

Results: In the absence of PDE inhibitors, cGMP levels in cultured RPE cells are very low. cGMP accumulation was readily detected in cultured human RPE cells after incubation with Bay60–7550 as a selective PDE2 inhibitor, sildenafil as a selective PDE5 inhibitor or Sch51866 as a selective PDE9 inhibitor. In the presence of PDE inhibition, cGMP content increased markedly after stimulation of the particulate guanylyl cyclase. mRNA of PDE2,PDE5 and PDE9 was detected in all cultured human RPE cells and also in rat RPE cell layers.

Conclusions: PDE2, PDE5 and PDE9 have a role in cGMP metabolism in RPE cells.

ndividual cells were grouped in defined grey value classes. Numbers are the means of three experiments (six pictures were taken per incubation in each experiment) and they express the percentage of cells in each of the four intensity classes.

Cyclic 3',5'-guanosine monophosphate (cGMP), a central molecule in the phototransduction cascade,[1][2] is also involved in several other physiological processes in the retina. cGMP stimulates the absorption of subretinal fluid by activating the retinal pigment epithelium (RPE) cell pump.[3][4] Recently, we found that retinal detachment was associated with a decrease in the cGMP concentration in the subretinal fluid as compared with controls.[5] These findings prompted us to investigate the mechanisms involved in retinal cGMP metabolism.

Intracellular concentrations of cGMP represent the net balance between synthesis by guanylyl cyclases and breakdown by 3',5' cyclic nucleotide phosphodiesterases (PDEs).[6] PDEs comprise a large group of enzymes that hydrolyse cyclic adenosine monophosphate (cAMP) and cGMP to their inactive 5' derivates. Eleven different subfamilies of PDE isozymes (PDE1–PDE11) are known. The classification is based on their affinities for cGMP and cAMP, and several proteomic and genomic characteristics.[7] PDE2, PDE5, PDE 6, PDE 9 and PDE10 are the major cGMP-degrading enzymes.[8][9–12] PDE10, which hydrolyses both cAMP and cGMP, was however not detected in the eye, and PDE6 is known to be present only in retinal photoreceptor cells.[13][14]

cAMP-hydrolysing and cGMP-hydrolysing activities have been detected in homogenates of cultured pigment epithelium from rats.[15] Although the first papers about PDE activity in RPE cells were already published in the early 1980s,[16][17] no data are available on the expression of the individual PDE isoforms that have been characterised over the past 10 years.

RPE cells are in close contact with the photoreceptor layer and facilitate the supply of necessary substrates, including oxygen, to the photoreceptor cells. We have found that RPE cells are capable of producing cGMP and most cGMP is generated after stimulation of the particulate guanylyl cyclase pathway and simultaneous non-selective PDE inhibition with 3-isobutyl-1-methylxanthine (IBMX; Diederen, unpublished data).

The aim of this study was to identify the PDE isoforms involved in the cGMP breakdown in RPE cells. To investigate PDE activity in RPE cells, we studied cGMP accumulation in the RPE cells after stimulating particulate or soluble guanylyl cyclase in the presence of PDE inhibitors with different selection properties. We used IBMX as a non-specific PDE inhibitor, Bay 60–7550 as a selective PDE2 inhibitor,[18] sildenafil as a selective PDE5 inhibitor and Sch 51866 as a selective PDE9 inhibitor.[18] In addition, mRNA expression of PDE2, PDE5 and PDE9 was studied in cultured human RPE cells using non-radioactive in situ hybridisation. As it is impossible to detect the in situ hybridisation signal in pigmented RPE cells, we studied the in vivo situation by analysing the mRNA expression of PDE2, PDE5 and PDE9 in the unpigmented RPE cell layer of albino Lewis rats.

Our results indicate that PDE2, PDE5 and PDE9 are present in cultured human RPE cells and rat RPE cell layers, and that these different PDE isoforms have a role in controlling cGMP levels in RPE cells.

METHODS

Cell culture
Human RPE cells (D407 cell line)[19] were suspended in Dulbecco's modified Eagle's medium containing 5% fetal calf serum, 2 mM glutamine and 100 µg/ml penicillin streptomycin, at a concentration of 0.5–1.0×10⁶ viable cells/ml. Portions of the suspension (1 ml) were seeded on to 40 mm diameter

Table 1 cyclic 3'5' guanosine monophosphate fluorescence intensity in human retinal pigment epithelium cells after incubation with different phosphodiesterase inhibitors and guanylyl cyclase stimulation

Treatment	n	Grey Values			
		300–600	600–1500	1500–2700	2700–4095
Control	3	95	5	0	0
+SNP	3	87	13	0	0
+ANP	3	95	5	0	0
IBMX	3	65	24	11	0
+SNP	3	64	34	2	0
+ANP*	3	22	39	32	7
Sildenafil	3	91	9	0	0
+SNP	3	96	4	0	0
+ANP*	3	18	60	10	12
BAY 60-7550	3	99	1	0	0
+SNP	3	86	14	0	0
+ANP*	3	01	88	5	6
Sch51866	3	99	1	0	0
+SNP	3	93	7	0	0
+ANP*	3	40	46	14	0

ANP, atrial natriuretic peptide; IBMX, 3-isobutyl-1-methylxanthine; SNP, sodium nitroprusside
*$p < 0.001$ when compared with control +ANP.

plastic petridishes and incubated at 37°C in a humidified atmosphere of 95% air and 5% CO_2.

Pharmacology

Twenty four hours after seeding, the subconfluent RPE cells were incubated for 40 min in aerated Krebs buffer (pH 7.4) with or without the following compounds: 1 mM IBMX (non-specific PDE inhibitor; Sigma), 1.0 μM Bay 60–7550 (selective PDE2 inhibitor),[18] 10 μM sildenafil (selective PDE5 inhibitor) and 10 μM Sch51866 (selective PDE9 inhibitor).[13] During the last 10 min of the incubation, the cells were stimulated with100 μM of the NO donor sodium nitroprusside (SNP) or 0.1 μM atrial natriuretic peptide (ANP).

Immunohistochemistry

After fixation with 4% freshly depolymerised paraformaldehyde in the cold (4°C), the cells were washed 3×5 min, twice with TRIS-buffered saline (TBS) and once with TBS containing 0.3% Triton X-100 (TBS-T). Cells were incubated overnight at 4°C

Figure 1 Cyclic 3',5'guanosine monophosphate fluorescence intensity in human retinal pigment epithelium cells after incubation with different phosphodiesterase inhibitors and guanylyl cyclase stimulation with 0.1 μM atrial natriuretic peptide. Individual cells were grouped in defined grey value classes. Numbers are the means of three experiments (six pictures were taken per incubation in each experiment) and they express the percentage of cells in each of the four intensity classes.

with the primary antibodies. cGMP was visualised using sheep polyclonal anti-formaldehyde-fixed cGMP antiserum diluted 1:4000 in TBS-T.[20] Cells were washed for 15 min with TBS, TBS-T and TBS, respectively. The cells were then incubated with Alexa 488 conjugated donkey anti-sheep immunoglobin (Ig)G (Molecular Probes) diluted 1:100 in TBS-T for 1.5 h at room temperature. Negative controls were processed in exactly the same way, with the omission of the primary antibody. After three further washings with TBS, the cells were cover-slipped with TBS/glycerol (1:2 v/v).

Rats

Adult male Lewis rats (200–240 g) were reared under standard conditions and were cared for in accordance with the guidelines of the Association for Research in Vision and Ophthalmology Statement for the use of animals in ophthalmic and vision research. The animals were decapitated and their eyes were immediately frozen. Frozen sections of 10 μm were cut and kept at −80°C until the experiment was completed.

In situ hybridisation of PDE2, PDE5 and PDE9

In situ hybridisation was performed with digoxigenin (DIG) labelled RNA probes as described previously.[21] Frozen sections were thawed for 10 min at 50°C and thereafter fixed with 4% paraformaldehyde in 0.1 M phosphate buffer for 20 min at room temperature. The RPE cells were fixed with 4% paraformaldehyde in 0.1 M phosphate buffer for 30 min at 4°C. The samples (sections and cells) were then washed shortly with phosphate buffered saline and incubated for 10 min with 0.1 M triethanolamine containing 0.25% acetic anhydride. Samples were washed two times with 2× SSC and thereafter washed at 37°C with 2× SSC containing 50% formamide. Hybridisation was performed overnight in a humid chamber at 55°C under cover slips in 100–200 μl hybridisation mix (50% (v/v) deionised formamide, 250 μg/ml salmon sperm DNA, 1 mg/ml tRNA, 10% dextran sulphate, 2× SSC, 1× Denhardt's solution and 200 ng/ml DIG-labelled RNA probe). After hybridisation, the samples were washed in 2× SSC, 1× SSC and 0.1× SSC: all solutions containing 50% formamide. Each wash step was performed at 55°C for 20 min. Next, the samples were treated with RNAse T1 2 U/ml (Roche) in 2× SSC containing 1 mM EDTA for 15 min at 37°C, followed by a 20 min wash with 1× SSC and a 10 min wash with 2× SSC. The samples were then incubated for 5 min with buffer 1
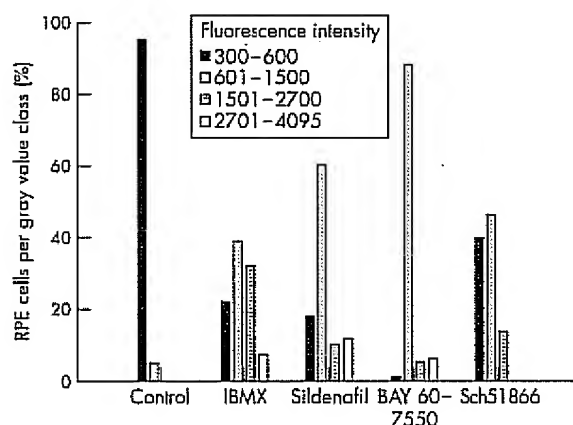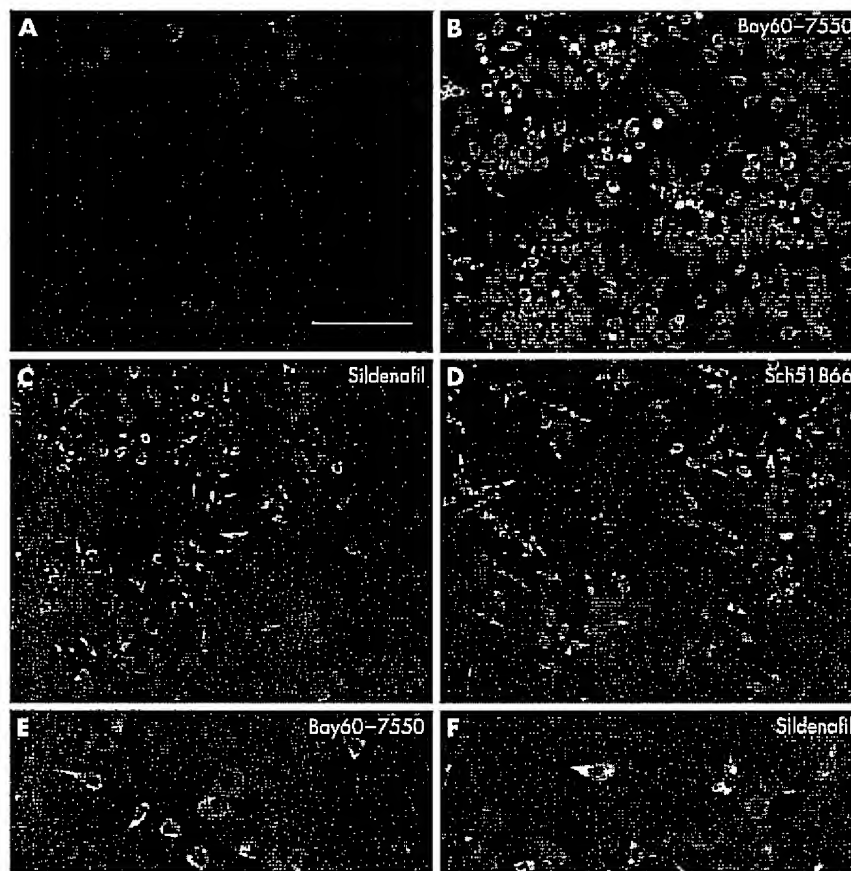
Figure 2 Cyclic 3',5'guanosine monophosphate immunoreactivity in human retinal pigment epithelium cell. (A) Without phosphodiesterase inhibition. (B, E) Combination of 1.0 µM Bay 60–7550 and 0.1 µM atrial natriuretic peptide. (C, F) Combination of 10 µM sildenafil and 0.1 µM ANP. (D) Combination of 10 µM Sch51866 and 0.1 µM ANP. Sections incubated without primary antibody show no cGMP immunoreactivity (not shown). Pictures are not taken from the same experiment. Scale bar is 100 µm in B–D 50 µm in A, E and F.

(0.15 M NaCl and 0.1 M maleic acid (pH 7.5)) followed by blocking for 2 hr at reverse transcription with buffer 2 (0.15 M NaCl, 0.1 M maleic acid (pH 7.5) and 1% blocking reagent (Roche, 1096176)) containing 5% sheep serum. Next, samples were incubated overnight with a 1:2000 dilution of anti-DIG-alkaline phosphatase (Roche) in buffer 2 containing 1% sheep serum. Samples were washed three times with buffer 1, followed by washing for 10 min with TBS containing 0.025% Tween 20 and thereafter, three times for 5 min with TBS. After two washes in buffer 3 (0.1 M TRIS–HCl (pH 9 5), 0.1 M NaCl and 0.05 M magnesium chloride), the samples were incubated with freshly prepared nitroblue tetrazolium and 5-bromo-4-chloro-3-indolyl-phosphate in buffer 4 (0.05 M TRIS (pH 9.5) 0.1 M NaCl, 6% polyvinylalcohol, 0.05 M $MgCl_2$, 1 mM levamisole) and stained overnight in the dark at 25°C. The colour reaction was stopped with 0.01 M TRIS–HCl–1 mM EDTA (pH 8.0).

Quantification of immunostainings

Immunostainings were examined using an Olympus A×70 microscope equipped with a cooled charge couple devices Olympus F-view camera. Experiments were repeated three times. From each incubation setting, six images were randomly chosen. Each image contained at least 50 RPE cells. Fluorescence intensities were converted into grey values (AnalySIS, Softimaging system) ranging from 0 (blank) to 4096 (white). After establishing a threshold setting using a blank preparation incubated with the secondary antibody only, five classes with increasing grey values were set as 0–300 (blank), 301–600, 601–1500, 1501–2700 and 2701–4096. All cells were classified according to the highest grey value they showed (table 1). The mean percentage of cells in each class was calculated for the six images taken from each incubation setting. The mean percentage was calculated for the three experiments. The distributions of the cells over the different classes were analysed using the χ^2 test.

RESULTS

Effect of PDE inhibition on cGMP levels in cultured human RPE cells

In unstimulated cells incubated without PDE inhibition, a low level of cGMP immunoreactivity was visualised in the cells (table 1; fig 2A). Hardly any differentiation in the intensity of the cGMP immunofluorescence was present. Addition of 1 mM IBMX to the incubation medium resulted in a general increase in the intensity of the cGMP immunostaining. We also observed more differentiation in the intensity of the cGMP immuno-fluorescence seen compared with the intensity after incubation without PDE inhibition (table 1).

Incubation of the cells without stimulation of sGC or pGC, although in the presence of Bay 60–7550 (PDE2 inhibitor), sildenafil (PDE5 inhibitor) and Sch51866 (PDE9 inhibitor), did not increase cGMP immunoreactivity compared with incubation without PDE inhibition (table 1).
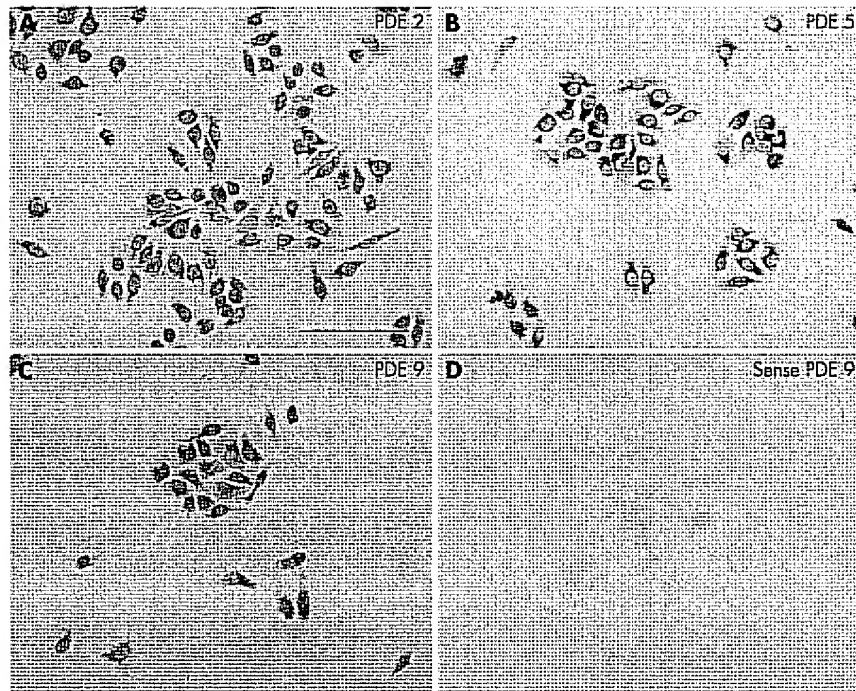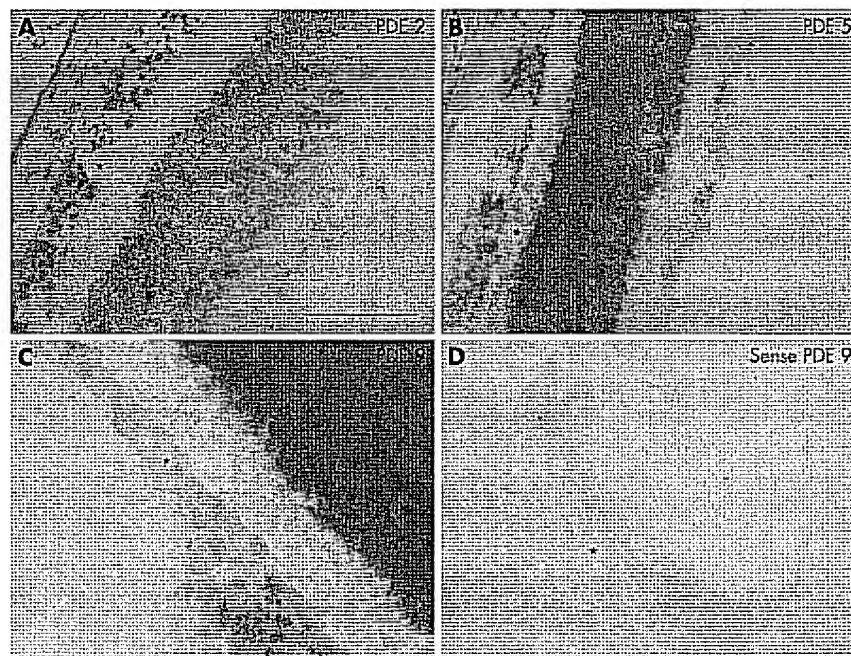
Figure 3   In situ hybridisation of phosphodiesterase PDE2, PDE5 and PDE9 in human retinal pigment epithelium cells. Localisation of (A) PDE2 mRNA, (B) Localisation of PDE5 mRNA and (C) PDE9 mRNA. (D) Hybridisation with the sense probe of PDE9. Scale bar is 100 µm.

Exposure of RPE cells to 0.1 µM ANP in combination with Bay60–7550, sildenafil or Sch51866 resulted in a strong increase in cGMP immunoreactivity in a large number of cells (figs 1 and 2). Figures 1 and 2 show that the effect of sildenafil and IBMX are quite similar, both with several cells in the highest grey value intensity class. The effect of Bay60–7550 is more homogenous in all cells, resulting in 88% of the cells in the second grey value intensity class. The distribution of GMP

Figure 4   In situ hybridisation of phosphodiesterase PDE2, PDE5 and PDE9 rat retinal pigment epithelium cell layers. Localisation of (A) PDE2 mRNA, (B) PDE5 mRNA and (C) PDE9 mRNA (D) Hybridisation with the sense probe of PDE9. *RPE cell layer. Scale bar is 100 µm in A, B and D. Scale bar is 50 µm in C.

throughout the cytoplasm is not homogeneous but seemed to be compartmentalised in many cells (fig 2). This holds true for all three PDE inhibitors. These results show that Bay 60–7550 sildenafil and Sch51866 were able to inhibit PDE activity. We found no major stimulating effect of SNP on cGMP synthesis in the presence of all three PDE inhibitors.

mRNA expression

Non-radioactive in situ hybridisation was used to study the mRNA expression patterns of PDE2, PDE5 and PDE9. RPE cells were hybridised with antisense and sense probes from these three different PDE families. In human RPE cell cultures, PDE 2, PDE5 and PDE9 mRNAs were detected in all cells, and most of the mRNA was visualised concentrated around the nucleus (fig 3). Control sections hybridised with sense probes did not show any specific staining.

Rat RPE cell layers were also hybridised with antisense and sense probes from PDE2, PDE5 and PDE9, andmRNA of PDE 2, PDE5 and PDE9 was shown to be present (fig 4). The in situ hybridisation signal was present in all RPE cells almost to the same extent. Control sections hybridised with sense probes did not show any specific staining.

DISCUSSION

We investigated the contribution of three isoforms of the PDE family of enzymes in controlling cGMP levels in human RPE cell cultures. Data obtained by using selective PDE inhibitors in combination with cGMP immunocytochemistry indicate that at least PDE 2, PDE5 and PDE9 are present in cultured human RPE cells. This was confirmed by the presence of mRNA of PDE 2, PDE5 and PDE9 in the human RPE cells and rat RPE cell layers studied by using in situ hybridisation. These three different PDE isoforms seem to be involved in controlling cGMP levels in RPE cells, as PDE10 was found not to be present in the eye.[13] Differences in mRNA expression between cells may be caused by cells being in a different cell cycle phase. Therefore, it is not surprising that a similar difference in the localisation of cGMP immunocytochemistry was observed in the cells, irrespective of the PDE inhibitor being present during the incubation.

PDE2 has an almost equal affinity for cGMP and cAMP. However, cAMP hydrolysis is greatly stimulated by low levels of cGMP.[14] The compound Bay60–7550 is a highly selective inhibitor of PDE2 and more potent than erythro-9-(2-hydroxy-3-nonyl) adenine, which is generally used as a PDE2 inhibitor.[16] In addition, in contrast to erythro-9-(2-hydroxy-3-nonyl) adenine, Bay 60–7550 is devoid of adenosine deaminase activity.[16]

PDE5 has been implicated in the control of vascular resistance.[14] Also in the retina, PDE5 was shown to have a possible role in the regulation of retinal blood flow.[20] Sildenafil, a relatively selective inhibitor for PDE5, also weakly inhibits PDE6, an enzyme involved in the process of phototransduction, with an efficacy of 1/10 of that for PDE5.[23] A single oral dose of 100 mg sildenafil causes impaired photoreceptor function, which is being attributed to weak inhibition of PDE6 by sildenafil.[24 25] To date, PDE6 is known to be present only in retinal photoreceptor cells.[14]

As PDE9 has the highest affinity for cGMP of all the mammalian PDEs, this enzyme can have a fundamental role in keeping cGMP at a low basal level.[9] In contrast with the other PDEs, PDE9 is not inhibited by IBMX.[11 13] Sch51866 is a somewhat selective inhibitor of PDE9 as it also weakly inhibits PDE5, with an efficacy of 1/15 of that for PDE9.[19] So the effect of Sch51866 on the cGMP immunoreactivity in the current study cannot be solely attributed to inhibition of PDE9.

Using in situ hybridisation, we showed the presence of PDE2, PDE5 and PDE9 mRNA in RPE cells, but this is not a quantitative technique. The immunohistochemistry data clearly show that a combination of sildenafil and ANP results in the largest percentage of cells in the highest grey value intensity class compared with other incubation settings. This may indicate a prominent role of PDE5 in cGMP breakdown in RPE cells.

The D407 cell line was shown to retain many of the metabolic and morphological characteristics of RPE cells in vivo, although there are some minor differences.[18] Given our results, it may be concluded that the expressions of PDE2, PDE5 and PDE9 are similar in the D407 cell line compared with those in rat RPE cells in vivo.

The major function for PDEs in the cell is to terminate the amplitude and duration of the cyclic nucleotide second messenger signal.[14] As shown previously, retinal detachment is associated with a decrease in the cGMP concentration in the subretinal fluid.[5] Hypoxia due to retinal detachment may cause a reduced activity of guanylyl cyclases that produce cGMP. This could lead to a reduced expression of cGMP by retinal cells after retinal detachment. By knowing the specific PDE families located in retinal cells, these enzymes could in the future become therapeutic targets to limit cGMP breakdown by using selective PDE inhibitors. Clinically, this could be important as cGMP is known for its stimulating role in the reabsorption of the subretinal fluid by activating the RPE pump.[3 4]

In conclusion, our results show that there is a complex regulation of cGMP synthesis in RPE cells. The three PDE isoforms, PDE2, PDE5 and PDE9, are involved in the breakdown of cGMP in these cells. This process of controlling cGMP levels might have a role in the regulation of fluid absorption from the subretinal space by RPE cells.

. . . .
Authors' affiliations
R M H Diederen, M Markerink-van Ittersum, J de Vente, Department of Psychiatry and Neuropsychology, European Graduate School of Neuroscience, University of Maastricht, Maastricht, The Netherlands
E C La Heij, A Kijlstra, F Hendrikse, Department of Ophthalmology, Eye Research Institute Maastricht, University Hospital Maastricht, Maastricht, The Netherlands

REFERENCES
1 Baylor DA. Photoreceptor signals and vision. Proctor lecture. Invest Ophthalmol Vis Sci 1987;28:34–49.
2 Yamazaki A, Moskvin O, Yamazaki RK. Phosphorylation by cyclin-dependent protein kinase 5 of the regulatory subunit (Pgamma) of retinal cgmp phosphodiesterase (PDE6): its implications in phototransduction. Adv Exp Med Biol 2002;514:131–53.
3 Marmor MF, Negi A. Pharmacologic modification of subretinal fluid absorption in the rabbit eye. Arch Ophthalmol 1986;104:1674–7.
4 Marmor MF. Control of subretinal fluid: experimental and clinical studies. Eye 1990;4:340–4.
5 La Heij EC, Blaauwgeers HG, de Vente J, et al. Decreased levels of cGMP in vitreous and subretinal fluid from eyes with retinal detachment. Br J Ophthalmol 2003;87:1409–12.
6 Francis SH, Corbin JD. Cyclic nucleotide-dependent protein kinases: intracellular receptors for cAMP and cGMP action. Crit Rev Clin Lab Sci 1999;36:275–328.
7 Beavo JA, Conti M, Heaslip RJ. Multiple cyclic nucleotide phosphodiesterases. Mol Pharmacol 1994;46:399–405.
8 Gillespie PG, Beavo JA. Characterization of a bovine cone photoreceptor phosphodiesterase purified by cyclic GMP-sepharose chromatography. J Biol Chem 1988;263:8133–41.
9 Thomas MK, Francis SH, Corbin JD. Characterization of a purified bovine lung cGMP-binding cGMP phosphodiesterase. J Biol Chem 1990;265:14964–70.
10 Sonnenburg WK, Mullaney PJ, Beavo JA. Molecular cloning of a cyclic GMP-stimulated cyclic nucleotide phosphodiesterase cDNA. Identification and distribution of isozyme variants. J Biol Chem 1991;266:17655–61.

11 Fisher DA, Smith JF, Pillar JS, *et al.* Isolation and characterization of PDE9A, a novel human cGMP-specific phosphodiesterase. *J Biol Chem* 1998;19:15559–64.

12 Fujishige K, Kotera J, Michibata H, *et al.* Cloning and characterization of a novel human phosphodiesterase that hydrolyzes both cAMP and cGMP (PDE10A). *J Biol Chem* 1999;274:18438–45.

13 Soderling SH, Bayuga SJ, Beavo JA. Isolation and characterisation of a dual-substrate phosphodiesterase gene family: PDE10A. *Proc Natl Acad Sci USA* 1999;96:7071–6.

14 Beavo JA. Cyclic nucleotide phosphodiesterases: functional implications of multiple isoforms. *Physiol Rev* 1995;75:725–48.

15 Kurtz MJ, Edwards RB, Schmidt SY. Cyclic nucleotide phosphodiesterases in cultured normal and RCS rat pigment epithelium: kinetics of cyclic AMP and cyclic GMP hydrolysis. *Exp Eye Res* 1987;45:67–75.

16 Miller S, Farber D. Cyclic AMP modulation of ion transport across frog retinal pigment epithelium. Measurements in the short-circuit state. *J Gen Physiol* 1984;83:853–74.

17 Sanyal A, Fletcher R, Liu YP, *et al.* Cyclic nucleotide content and phosphodiesterase activity in de rds mouse (020/A) retina. *Exp Eye Res* 1984;38:247–56.

18 Boess FGHM, Hendrix M, van der Staay FJ, *et al.* Inhibition of phosphodiesterase 2 increases cGMP neuronal plasticity and memory performance. *Neuropharmacology* 2004;47:1081–92.

19 Davis AA, Bernstein PS, Bok D, *et al.* A human retinal pigment epithelial cell line that retains epithelial characteristics after prolonged culture. *Invest Ophthalmol Vis Sci* 1995;36:955–64.

20 De Vente J, Steinbusch HW. On the stimulation of soluble and particulate guanylate cyclase in the rat brain and the involvement of nitric oxide as studied by cGMP immunocytochemistry. *Acta Histochem* 1992;92:13–38.

21 Van Staveren WC, Steinbusch HW, Markerink-Van Ittersum M, *et al.* mRNA expression patterns of the cGMP-hydrolyzing phosphodiesterases types 2, 5, and 9 during development of the rat brain. *J Comp Neurol* 2003;467:566–80.

22 Poche M, Meyer P, Prünte C, *et al.* Sildenafil induces retinal vasodilatation in healthy subjects. *Br J Ophthalmol* 2002;86:156–8.

23 Ballard SA, Gingell CJ, Tang K, *et al.* Effects of sildenafil on the relaxation of human corpus cavernosum tissue in vitro and on the activities of cyclic nucleotide phosphodiesterase isozymes. *J Urol* 1998;159:2164–71.

24 Vobig MA, Klotz T, Staak M, *et al.* Retinal side-effects of sildenafil. *Lancet* 1999;353:375.

25 Vobig MA. Retinal side-effects of sildenafil. *Lancet* 1999;353:1442.

The role of phosphodiesterase isoforms 2, 5, and 9 in the regulation of NO-dependent and NO-independent cGMP production in the rat cervical spinal cord

J. de Vente [a,*], M. Markerink-van Ittersum [a], J.S.H. Vles [b]

[a] European Graduate School of Neuroscience (EURON), Maastricht University, Department of Psychiatry and Neuropsychology, UNS50, POB 616, 6200 MD Maastricht, The Netherlands
[b] Department of Neurology, University Hospital Maastricht, 6202 AZ Maastricht, The Netherlands

Abstract

NO-responsive, cGMP-producing structures are abundantly present in the cervical spinal cord. NO-mediated cGMP synthesis has been implicated in nociceptive signaling and it has been demonstrated that cGMP has a role establishing synaptic connections in the spinal cord during development. As cGMP levels are controlled by the activity of soluble guanylyl cyclase (synthesis) and the phosphodiesterase (PDE) activity (breakdown), we studied the influence of PDE activity on NO-stimulated cGMP levels in the rat cervical spinal cord.

cGMP-immunoreactivity (cGMP-IR) was localized in sections prepared from slices incubated in vitro. A number of reported PDE isoform-selective PDE inhibitors was studied in combination with diethylamineNONOate (DEANO) as a NO-donor including isobutyl-methylxanthine (IBMX) as a non-selective PDE inhibitor. We studied 8-methoxy-IBMX as a selective PDE1 inhibitor, erythro-9-(2-hydroxy-3-nonyl)adenine (EHNA) and BAY 60-7550 as selective PDE2 inhibitors, sildenafil as a selective PDE5 inhibitor, dipyridamole as a mixed type PDE5 and PDE10 inhibitor, rolipram as a PDE4 inhibitor, and SCH 81566 as a selective PDE9 inhibitor. cGMP-IR structures (nerve fibers, axons, and terminals) were characterized using the following neurochemical markers: vesicular transporter molecules for acetylcholine, GABA, and glutamate (type 1 and type 2), parvalbumin, glutamate transporter molecule EAAT3, synaptophysin, substance P, calcitonin gene-related peptide, and isolectin B4. Most intense cGMP-IR was observed in the dorsal lamina. Ventral motor neurons were devoid of cGMP-IR. cGMP-IR was observed in GABAergic, and glutamatergic terminals in all gray matter laminae. cGMP-IR was abundantly colocalized with anti-vesicular glutamate transporter 2 (vGLUT2), however not with the anti-vesicular glutamate transporter 1 (vGLUT1), suggesting a functional difference between structures expressing vGLUT1 or vGLUT2. cGMP-IR did not colocalize with substance P- or calcitonin-gene related peptide-IR structures, however did partially colocalize with isolectin B4 in the dorsal horn. cGMP-IR in cholinergic structures was observed in dorsal root fibers entering the spinal cord, occasionally in laminae 1–3, in laminae 8 and 9 in isolated boutons and in the C-type terminals, and in small cells and varicosities in lamina 10. This latter observation suggests that the proprioceptive interneurons arising in lamina 10 are also NO-responsive.

No region-specific nor a constant co-expression of cGMP-IR with various neuronal markers was observed after incubation of the slices with one of the selected PDE inhibitors. Expression of the mRNA of PDE2, 5, and 9 was observed in all lamina. The ventral motor neurons and the ependymal cells lining the central canal expressed all three PDE isoforms.

Incubation of the slices in the presence of IBMX, DEANO in combination with BAY 41-2272, a NO-independent activator of soluble guanylyl cyclase, provided evidence for endogenous NO synthesis in the slice preparations and enhanced cGMP-IR in all lamina. Under these conditions cGMP-IR colocalized with substance P in a subpopulation of substance P-IR fibers.

It is concluded that NO functions as a retrograde neurotransmitter in the spinal cord but that also postsynaptic structures are NO-responsive by producing cGMP. cGMP-IR in a subpopulation of isolectin B4 positive fibers and boutons is indicative for a role of NO-cGMP signaling in nociceptive processing. cGMP levels in the spinal cord are controlled by the concerted action of a number of PDE isoforms, which can be present in the same cell.
© 2006 Elsevier B.V. All rights reserved.

Keywords: Nitric oxide; cGMP; Phosphodiesterase; Spinal cord; Micropharmacology; Nociception

---

* Corresponding author. Tel.: +31 43 3881022; fax: +31 43 3761096.
E-mail address: j.devente@np.unimaas.nl (J. de Vente).

1. Introduction

NO has an important messenger function in the nervous system of probably all animals species (Alonso et al., 2000; Scholz and Truman, 2000). NO synthesis is catalyzed by the enzyme nitric oxide synthase (NOS). In the mammalian central nervous system, the constitutively expressed neuronal isoform of the enzyme (nNOS) has a wide-spread localization and can be observed in virtually every (sub)region. Nevertheless, there are large differences in the amount of NOS expressed in the various regions of the CNS (Bredt et al., 1990; Vincent and Kimura, 1992; Southam and Garthwaite, 1993; De Vente et al., 1998). The target molecule for NO is the so-called soluble isoform of guanylyl cyclase sGC (Murad, 1994), also designated $NO_{GC}R$ (Denninger and Marletta, 1999; Friebe and Koesling, 2003; Koesling et al., 2004).

NO-independent cGMP signaling can occur through activation of the receptor-operated, membrane-bound particulate GC (pGC) by natriuretic peptides (Tamura et al., 2001) (see the accompanying paper by De Vente et al.). In addition, compounds like YC-1 (Wu et al., 1995a, 1995b) and BAY 41-2272 and related compounds (Becker et al., 2001; Stasch et al., 1991) are NO-independent activators of sGC and potentiate the action of NO on the enzyme. It has been proposed that these compounds can be used to sense endogenous NO production (Ott et al., 2004; Van Staveren et al., 2005).

NO-cGMP signaling in the brain has been observed in virtually every region of the brain (e.g. Southam and Garthwaite, 1993; De Vente et al., 1998). Less data are available on NO-cGMP signaling in the spinal cord. Using in vitro experiments with spinal cord slices NO-mediated cGMP production was demonstrated throughout the gray matter of the spinal cord (Vles et al., 2000). These experiments were all performed in the presence of isobutyl-methylxanthine (IBMX) as a non-specific phosphodiesterase (PDE) inhibitor in order to inhibit cGMP hydrolysis, as PDE activity in neural tissue is high, and it is almost impossible to localize the sites of synthesis of cGMP by means of cGMP-immunocytochemistry (cGMP-ICC) without inhibiting PDE activity. Presently, 11 subfamilies of PDE's are known. Subfamilies have been classified on the basis of structural data, and on the basis of substrate and inhibitor profiles (Beavo, 1995; Conti and Jin, 1999; Francis et al., 2001). PDE's which are important in controlling cGMP metabolism in the CNS are PDE1, PDE2, PDE5, PDE6, PDE9, and PDE10. Of these, PDE6 is only present in the retina (Beavo, 1995). Specific isoforms of the PDE's show a selective regional localization in the brain and it has become evident that several PDE isoforms can be expressed in the same cell (Juilfs et al., 1997; Andreeva et al., 2001; Bellamy and Garthwaite, 2001; Van Staveren et al., 2003).

There is evidence that cGMP is involved in (anti)nociceptive processing in the spinal cord (Kitto et al., 1992; Siegan et al., 1996; Inoue et al., 1998; Ferreira et al., 1999; Tegeder et al., 2004). It has been demonstrated that during development cGMP is involved in patterning of the sensory input into the spinal cord and also in synaptic arrangements in the gray matter (Inglis et al., 1998; Schmidt et al., 2002). As cGMP levels are controlled by PDE activity, and there is no information on the cellular localization of PDE's in the spinal cord, we investigated the localization of the mRNA of the cGMP-hydrolyzing PDE's2, 5, and 9. In addition, in an attempt to study the contribution of these three PDE's to NO-cGMP signaling in the spinal cord, we investigated the effects of a number of PDE inhibitors of different selectivity on the localization of NO-mediated cGMP synthesis in the slices of the rat cervical spinal cord and attempted to characterize the cGMP-immunoreactive (cGMP-IR) structures in terms of known neurotransmitters in the spinal cord.

2. Materials and methods

2.1. Materials

DiethylamineNONOate (DEANO), dipyridamole, erythro-9-(2-hydroxy-3-nonyl)adenine (EHNA), N^ω-nitro-L-arginine (L-NAME), isobutyl-methyl-xanthine, 8-methoxy-IBMX, and TRITC-conjugated isolectin B4 were from Sigma–Aldrich. Rolipram was from RBI. 1H-[1,2,4]oxadiazolo[4,3-a]-quinoxalin-1-one (ODQ) was from Tocris Cookson Ltd. Sildenafil was a gift of Pfizer, Sandwich, UK. SCH 51866 was a gift of Schering-Plough, Kenilworth, NJ, USA. 5-Cyclopropyl-2-[1-(2-fluoro-benzyl0-1H-pyrazolo[3,4-b]pyridin-3-yl]-pyrimidin-4-ylamine (BAY 41-2272) and 2-(3,4-dimethoxybenzyl)-7-{(1R)-1-[(1R)-1-hydroxyethyl]-4-phenylbutyl}-5-methyl-imidazo[5,1-f][1,2,4]triazin-4(3H)-one (BAY 60-7550) were gifts of Bayer, Wuppertal, Germany. Rabbit antibodies: anti-parvalbumin was a gift of P.C. Emson (Cambridge, UK); anti-neuronal glutamate transporter (EAAT3) (Furuta et al., 1997) was a gift of J.D. Rothstein (Baltimore, MD, USA); antiserum against the β1-subunit of sGC was from S. Behrends (Toronto, Canada) (Behrends et al., 2001); anti-vesicular acetylcholine transporter (vAChT) was from Phoenix Pharmaceuticals; anti-synaptophysin from Chemicon; anti-substance P (SP) from Santa Cruz Biotechnology; anti-CGRP from Calbiochem; anti-vesicular GABA transporter (vGAT), anti-vesicular glutamate transporter 1 (vGLUT1), and anti-vesicular glutamate transporter 2 (vGLUT2) were from Synaptic Systems. Anti-formaldehyde-fixed-cGMP serum (De Vente et al., 1987; Tanaka et al., 1997) was raised in sheep. Alexa Fluor 488 donkey anti-sheep and Alexa Fluor 594 donkey anti-rabbit IgG conjugates were from Invitrogen. Donkey anti-sheep FITC conjugate and donkey anti-rabbit CY-3 conjugate were obtained from Jackson.

2.2. Animals

Male Lewis rats (aged three to four months) were reared under standard conditions at the local animal facility. Experiments were approved by the University committee on animal welfare according to Dutch governmental rules.

2.3. In vitro incubation of spinal cord slices

Animals were decapitated and the cervical and thoracal spinal column was removed within 1 min, and put in ice-cold aerated Krebs buffer. The spinal cord was dissected out and the meninges were carefully removed. This procedure took approximately 5 min. The tissue was kept constantly under ice-cold areated Krebs buffer of the following composition: 121.1 mM NaCl, 1.87 mM KCl, 1.17 mM KH_2PO_4, 1.15 mM $MgSO_4$, 26.2 mM $NaHCO_3$, 2.0 mM $CaCl_2$ and 11.0 mM glucose, aerated with 95% O_2 and 5% CO_2 (carbogen) at pH 7.4.

The caudal side of the cervical spinal cord was glued onto a support with superglue and supported by a block of agar. Transverse slices (400 μm) were cut of the cervical spinal cord while submerged in Krebs buffer as described above, under controlled temperature of 4 °C and constant aeration with carbogen. Cutting was performed using an Integra-slicer 7550 PSDS (Campden Instruments) equipped with a ceramic knife.

Longitudinal slices (400 μm) were prepared using a McIlwain tissue chopper (The Miccle Engineering Company Ltd.). The slices were separated from each other while submerged in ice-cold Krebs buffer as described above.

After sectioning, slices were equilibrated in Krebs buffer bubbled with carbogen at room temperature for 15 min and then transferred into incubation wells and incubated for 40 min, while the temperature was slowly raised till 35.5 °C, in Krebs buffer in the presence or absence of PDE inhibitors under an atmosphere of carbogen. The final 10 min of incubation were in the presence of the NO-donor diethylamineNONOate (DEANO). NO-independent stimulation of sGC was investigated with BAY 41-2272 and this compound was present during the last 25 min of the incubation period. DEANO and IBMX were dissolved in Krebs buffer. The PDE inhibitors, ODQ and BAY 41-2272 were dissolved in dimethylsulfoxide (DMSO), resulting in a final concentration of 0.5% DMSO during the incubation. A similar concentration of DMSO was used in the appropriate controls. This concentration of DMSO has no measurable effect on cGMP levels in the spinal cord.

It has to be noted that our approach using spinal cord slices incubated in vitro leads to a comparison of drug effects in regions of the spinal cord that are not strictly the same as each experimental condition has to be tested in a separate slice. All PDE inhibitors were tested initially at three different concentrations: 1, 10, and 100 μM (BAY 60-7220 at 0.01, 0.1, 1.0, 10, and 100 μM). Each PDE inhibitor was studied in four to six experiments (indicated in the tables) at the next higher concentration than the concentration that in combination with DEANO resulted in an observable cGMP-IR in the sections. This procedure was adopted in an attempt to minimize interaction of the selective PDE inhibitors with other PDE's, as it is known that at high concentrations the PDE inhibitors tend to become unselective (e.g. Bellamy and Garthwaite, 2001). Selectivity data on the PDE inhibitors used is presented in Table 8.

As a control, one slice with 1 mM IBMX in combination with 100 μM DEANO was included in all experiments. In addition, in each experiment we included a slice incubated in the presence of the PDE inhibitor under study without DEANO.

2.4. Immunocytochemistry

After the incubation period, slices were fixed with an ice-cold fixative solution of 4% freshly prepared depolymerised paraformaldehyde in 0.1 M phosphate buffer (pH 7.4) for 30 min at 4 °C. Thereafter, slices were fixed for another 90 min with 4% formaldehyde containing 10% sucrose. After washing at 4 °C in 0.1 M phosphate buffer (pH 7.4) containing 10% sucrose for at least 30 min, slices were aligned in a plane and snap-frozen with CO_2 in Tissue-Tek O.C.T. compound (Sakura Finetek). Cryostat sections (10 μm) were cut and thawed onto laboratory-prepared chrome-alumn/gelatin coated slides and stored at −20 °C, or processed for immunocytochemistry.

Frozen sections were dried for 20 min at room temperature, followed by three 5 min washes with 0.1 M Tris-buffered saline, pH 7.4 (TBS). No blocking steps were included in immunostaining protocols. Incubation of the sections with the antibodies was done using two different protocols. Sections incubated with primary antibodies that were to be combined with donkey anti-sheep FITC conjugate (1:50) or donkey anti-rabbit CY-3 conjugate (1:800), were incubated overnight at 4 °C with the primary antibodies diluted in TBS containing 0.3% Triton X-100 (TBS-T). These secondary antibodies were diluted in TBS-T.

The Alexa Fluor 488 and Alex Fluor 594 cannot be used in TBS-T as we found that the Triton-X-100 unmasks an epitope in myelin which cross-reacts with the Alexa antibodies (see also Weruaga et al., 1998). In combination with the Alexa Fluors (1:100) we incubated the sections with primary and secondary antibodies diluted in TBS only. Incubations with the primary antibodies were 72 h at 4 °C, secondary antibodies were incubated for 2 h at room temperature, and the in-between washing protocols lasted 2 h each.

Dilutions of the primary antibodies were as follows: sheep anti-formaldehyde-fixed-cGMP (1:4000) (Tanaka et al., 1997); rabbit anti-vesicular acetylcholine transporter (1:2000); rabbit anti-parvalbumin (1:1500); rabbit anti-glutamate transporter (EAAT3, 1:300); rabbit anti-synaptophysin antibody (1:1000); rabbit anti-substance P (1:1000); rabbit anti-CGRP (1:3000); rabbit anti-vGAT (1:1500); rabbit anti-vGLUT1 (1:1000); and rabbit anti-vGLUT2 (1:1000); rabbit anti-β1 subunit antiserum (1:2000). TRITC-conjugated isolectin B4 (IB4) was used in a dilution of 1:500. After washing, the sections were mounted with TBS-glycerol (1:3, v/v).

As a control on the immunostainings we always incubated sections without the primary antibodies but in combination with the secondary antibodies used. Preabsorbtion studies with the cGMP-antibody have been reported repeatedly (see Tanaka et al., 1997).

2.5. In situ hybridization

2.5.1. Probe preparation

For the in situ hybridization of PDE2, a pBS+ vector containing a portion of rat PDE2 (nt 1964-2314, GenBank accession no. NM_031079) was used. This construct (GenBank accession no. M94540) and the specificity of the probe has been previously described (Repaske et al., 1993).

The expression of PDE5 was studied by cloning a part of the rat PDE5 sequence (nt 2206-2580, GenBank accession no. D89093) into the SacI and EcoRI sites of a pCRIITOPO vector (Invitrogen). A probe comprising this part of PDE5 has been earlier described (Kotera et al., 1997).

PDE9 riboprobes were constructed from the mouse PDE9A1 as a template (Van Staveren et al., 2002).

All constructs were analyzed by DNA sequencing before probe synthesis. After restriction digestion of each construct, as described above, antisense and sense riboprobes were made from 5 μg DNA template by in vitro transcription with digoxigenin (DIG) labeled UTP using a DIG RNA labeling kit (Roche) according to the manufacturer's instructions.

2.5.2. Hybridization procedures

Animals were decapitated and their spinal cords were dissected, frozen in CO_2 and stored at −80 °C until sectioning. Frozen serial sagittal sections (14 μm) were cut and thawed onto SuperFrost Plus slides (Menzel-Gläser) and stored at −80 °C until use. Three animals were studied and from each animal consecutive sections were used for hybridization of PDE2, PDE5 and PDE9 with sense and antisense probes, exactly as described previously (Van Staveren et al., 2003). These experiments were repeated three times.

2.6. Microscopy

Sections were examined using an Olympus AX70 microscope equipped with an Olympus F-view cooled CCD camera. For the epifluorescence detection we used a narrow band pass MNIBA filter for Alexa Fluor 488 in combination with a narrow beam excitation filter U-M41007A for the detection of Alexa Fluor 594 (both filters are from Chroma Technologies). This filter combination prevented bleeding of the Alexa Fluors (see Fig. 1). Images were initially stored as 16 bits images and gray values were reduced to 4095 using a linear function (analySIS vers.3.0 software, Soft Imaging System). Color images were obtained by merging the corresponding black and white images. For use in the Adobe Photoshop 7.0.1, the images were converted to 8 bits images and the number of gray values reduced to 265.

3. Results

3.1. Non-specific PDE inhibition using IBMX

cGMP-IR in slices of the cervical spinal cord incubated in vitro was virtually absent if no PDE inhibitor was present (Fig. 2(a)). Addition of 1 mM IBMX resulted in the appearance of cGMP-IR in varicosities and fibers in the gray matter of the slices, especially in lamina 1–3 (Fig. 2(b)). The effect of IBMX could be inhibited by 10 μM ODQ or 0.1 mM L-NAME. These results suggest ongoing NO synthesis in the spinal cord slices (see also the section on the effects of BAY 41-2272). Addition of 100 μM DEANO to the slices in the presence of 1 mM IBMX resulted in abundant cGMP-IR throughout the gray matter, and in glial somata and ramifications in the white matter (Fig. 2(c)).
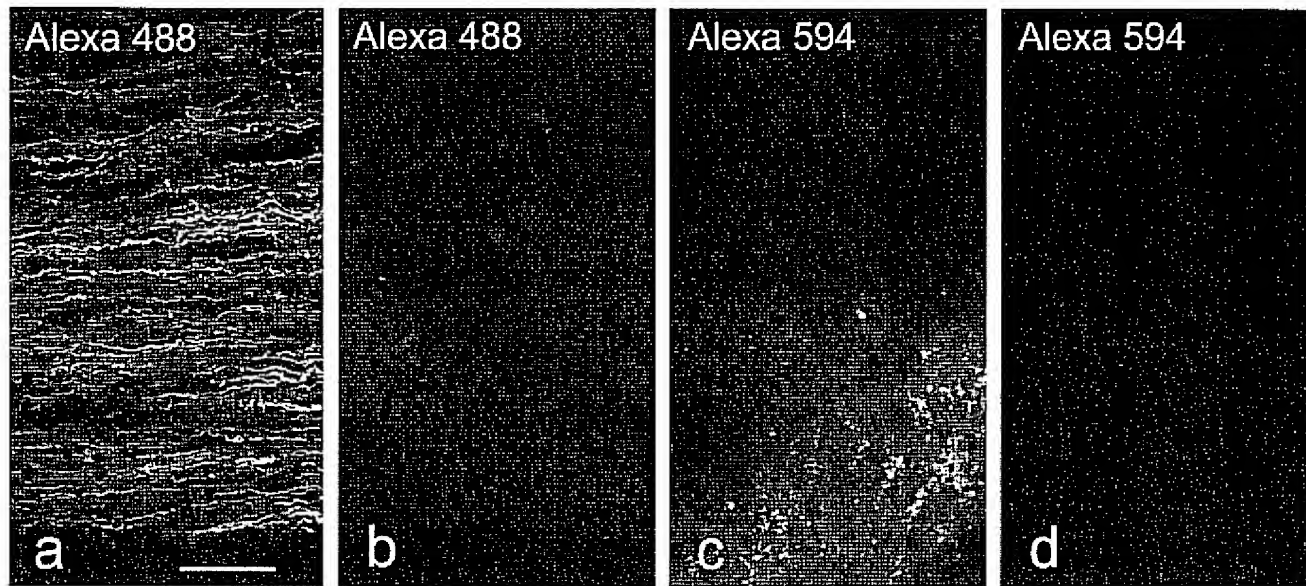
Fig. 1. Absence of bleed-through with the optical filters used in this study for the fluorescence of the secondary antibodies used; (a) cGMP-immunofluorescence using Alexa Fluor 488 through the band pass MNIBA filter (longitudinal slice); (b) same specimen as in (a): fluorescence of Alexa Fluor 488 through the U-M41007A filter; (c) CGRP-immunofluorescence using Alexa Fluor 594 through the U-M41007A filter (transverse slice); and (d) same specimen as in (c): fluorescence of Alexa Fluor 594 through the MNIBA filter. Bar represents 50 μm.

Characterization of the cGMP-IR structures after incubation of the slices in the presence of IBMX and DEANO, revealed that cGMP-IR colocalized to some extent with synaptophysin in all lamina of the gray matter (Fig. 3(a–f)). Colocalization between cGMP-IR and EAAT3 was observed only in layers 1 and 2 (Figs. 3(g–I) and 12(d–f)). cGMP-IR was also observed in a subpopulation of parvalbumin-positive cells and fibers in the gray matter (see Vles et al., 2000). In addition, cGMP-IR was observed in the large cholinergic boutons surrounding the motor neurons in laminae 8 and 9 (Fig. 3(j)) and in varicose fibers in lamina 10 surrounding the central canal (see Vles et al., 2000). cGMP-IR did not colocalize with substance P (Fig. 4) or

with CGRP (Fig. 5) in all laminae. Nevertheless, it was remarkable that cGMP-IR fibers ran often closely parallel to SP- (Fig. 4(d–f)) or CGRP-IR (Fig. 5(d)) fibers. A subpopulation of fibers and boutons that stained with IB4 were cGMP-IR (Fig. 5(e–j)). These data are summarized in Table 1.

3.2. PDE1 inhibition using 8-methoxy-IBMX

8-Methoxy-IBMX (8-Met-IBMX) has been described as a selective inhibitor of PDE1 (Loughney et al., 1996; Yu et al., 1997). Stimulation of cGMP synthesis by DEANO in the presence of 100 μM 8-Met-IBMX resulted in the appearance of
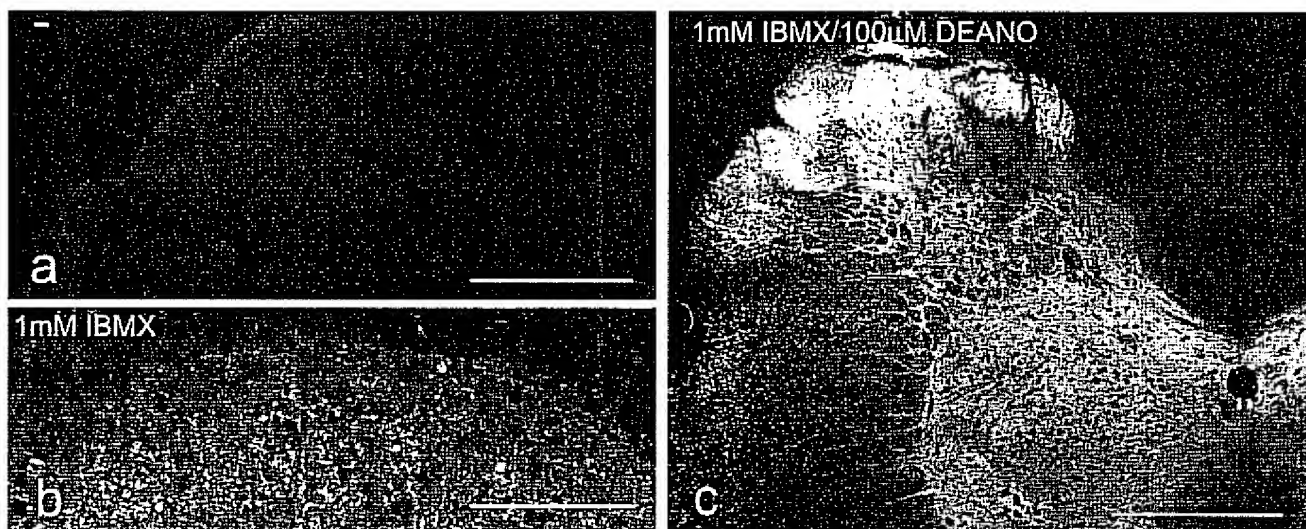
Fig. 2. Effect of IBMX on the localization of cGMP-IR in the cervical spinal cord. Slices were incubated in absence of drugs (a); in the presence of 1 mM IBMX (b); and in the combined presence of 1 mM IBMX and 100 μM DEANO (c). Bars indicate 500 μm in (a and c), and 100 μm in (b).
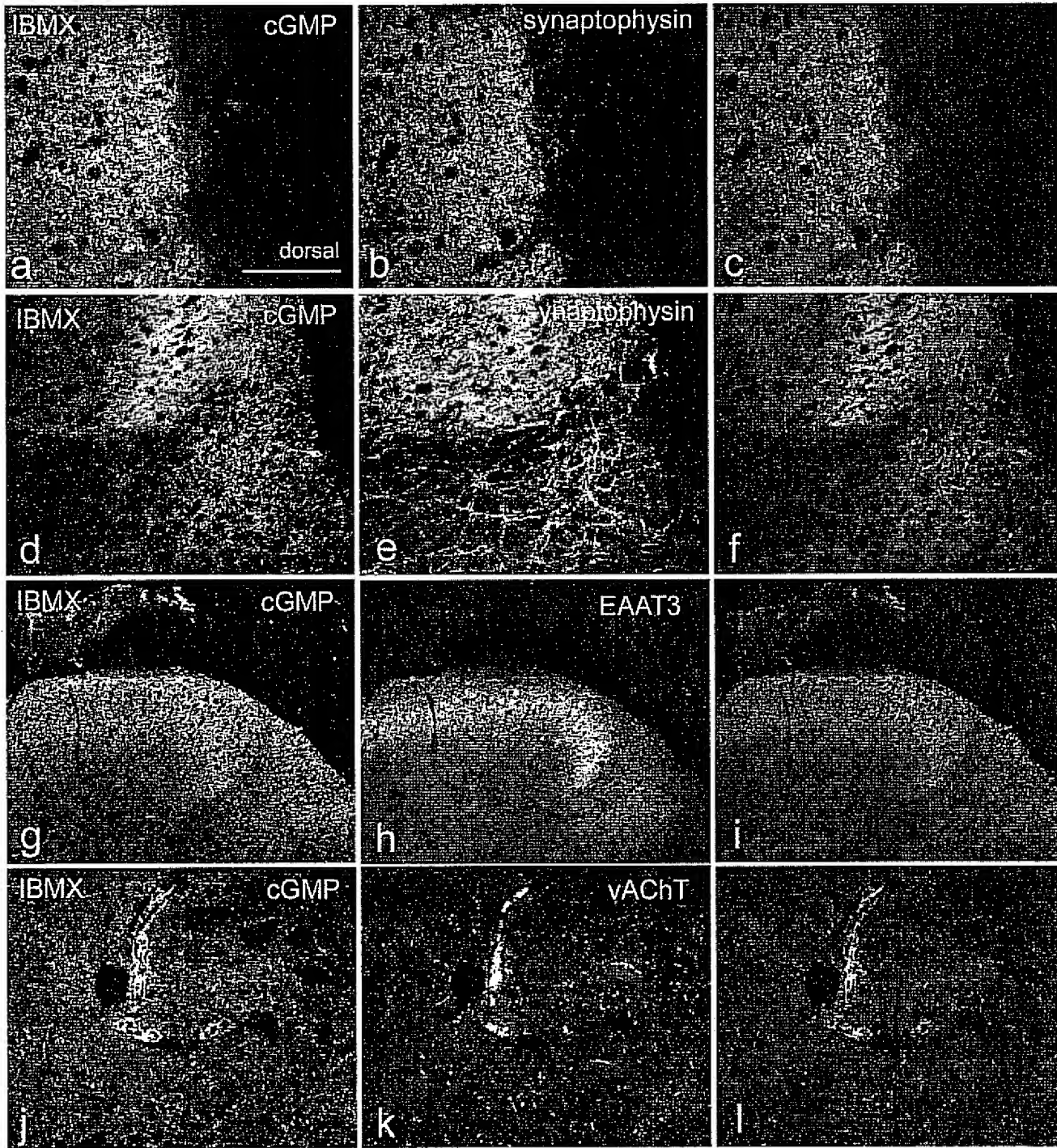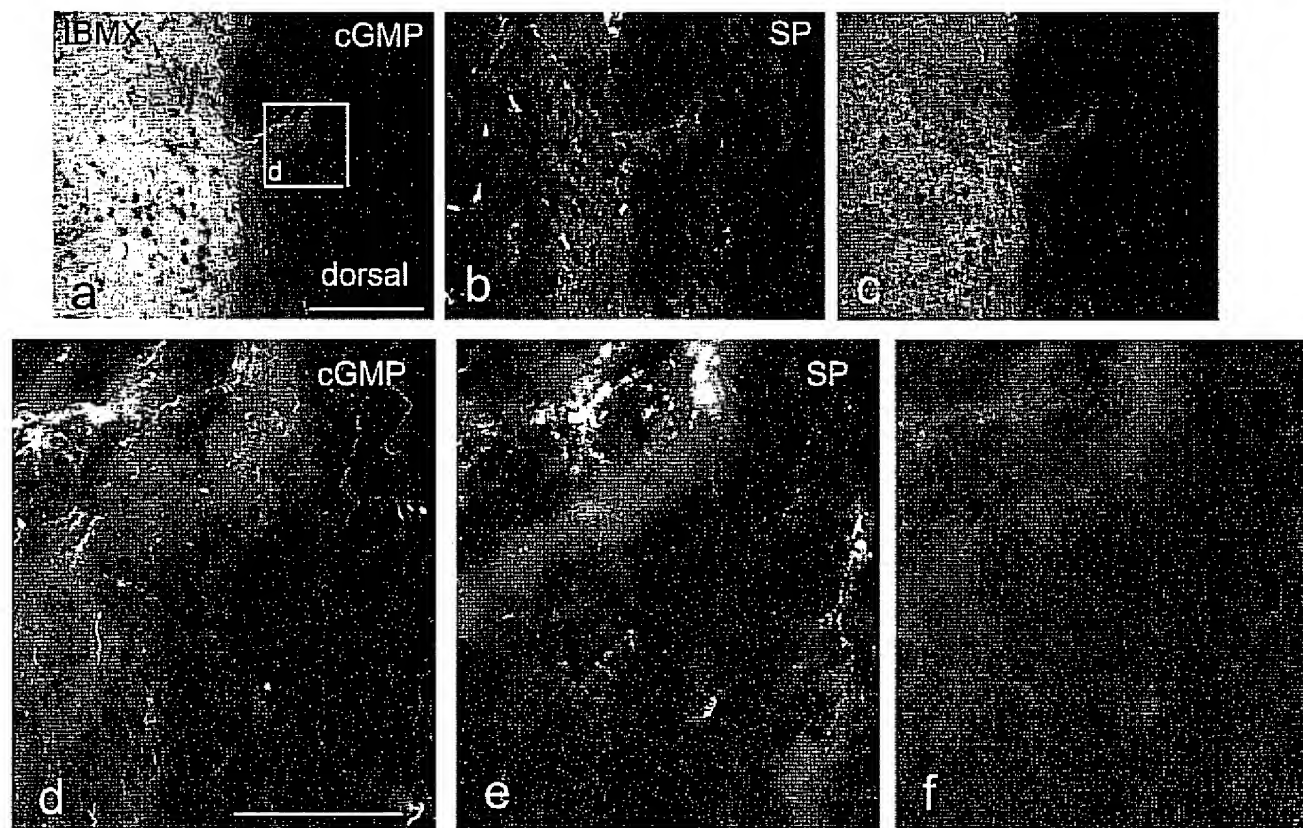
Fig. 3. Effect of IBMX on the localization of cGMP-IR in the cervical spinal cord. Slices were incubated in the presence of 1 mM IBMX and 100 μM DEANO. The section shown in (a–c) is from a longitudinal slice; all other sections are from transverse slices. Sections (a) and (d) were double-immunostained for cGMP-IR and synaptophysin (b and e) showing extensive colocalization; section (g) was double-immunostained cGMP-IR and EAAT3 (h) and (i) showing very little colocalization; section (j) shows colocalization of cGMP-IR with vAChT in the ventral horn in varicosities and C-terminals. Bar in (a) represents 100 μm for (a–f); bar in (g) represents 200 μm, also for (h); bar in (i) represents 50 μm also for (j).

cGMP-IR in the same structures as observed when using IBMX (Fig. 6). cGMP synthesis was stimulated in varicose fibers throughout the gray matter and was clearly visible in the large cholinergic boutons (C-terminals) surrounding the motor neurons in the ventral horn (Fig. 6(b)). In addition, cGMP-IR was observed in cell somata which are positioned between the ependymal cells of the central canal and the gray matter of layer 10 (Fig. 6(c)). These cells often show finger-like protrusions through the ependymal cell layer making contact with the lumen of the central canal (arrow in Fig. 6(c)).

Fig. 4. Effect of IBMX on the localization of cGMP-IR in the cervical spinal cord. Slices were incubated in the presence of 1 mM IBMX and 100 μM DEANO. Sections were double-immunostained for cGMP-IR and SP ((a–c), from a longitudinal slice). There is no colocalization between cGMP-IR and SP. The boxed area in (a) is shown enlarged in (d) using a 40× objective. Bar in (a) represents 100 μm for (a–c); and bar in (d) represents 50 μm for (d–f).

3.3. PDE2 inhibition using EHNA or BAY 60-7550

Bay 60-7550 is a highly selective PDE2 inhibitor (Boess et al., 2004). At a concentration of 1 μM, the presence of this compound in combination with DEANO resulted in strong cGMP-IR in all gray matter layers and in fiber tracts and dot-like structures in the white matter. Colocalization studies gave the same results as described under EHNA. Colocalization betweeen cGMP-IR and synaptophysin was prominent in the dorsal and ventral horn, and in fibers running through the ventral white matter (Fig. 7(a–f)). C-terminals showed cGMP-IR frequently when using BAY 60-7550 as a PDE inhibitor. These results are summarized in Table 2.

Until recently EHNA was the only available selective inhibitor of PDE2. In the presence of 100 μM EHNA, DEANO stimulates cGMP synthesis strongly in varicose fibers of the ventral horn (Fig. 7(g–i)) and in the dorsal horn (Fig. 7(j–l)). In addition, cGMP-IR is visualized in the neuropil of all layers of the gray matter. cGMP-IR was also observed in the white matter where it appeared as a dot-like staining. cGMP-IR colocalized

partly with the EAAT3 immunostaining, especially in varicosities in the dorsal horn (Fig. 7(j–l)) but never in the cell somata. This colocalization was minor in the ventral horn (not shown). Using EHNA as a PDE inhibitor, cGMP-IR was observed in parvalbumin-immunopositive structures in the dorsal horn (Fig. 12(g–I)) but was almost totally absent in the ventral horn (Fig. 7(g–I)). Synaptophysin was observed to colocalize with cGMP-IR in the dorsal and ventral horn. In addition, we found synaptophysin to be present in the large cholinergic boutons around the motor neurons and a few of the boutons were also cGMP-immunoreactive (not shown). These observations are summarized in Table 3.

3.4. PDE5 inhibition using dipyridamole or sildenafil

Dipyridamole inhibits PDE5 and PDE10 (Lugnier et al., 1986; Soderling et al., 1999; Fujishige et al., 1999a, 1999b). In combination with DEANO a strong stimulation of cGMP synthesis is observed in layers 1 and 2 of the dorsal horn, and to a lesser extent in the other gray matter layers. Contrary to the

Fig. 5. Effect of IBMX on the localization of cGMP-IR in the rat cervical spinal cord. Slices were incubated in the presence of 1 mM IBMX and 100 μm DEANO. Sections were double-immunostained for cGMP-IR with CGRP ((a-c), from (a) longitudinal slice) and with IB4 ((e-g), from a longitudinal slice; (h-j), from a transverse slice). There is no colocalization between cGMP-IR and CGRP. The boxed area in (c) is shown enlarged in (d) using a 40× objective. There is colocalization between cGMP-IR and IB4 in subpopulations of fibers (e.g. arrows in (j)) and boutons. Bar in (a) represents 100 μm for (a-c) and (e-g); bar in (d) represents 25 μm; bar in (j) represents 50 μm in (h-j).
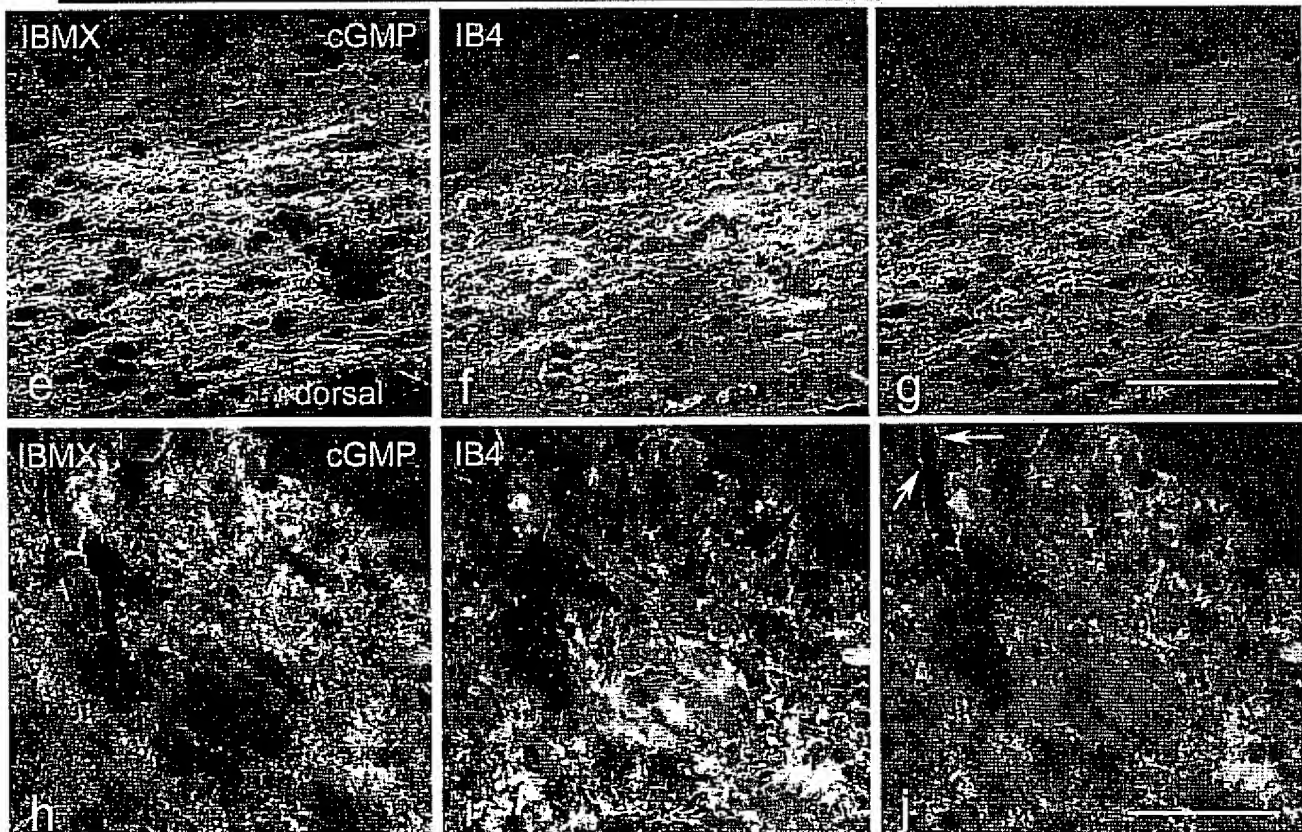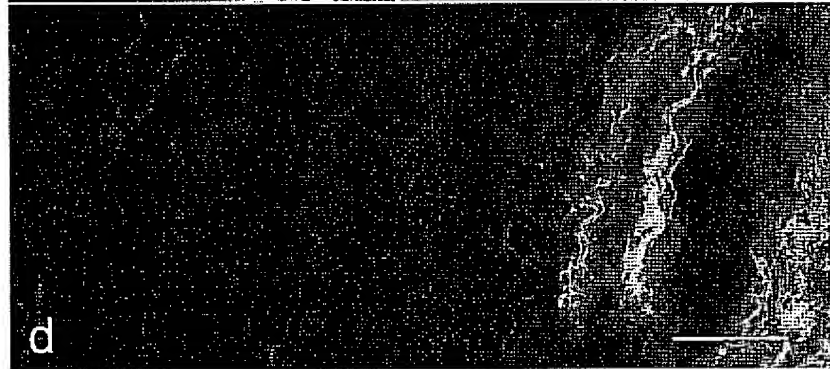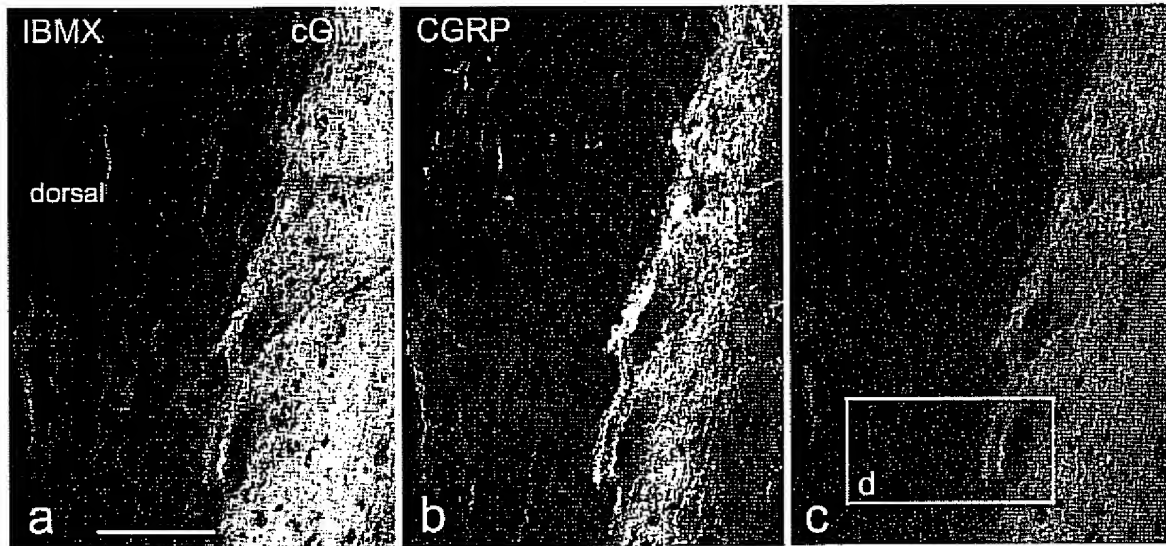
Table 1

Effect of incubation of slices of the rat cervical spinal cord in the presence of 1 mM IBMX and 100 μM DEANO (n = 32) on the colocalization observed between cGMP-IR and 10 neuronal marker molecules in the various lamina

	Lamina						White matter		Dorsal root
	1	2	3	4–7	8–9	10	dl	l	
cGMP	+++	+++	+++	+	++	++	+	+	+
Colocalization									
vAChT	–	–	–	–	+	±	–		+
Parvalbumin	+	+	+	+	+	+	+		+
EAAT3	+	–	–	–	–	–	–		+
Synaptophysin	++	++	++	+	+	+	–		
Substance P	–[a]	–[a]	–[a]	–	–	–	–		–
CGRP	–	–	–	–	–	–	–		–
IB4	++	++	m)	m)	m)	m)			
vGAT	++	++	+	+	+	+	–		–
vGLUT1	–	–	–	–	–	–	–		–
vGLUT2	++	++	++	++	++	++	–		–

(+) detectable; (++) fairly strong; (+++) intense; (±) sparse. m): only in microglia; dl: dorsolateral; l: lateral.
[a] See results obtained with slices incubated with 1 mM IBMX, 1.0 μM BAY 41-2272, and 100 μM DEANO.
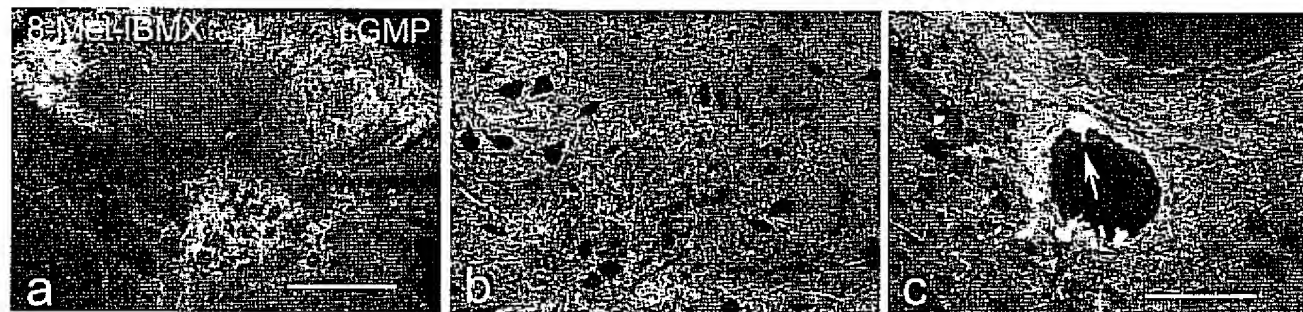
Fig. 6. Effect of the selective PDE1 inhibitor 8-methoxy-IBMX on cGMP-IR in the rat cervical spinal cord. Slices were incubated in the presence of 100 μM 8-methoxy-IBMX and 100 μM DEANO. cGMP-immunostaining in (a) layers 1–4; (b) layers 8 and 9; and (c) layer 10. Bars represent 200 μm in (a and b), and 100 μm in (c).

observations using IBMX as a PDE inhibitor, no colocalization was observed between cGMP-IR and parvalbumin in the dorsal horn (Fig. 8(a, b and e)), however, some colocalization was observed in layers 8 and 9. cGMP-IR was strong in the large

cholinergic boutons in the ventral horn (Fig. 8(c, d and f)). A summary of these results is given in Table 4.

Inhibition of PDE5 by 10 μM sildenafil in combination with DEANO resulted in moderate cGMP-IR in all gray

Table 2

Effect of incubation of slices of the rat cervical spinal cord in the presence of 1 μM Bay 60-7550 and 100 μM DEANO (n = 6) on the colocalization observed between cGMP-IR and nine neuronal marker molecules in the various laminae

	Lamina						White matter	
	1	2	3	4–7	8–9	10	dl	l
cGMP	+++	+++	+++	++	+++	+++	+	+
Colocalization								
vAChT	–	–	–	–	+	–	–	
Parvalbumin	±	±	–	–	–	–	–	–
EAAT3	+	+	+	–	–	–	+	
Synaptophysin	±	±	±	±	+	+	+	
Substance P	–	–	–	–	–	–	–	
CGRP	–	–	–	–	–	–		
vGAT	+	+	+	+	+	+	–	
vGLUT1	–	–	–	–	–	–	–	
vGLUT2	+	+	+	+	+	+	–	

See Table 1 for explanation of the symbols.

Fig. 7. Effect of the PDE2 inhibitors BAY 60-7550 and EHNA on the localization of cGMP-IR in the rat cervical spinal cord. Slices were incubated in the presence of 1 μM BAY 60-7550 (a–f) or 100 μM EHNA (g–h) in combination with 100 μM DEANO. Double-immunostaining of cGMP-IR with synaptophysin (a–f) reveals abundant colocalization of cGMP-IR in synaptophysin immunopositive boutons in all laminae of the spinal cord, including white matter. Double-immunostaining of cGMP-IR with parvalbumin (g–h) revealed no colocalization, whereas double-immunostaining with EAAT3 (j–l) did show colocalization in laminae 1 and 2. Bar in (a) is 100 μm for all images.

matter layers. No cGMP-IR was observed in parvalbumin or synaptophysin immunopositive structures. Some colocalization was observed between cGMP-IR and vAChT in varicosities in laminae 1–3 (Fig. 9(a, b and e)). Some of the large cholinergic boutons in the ventral horn showed cGMP-IR (Fig. 9(c, d and f)), but cGMP-IR was mainly confined to small varicosities. We observed immunostaining for vAChT in some cells in layer 10 and in the ependymal cells lining the central canal (Fig. 9(g–i)). Results are summarized in Table 5.
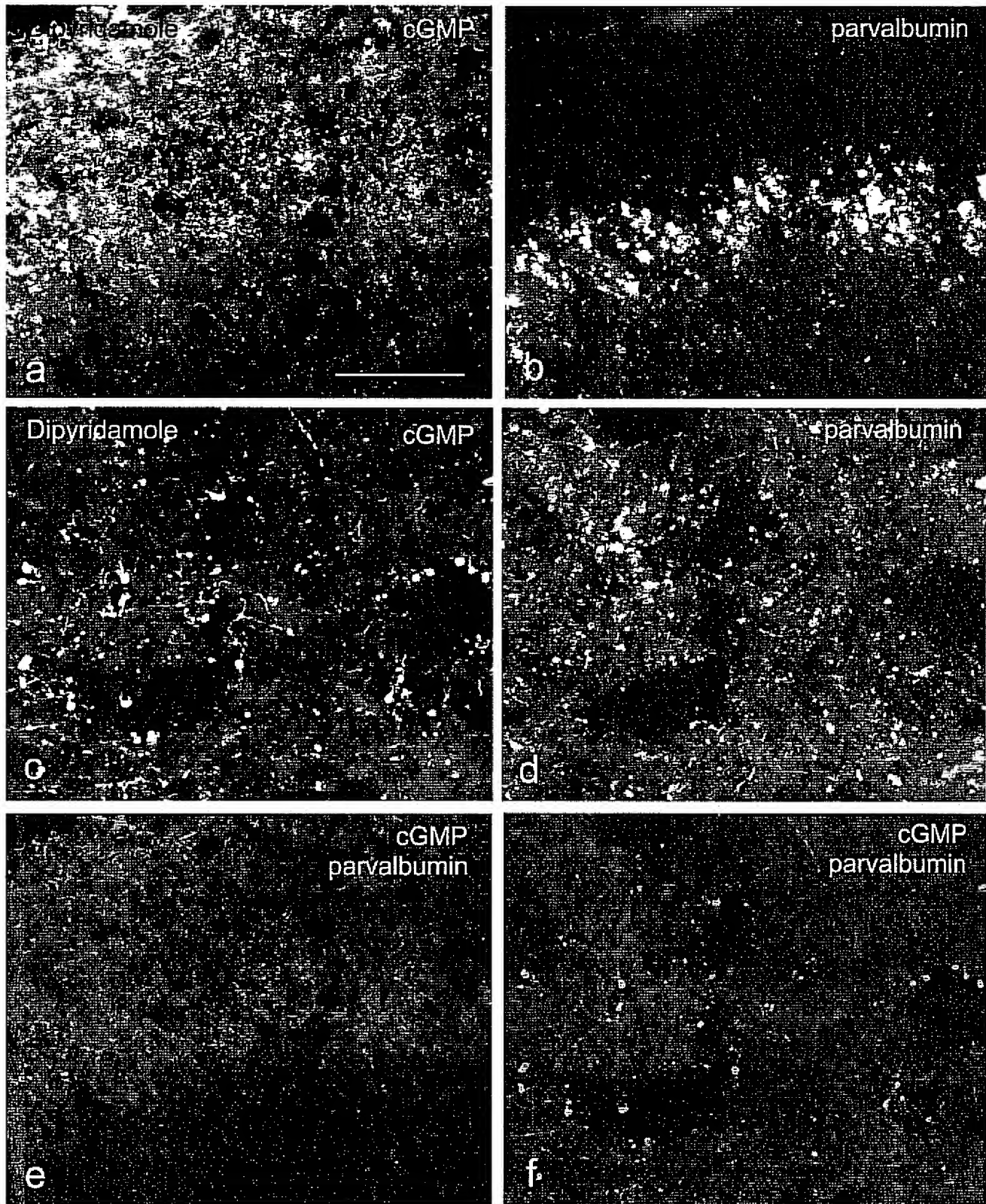
Fig. 8. Effect of the mixed typed PDE5–PDE10 inhibitor dipyridamole on the localization of cGMP-IR in the rat cervical spinal cord. Slices were incubated in the combined presence of 100 μM DEANO and 10 μM dipyridamole. Double-immunostaining of cGMP-IR with parvalbumin in laminae 1 and 2 (a, b, e) or laminae 8 and 9 (c, d, f) revealed partial colocalization in the ventral horn but not in the dorsal horn. Bar indicates 50 μm for all images.
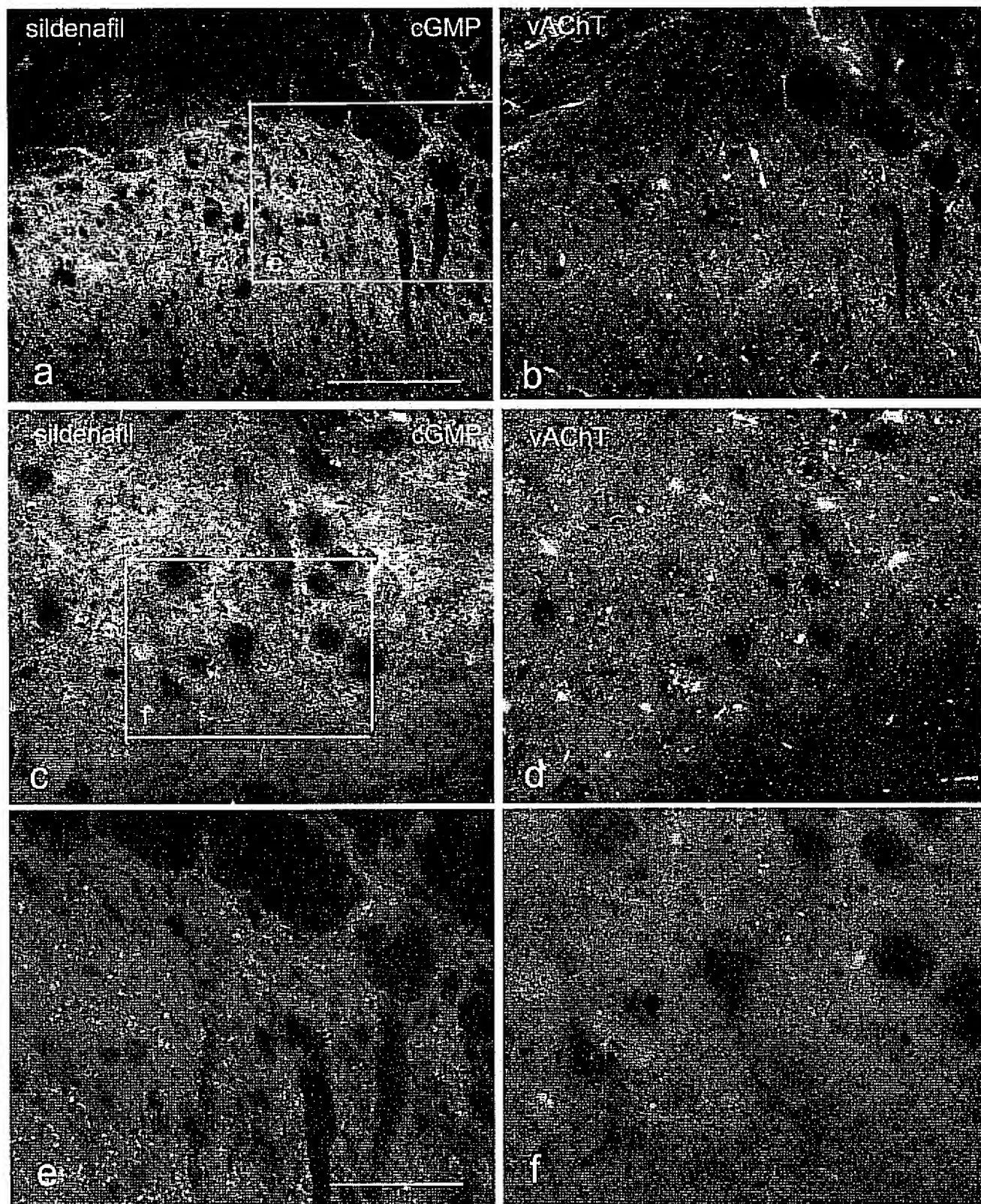
Fig. 9. Effect of the PDE5 inhibitor sildenafil on the localization of cGMP-IR in the rat cervical spinal cord. Slices were incubated in the presence 10 μM sildenafil and 100 μM DEANO. Slices were double-immunostained for cGMP-IR and vAChT. Some colocalization is observed between cGMP-IR and vAChT in the dorsal (a, b, e) and ventral (c, d, f) horns and around the central canal (layer 10) (g–i). Bar indicates 100 μm.
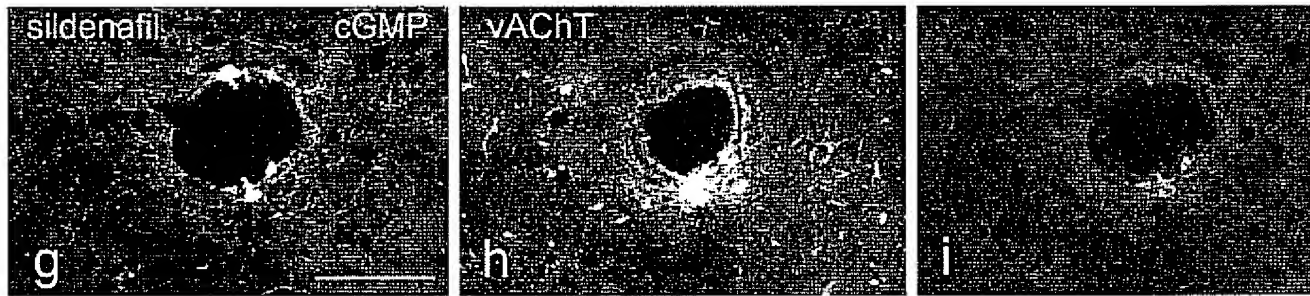
Fig. 9. (*Continued*).

Addition of 10 μM SCH 51866 alone had no effect on NO-mediated cGMP-IR. In combination with DEANO, stimulation of cGMP synthesis was observed in layers 1–3 (Fig. 11(a, d, g, i and k)) and layer 10 and in some cells touching on the ependymal cell layer lining the central canal (Fig. 11(j)). As can be seen in Fig. 11(j), these cells often have protrusions which make contact with the CSF. Colocalization between cGMP-IR and vGAT and vGLUT2 (but not vGLUT1) was observed in the layers 1–3 (Fig. 11(a–f)) but not in layer 10. No colocalization between cGMP-IR and CGRP was observed in the dorsal aspect (Fig. 11(g–i)), although cGMP-IR fibers and CGRP-IR fibers could be observed which were running closely parallel (Fig. 11(i)). A few CGRP-IR structures which were always observed near the ventral side of the ependymal cell layer (Fig. 11(j)). No colocalization was observed between cGMP-IR and SP in laminae 1 and 2 (Fig. 11(k)). These results are summarized in Table 7.

3.7. cGMP-IR in the dorsal root

In some preparations (IBMX $n = 3$; EHNA $n = 1$) we were able to study the effect of PDE inhibitors on cGMP synthesis in the dorsal root and the dorsal root entry zone. We observed cGMP-IR in the cholinergic fibers of the proximal dorsal root and the dorsal root entry zone (Fig. 12(a–c)) using IBMX as a PDE inhibitor. Similarly, we observed colocalization between cGMP-IR in a minor population of EAAT3-immunopositive structures of the dorsal root (Fig. 12(d–f)) and in layer 1 of the dorsal horn. Using EHNA as a PDE inhibitor, we found colocalization between cGMP-IR and parvalbumin in cells of the dorsal root and in layers 1 and 2 of the dorsal horn (Fig. 12(g–i)).

3.8. mRNA expression of PDE2, 5, and 9

Expression of PDE's2, 5, and 9 was studied using mRNA in situ hybridization. mRNA's of all three PDE's were observed in all layers of the gray matter (Fig. 13). In the dorsal horn mRNA expression of all three PDE's appeared in cells with the morphology of small neurons and also the motor neurons in the ventral appeared to express all three mRNA's. Ependym cells lining the central canal also expressed all three mRNA's.

3.9. Experiments using the NO-independent sGC activator BAY 41-2272

BAY 41-2272 was used to study endogenous NO synthesis in the spinal cord slice. Already a concentration of 0.1 μM BAY 41-2272 in combination with 1 mM IBMX resulted in cGMP-IR in the dorsal horn (Fig. 14(a); compare with Fig. 1(b)). Incubation of the slices in the presence of the NOS inhibitor L-NAME (100 μM) abolished the effect of 0.1 μM BAY 41-2272 almost completely (Fig. 14(b)). On the other hand, in the presence of IBMX the effect of 10 μM DEANO was greatly potentiated by 0.1 μM BAY 41-2272 in all gray matter areas. This is shown in Fig. 14(c) in a cross section of a slice made in the longitudinal direction. The intensity of cGMP-immunostaining was greatly increased and also the number of structures showing cGMP-IR was increased when compared with cGMP-IR in a slice that was incubated with

Table 6

Effect of incubation of slices of the rat cervical spinal cord in the presence of 100 μM rolipram and 100 μM DEANO ($n = 5$) on the colocalization observed between cGMP-IR and six neuronal marker molecules in the various laminae

	Lamina						White matter	
	1	2	3	4–7	8–9	10	dl	l
cGMP	±	±	++	−	−	+	+	
Colocalization								
vAChT	−	−	−	−	−	−	−	−
Parvalbumin	−	−	−	−	−	−	+	+
EAAT3	−	−	−	−	−	−	−	
Synaptophysin	+	+	+	−	−	−	+	
Substance P	−	−	−	−	−	−		
CGRP	−	−	−	−	−	−		

See Table 1 for explanation of the symbols.

J. de Vente et al./Journal of Chemical Neuroanatomy 31 (2006) 275–303
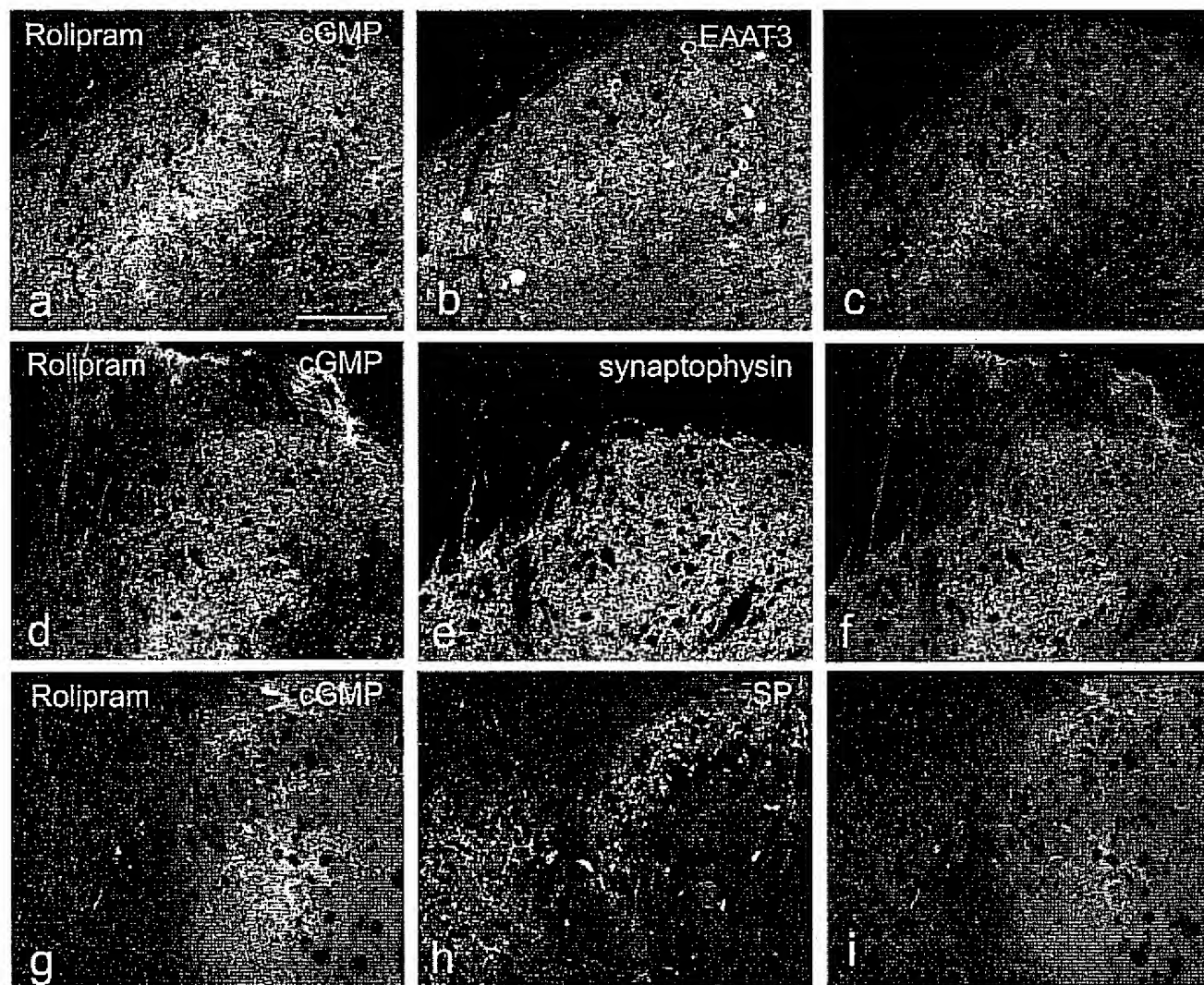

Fig. 10. Effect of the PDE4 inhibitor rolipram on the localization of cGMP-IR in the rat cervical spinal cord. Slices were incubated in the presence of 10 μM Rolipram and 100 μM DEANO. Slices were double-immunostained for cGMP-IR and EAAT3 (a–c), synaptophysin (d–f), or SP (g–i). Colocalization of cGMP-IR with EAAT3 was not observed in all layers, e.g. the dorsal horn (a–c). Some colocalization was also observed between cGMP-IR and synaptophysin in lamina 3 of the dorsal horn (j–I). No colocalization was observed between cGMP-IR and substance P (g–i). Bar indicates 100 μm for all images.

IBMX and DEANO only (Fig. 1(c)). In sections from slices incubated in the presence of all three compounds we observed long cGMP-IR fibers running in longitudinal direction through the white matter layers also (see arrows in Fig. 14(c), but also Figs. 15(a) and 18(a)).

cGMP-IR in the slice after incubation with a combination of IBMX, BAY41-2272 and DEANO did not colocalize with vGLUT1 in any of the gray matter layers. In Fig. 15 this is illustrated in a photomontage of part of a longitudinal slice. Colocalization of cGMP-IR with vGLUT2 in slices incubated under this condition is abundant in all gray matter layers (Fig. 16(a–c), ventral horn) and in varicosities of fibers running longitudinal through the white matter (Fig. 16(d–f), dorsolateral). Also with vGAT we observed abundant colocalization in all gray matter layers (Fig. 17(a–c), ventral horn; Fig. 17(d–f), dorsolateral). Colocalization with substance P under conditions of IBMX, BAY 41-2272 and DEANO was observed

in a minor subpopulation of dorsolateral running fibers (Fig. 18) and in some superficial dorsal fibers (Fig. 19(e–f)). No colocalization was observed under these conditions with CGRP-IR fibers (Fig. 19(a–c)). We observed cGMP-IR fibers which ran closely parallel to CGRP-IR fibers (Fig. 19(c)) or substance P-IR fibers (Fig. 19(d)) over some distance.

4. Discussion

In the spinal cord, cGMP has been implicated in the development and maintenance of hyperalgesia (Kawabata et al., 1993; Meller et al., 1994; Salter et al., 1996; Siegan et al., 1996; Ferreira et al., 1999; Sousa and Prado, 2001; Tao et al., 2000; Tao and Johns, 2002; Schmidtko et al., 2003; Tegeder et al., 2004). NO-cGMP signaling in the spinal cord is widespread and has been observed in all laminae of the spinal cord (Vles et al., 2000). Nevertheless, the role of cGMP in spinal

neurotransmission and/or homeostasis is still unclear. This might be caused by the scant knowledge about the localization of cGMP synthesis in relation to the hydrolysis of this cyclic nucleotide. We have investigated NO-cGMP signal transduction in the rat cervical spinal cord slice preparation by localizing the NO-mediated cGMP signal at the cellular level in combination with the use of different PDE inhibitors and an NO-donor. In addition, we studied the localization of mRNA of PDE2, 5, and 9 using in situ hybridization. Our results indicate that in the spinal cord slice preparation there is endogenous NO synthesis and that NO is an almost ubiquitous neurotransmitter

in the spinal cord performing both retrograde and postsynaptic transmitter functions. In addition, NO-cGMP signaling is controlled by the concerted action of a number of PDE's.

4.1. PDE expression in the spinal cord

PDE activity in the spinal cord is high, as no cGMP-IR could be observed in slices that were incubated in presence of an NO-donor but in the absence of PDE inhibitors. In situ hybridization of the mRNA of PDE2, 5 and 9 showed that all three PDE's have a wide-spread distribution in the rat cervical spinal
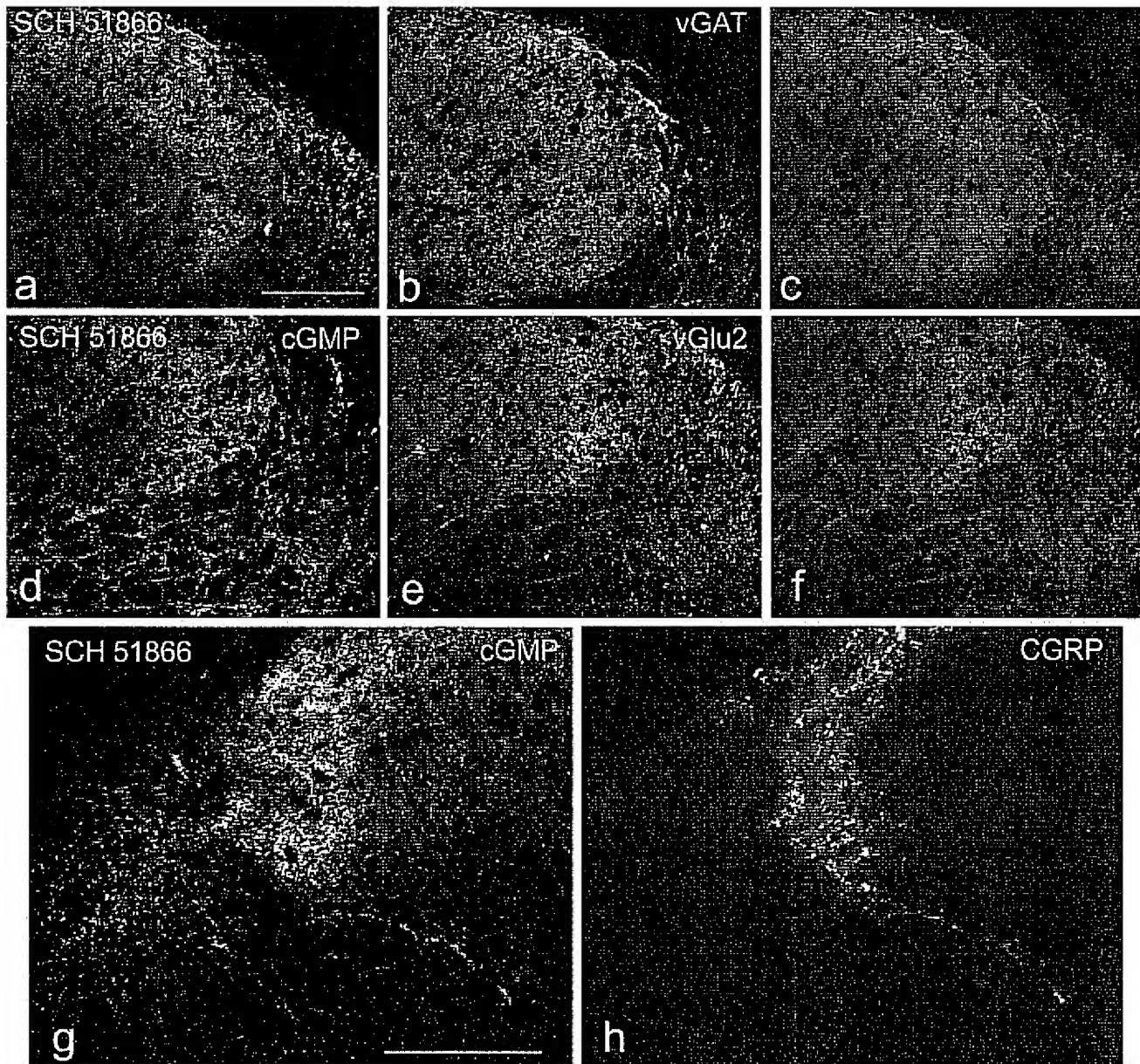

Fig. 11. Effect of selective PDE9 inhibitor SCH 51866 on the localization of cGMP-IR in cervical spinal cord. Slices were incubated in the presence of 10 μM 51866 and 100 μM DEANO. Sections were double-immunostained for cGMP-IR and vGAT (a–c), vGLUT2 (d–f), CGRP (g–j), or SP (k). Partial colocalization was observed between cGMP-IR and vGAT (a–c), cGMP-IR and vGLUT2 (d–f). Colocalization between cGMP-IR and CGRP (g–j) or substance P (k) was absent in the dorsal horn. Bar in (a) indicates 100 μm for the images (a–f); bar in (g) indicates 100 μm for the images (g–j); bar in (k) represents 25 μm.
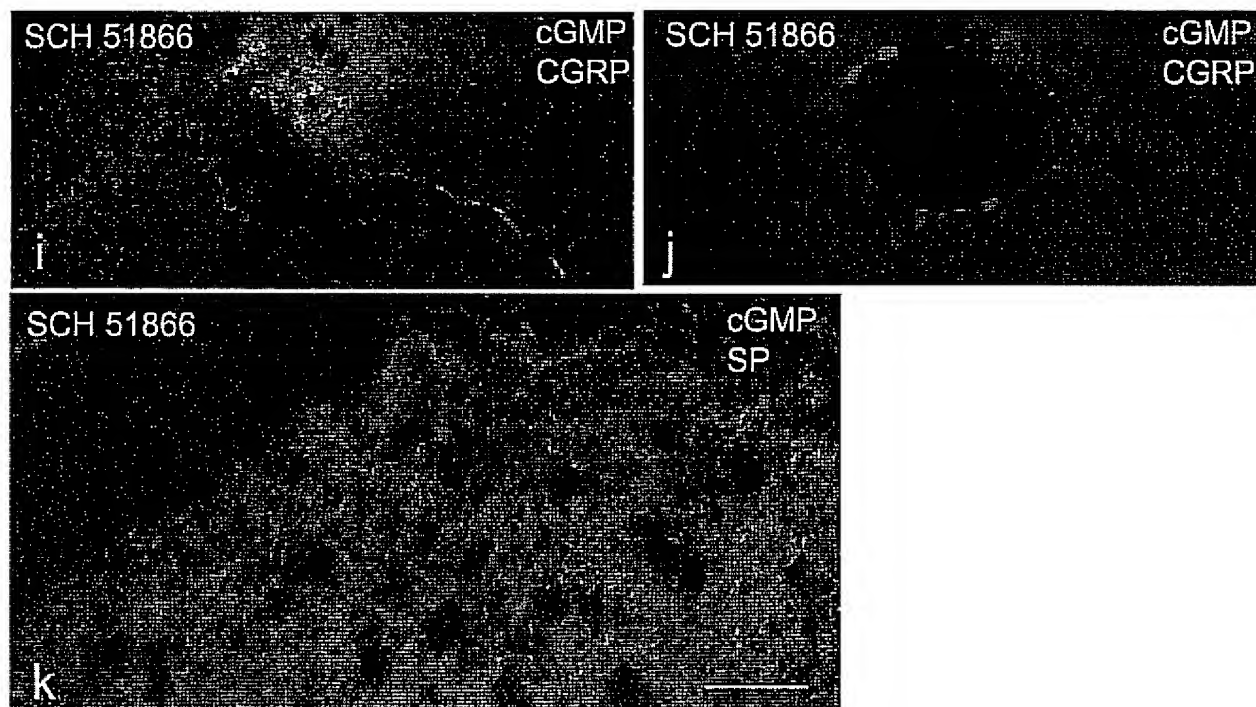
Fig. 11. (*Continued*).

cord. It is striking that the mRNA of all three PDE's has been observed in ventral motor neurons. Immunoreactivity for choline acetyltransferase or vAChT is destroyed when combined with the in situ hybridization technique and therefore it cannot be concluded from our data with certainty that expression of all three PDE's occurs in all motor neurons. However, considering the number of motor neurons which express these PDE's the latter possibility is highly likely.

In order to gain insight into the importance of PDE activity on cGMP accumulation in the spinal cord slices we used selective inhibitors in combination with DEANO on slices incubated in vitro. The cGMP-IR present in the sections from such slices might give an indication of the PDE activity in the cGMP-IR structures.

In Table 8 we present a compilation of IC50 values found in the literature of PDE inhibitors under study. From these IC50 values it might be concluded that a certain extent of inhibition of several PDE's by the high concentrations that we used is indicated. As stated in Section 2 we tested the inhibitors over a concentration range and performed our colocalization studies at the dose which was next higher than the lowest dose of the inhibitor which resulted in a cGMP response in the presence of DEANO. This procedure does not exclude non-selective PDE inhibition. The selectivity of, e.g. 8-methoxy-IBMX for PDE1 and SCH 51866 for PDE9 (see Table 8) is not high, and it is to be expected that the localization of cGMP-IR will be like that obtained with IBMX. On the other hand, it has been discussed in the literature (e.g. Thompson, 1991) that due to substrate interactions between the different PDE isoforms, it might be expected that the pharmacological inhibition constants obtained in cell cultures or tissues might be considerable

higher that the biochemical inhibition constants obtained on purified enzymes. A clear example of this was recently reported using a new PDE9 inhibitor (Wunder et al., 2005).

Although the inhibition constants indicate that rolipram is a highly selective PDE4 inhibitor, there might be already some inhibition of the other PDE isoforms at a concentration of 10 μM, and we indeed observed a considerable effect of rolipram on cGMP-IR at this concentration. This is in agreement with the finding that PDE4 hydrolyzes cGMP in a rolipram sensitive manner when the concentration of cGMP is high enough (Bellamy and Garthwaite, 2001). In addition, it cannot be excluded that an increase in the cAMP concentration caused by inhibition of PDE4 has an effect on cGMP metabolism.

Considering the abundance of PDE9 mRNA, the results using SCH 51866 in combination with DEANO were less than expected because cGMP-IR was observed only in the laminae 1–3 and around the central canal. Using SCH 51866 in combination with 1 mM IBMX and DEANO did not yield different results to those obtained with IBMX and DEANO. Therefore, we conclude in our experimental approach the contribution of PDE9 to hydrolysis of cGMP might be minimal.

4.2. cGMP-IR in GABAergic neurons

In the present study we used parvalbumin and vGAT as markers for GABAergic neurons. It has been known for considerable time that a subpopulation of GABAergic neurons is parvalbumin-IR (Antal et al., 1991). Our observations are in agreement with these results. Although we observed colocalization between parvalbumin and cGMP-IR in all gray matter
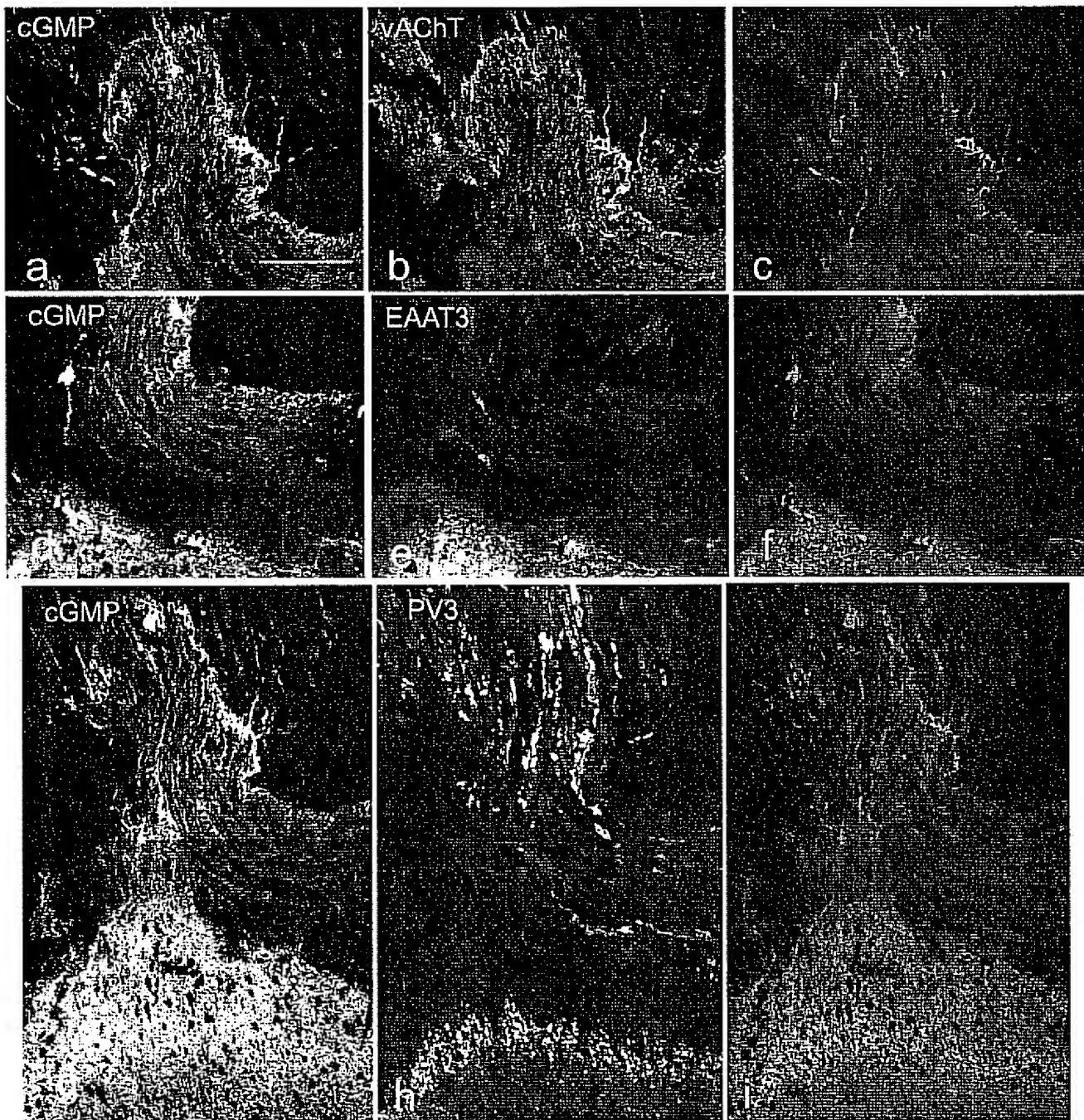
Fig. 12. Effect of IBMX and EHNA on the localization of cGMP-IR in the proximal part of the dorsal root and the dorsal root entry zone in the rat cervical spinal cord. Slices were incubated in the combined presence of 100 μM DEANO and 1 mM IBMX (a–f) or 100 μM EHNA (g–i). Sections were double-immunostained for cGMP-IR and vAChT (a–c), EAAT3 (d–f), or parvalbumin (g–i). Abundant colocalization is present between cGMP-IR and the three markers vAChT, EAAT3 and parvalbumin in the proximal part of the dorsal root. In addition, there is colocalization between cGMP-IR and parvalbumin in the layers 1 and 2 of the dorsal horn (g–i). Bar in (a) represents 100 μm for all images.

layers (Vles et al., 2000), this colocalization was only partial. Colocalization of cGMP-IR with vGAT was abundant in laminae 1–7, and somewhat less in laminae 8–10. When the slices were incubated with the different PDE inhibitors, we did not observe striking differences in the localization of cGMP-IR in GABAergic neurons. Abundant cGMP-IR in GABAergic neurons was observed when slices were incubated in the presence of IBMX, which was even more extensive when also BAY 41-2272 was present.

4.3. cGMP-IR in cholinergic neurons

vAChT is a good marker for labeling cholinergic fibers and terminals, but less appropriate to label cholinergic somata
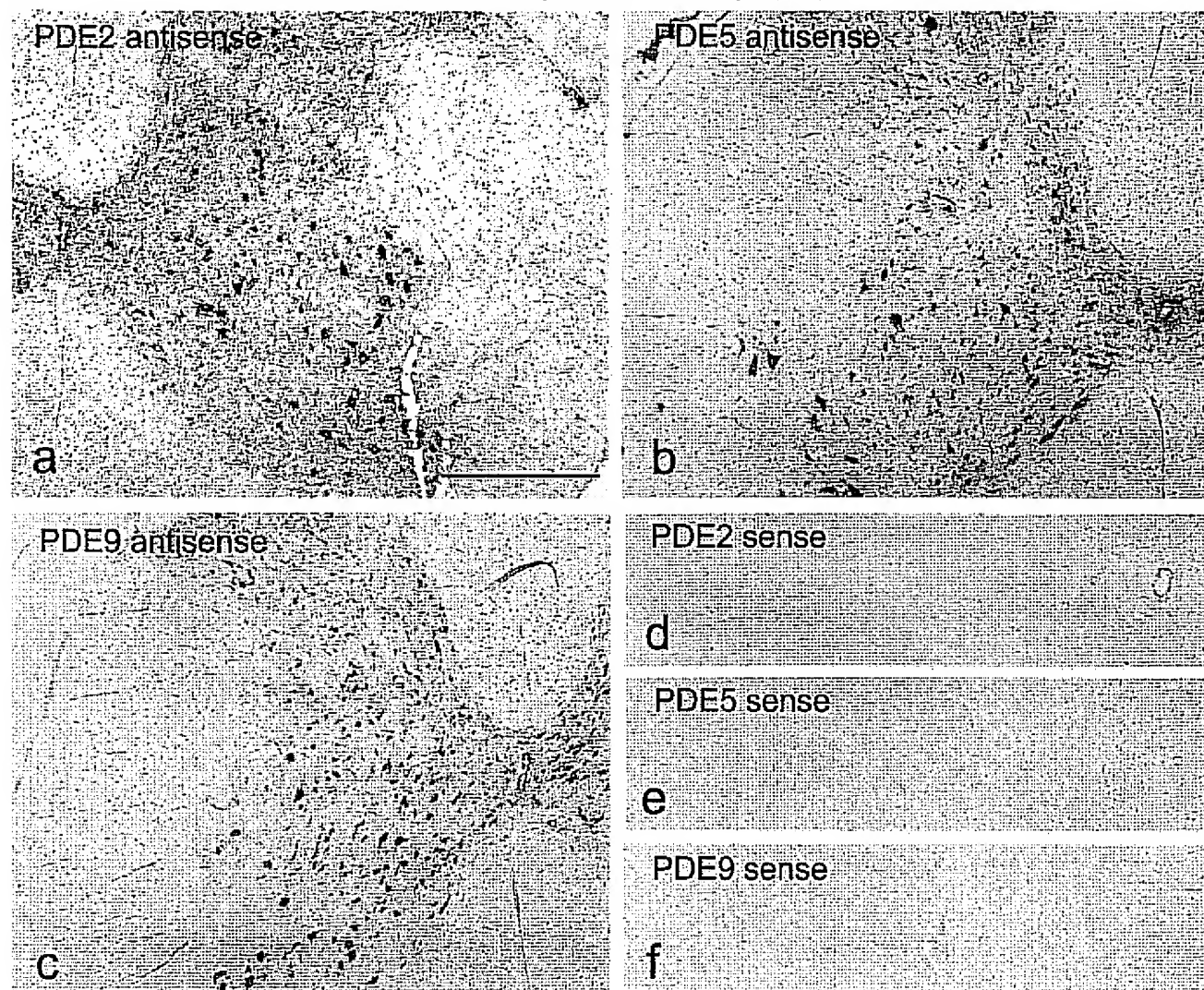
Fig. 13. Localization of mRNA of PDE2 (a), PDE5 (b), and PDE9 (c) in the rat cervical spinal cord visualized by in situ hybridization. Corresponding sense probes are shown in (d–f). Bar in (a) represents 400 μm for all images.

(Ichikawa et al., 1997). Our results showed some experimental variation in the immunostaining of ventral motor neurons with vAChT (Fig. 3(j); Fig. 9(d)), although the smaller cholinergic cells in lamina 10 generally did show vAChT-IR (Fig. 9(h)). cGMP-IR in cholinergic neuronal fibers and terminals was observed in all lamina, and also in the dorsal root and dorsal root entry zone (Fig. 12(b)). This latter finding suggests a sensory, cholinergic input to the superficial layers or the cervical spinal cord (Sann et al., 1995). Surprisingly we did observe colocalization between cGMP-IR and vAChT in laminae 8 and 9 in the C-terminals when slices were incubated with the PDE2 inhibitor BAY 60-7550, but not with EHNA. This might be caused by the higher affinity of BAY 65-7550 for PDE2 compared to EHNA. The cholinergic nature of the C-terminals has been described before (Nagy et al., 1993). Inhibition of PDE5 with dipyridamole or sildenafil also resulted in cGMP-IR in these C-type terminals. In agreement with a previous report (Sann et al., 1995) we observed vAChT-IR

fibers and cells in layer 10 and these cells were cGMP-IR when the slices were incubated with sildenafil. These cGMP/vAChT-IR cells might be the small short-axon propriospinal interneurons (Feng-Chen and Wolpaw, 1996; Arvidsson et al., 1997), the origins of the C-boutons on the ventral motor neurons. This suggestion was recently strengthened by the report that the C-type terminals develop in correspondence with the motor system (Wilson et al., 2004).

4.4. cGMP-IR glutamatergic neurons

We used three marker molecules as markers for the glutamatergic innervation, i.e. EAAT3, vGLUT1, and vGLUT2. Colocalization between cGMP-IR and EAAT3 was observed in laminae 1–3 and lamina 10 in the presence of the PDE2 inhibitors EHNA or BAY 60-6550. We have no ready explanation why no colocalization between cGMP-IR and EAAT3 could be observed after incubation in the presence of
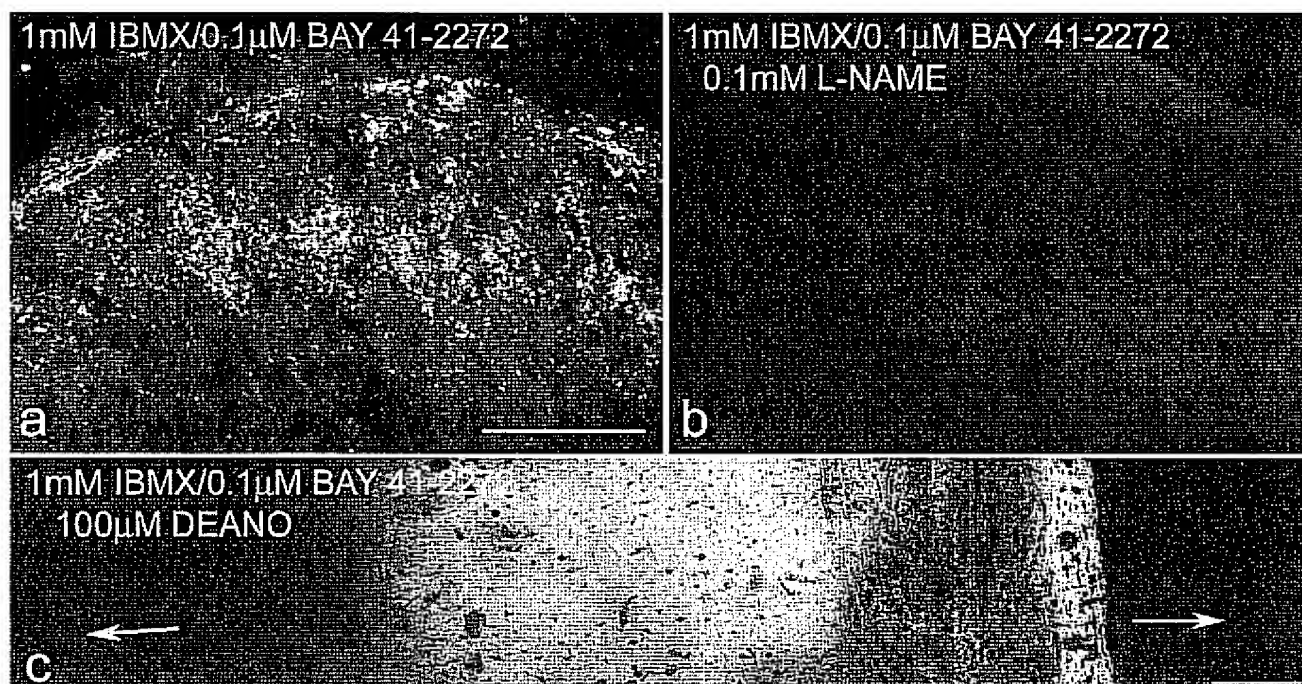
Fig. 14. Evidence for endogenous synthesis of NO in the cervical spinal cord slice. Slices were incubated in the presence of 1 mM IBMX, 0.1 μM BAY 41-2272 (a), in combination with 0.1 mM L-NAME (b), or 100 μM DEANO (c); (presenting the transverse overview of a longitudinal slice). The effect of BAY 41-2272 is almost completely abolished by 0.1 mM L-NAME. Bar represents 100 μm in (a and b) and 200 μm in (c). In (c) images were aligned using Adobe Photoshop 7.0.1. The arrows in (c) indicate the borders of the section.

IBMX. It might be that the higher affinity of EHNA and especially BAY 60-7550 for PDE2 compared to IBMX results in cGMP accumulation in PDE2 containing fibers. After incubation of the slices in the presence of IBMX, or even more after incubation with IBMX in the presence of BAY 41-2272 we observed abundant NO-mediated cGMP-IR in vGLUT2-IR fibers, however, not in vGLUT1 containing fibers. A functional differentiation between the vGLUT1-IR and vGLUT2-IR innervation of the spinal cord has been suggested before (Alvarez et al., 2004). vGLUT1 innervation was coming mainly from cutaneous and muscle mechanoreceptors (Alvarez et al., 2004), whereas vGLUT2 innervation was of intrinsic origin.

4.5. NO synthesis in the spinal cord

NO has been described as being a retrograde messenger (O'Dell et al., 1991; Hawkins et al., 1998). However, recently it has been demonstrated that NO functions as a messenger molecule with a presynaptic as well as a postsynaptic role (Wang et al., 2005). At all spinal levels nNOS is localized mainly in somata which are positioned in the superficial dorsal horn and around the central canal, whereas at thoracic and sacral levels nNOS is also present in the intermediolateral cell column (e.g. Valtschanoff et al., 1992). The presence of nNOS in a small population of the ventral motor neurons has been reported by a number of groups (Blottner and Baumgarten, 1992; Zhang et al., 1993; Wu et al., 1995a, 1995b; Urushitani et al., 1998) whereas others did not observe nNOS in the motor neurons (Dun et al., 1993; Spike et al., 1993; Clowry, 1993; He

et al., 1997; Wu et al., 1998). The above can be summarized as follows: nNOS-IR fibers traverse all through the gray matter of the spinal cord and also penetrate the white matter. Similar to the situation in the brain, the presence of nNOS is much more widespread than can be judged from the number of the nNOS-IR somata. In addition, the target for NO, i.e. sGC, was found to be present in all laminae and in white matter tracts (Maihöfner et al., 2000).

We found evidence for the presence of NOS activity in the spinal cord slices as the presence of only IBMX during the incubation resulted in cGMP-IR in varicosities and small fibers in the dorsal horn (compare Fig. 2(a and b)). This observation is in agreement with quantitative measurements of cGMP levels in the dorsal horn of the spinal cord in rabbits (Pavel et al., 2000). In addition, the effect of BAY 41-2272 without NO-donor was inhibited almost completely by 0.1 mM L-NAME (Fig. 14(a and b)). Although it has been reported that BAY 41-2272 inhibits PDE5 (Mullershausen et al., 2004), it is unlikely that this effect is responsible for the observed effect of BAY 41-2272 on cGMP levels in our slice preparations as the selective PDE5 inhibitor sildenafil has no effect on cGMP-IR in the absence of an NO-donor [present results]. The potentiation of the effect of NO on sGC by BAY 41-2272 is evidenced by an intense cGMP-IR in all lamina of the cervical spinal cord and in white matter tracts (e.g. Fig. 14(c)). cGMP-IR in the longitudinal sections shows long, thin fibers which can be traced over a distance of more than 100 μm (Figs. 1, 15 and 18).

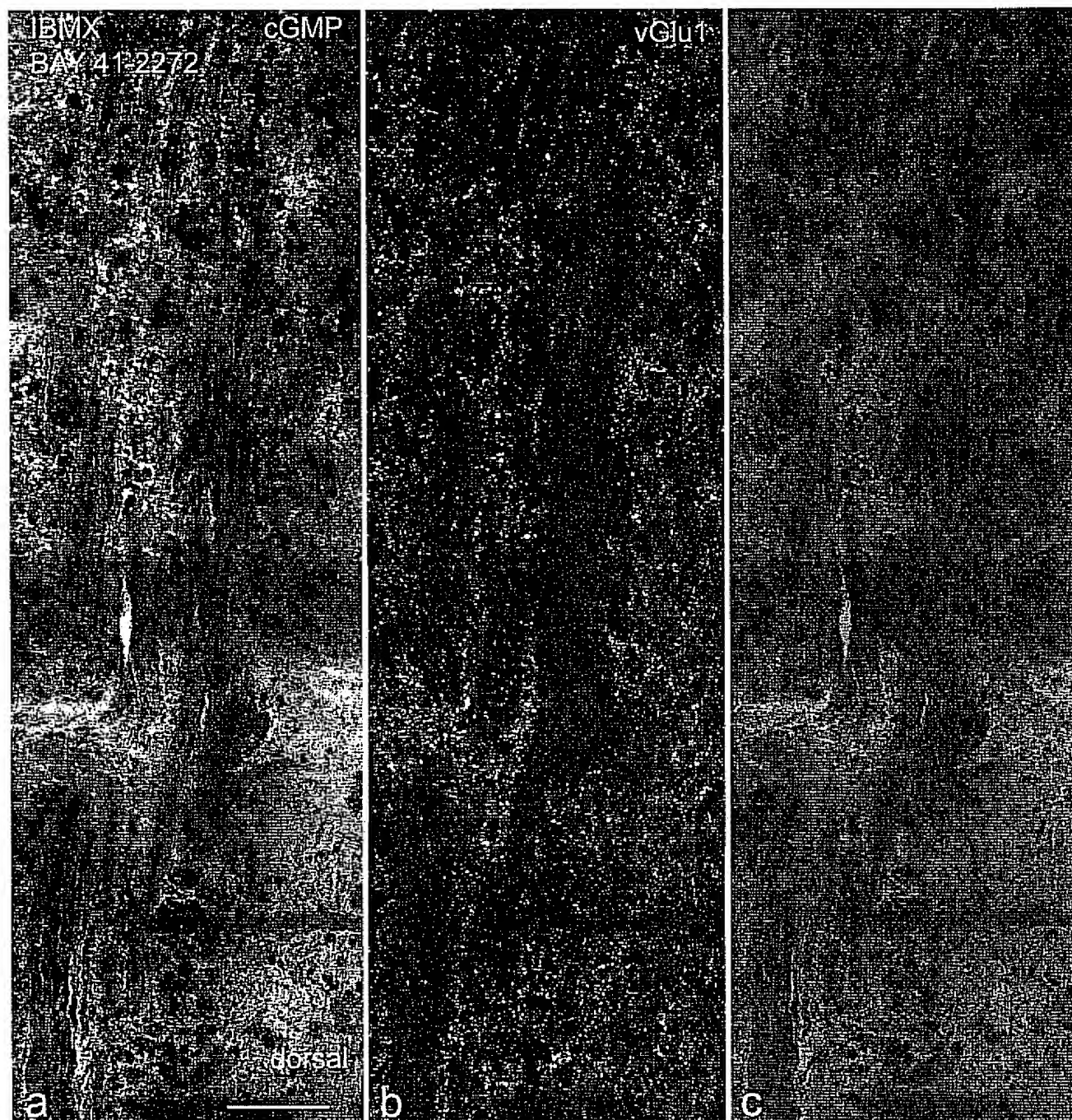The concomitant treatment of the slices with IBMX, BAY 41-2272 and DEANO resulted in abundant colocalization of

Fig. 15. Absence of colocalization between cGMP-IR and vGlu1 in the cervical spinal cord (longitudinal slice). Slice was incubated in presence of 1 mM IBMX, 1.0 μM BAY 41-2272 and 100 μM DEANO. Section was double-immunostained for cGMP-IR and vGLUT1. A total of four adjacent images were aligned using Adobe Photoshop 7.0.1. Bar represents 100 μm for all images.

cGMP-IR with synaptophysin in all laminae. This observation is agreement with the concept of NO being a retrograde messenger molecule. However, we also observed NO-mediated cGMP-IR in long fibers which often showed varicosities (see Figs. 15–18). This observation poses the question whether NO is a purely retrograde messenger molecule or not. Recently, it was shown that NO has both pre- and postsynaptic effects in the hippocampus which are mediated by cGMP (Wang et al.,

2005). We propose that also in the spinal cord there are pre- and postsynaptic effects of NO.

4.6. sGC in spinal motor neurons

There is little data on the role of NO-cGMP signaling in spinal motor neurons. In the mammalian spinal cord there is only some circumstantial evidence that spinal motor neurons
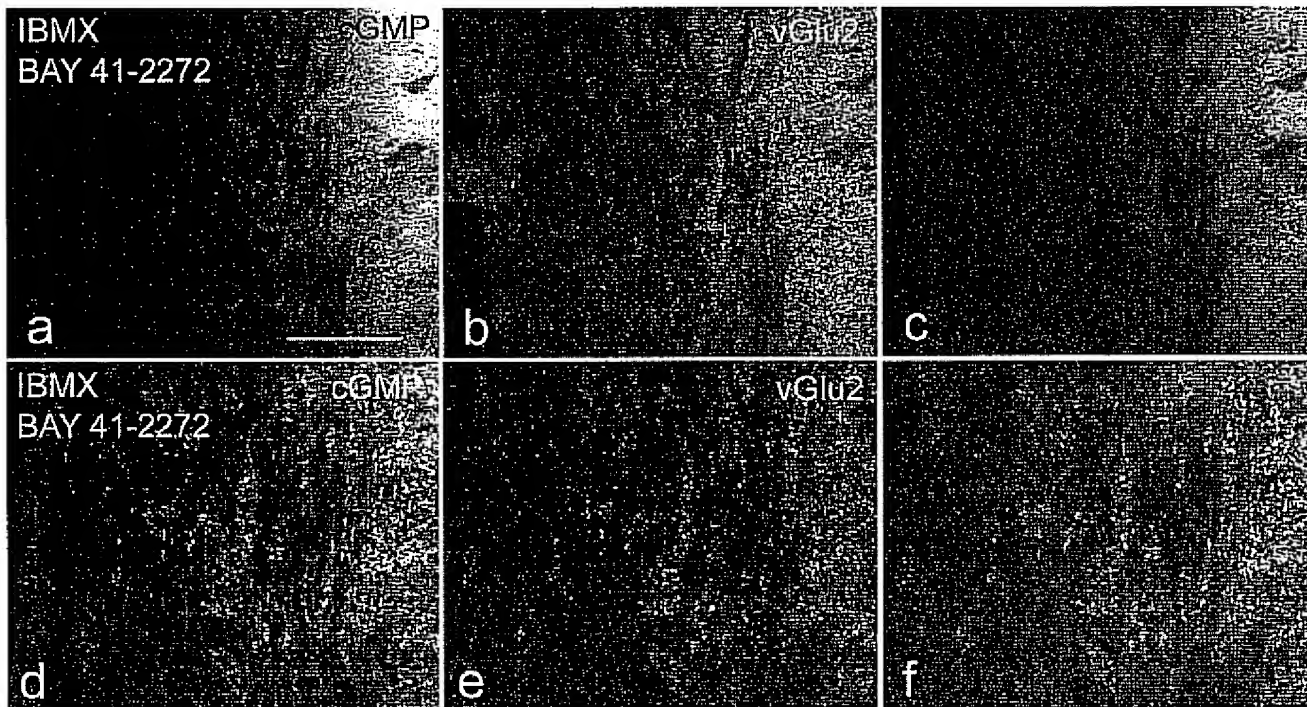
Fig. 16. Colocalization between cGMP-IR and vGLUT2 in the cervical spinal cord (longitudinal slice). Slice was incubated in the presence of 1 mM IBMX, 1.0 µM BAY 41-2272, and 100 µM DEANO. Sections were double-immunostained for cGMP-IR and vGlu2. A two times enlargement of the central region of (a–c) is shown in (d–f). Bar represents 100 µm for (a–c).

express sGC (Panahian and Maines, 2001). Development of motor neurons dendrites was dependent on NO, which suggests that cGMP has also a role in this process (Inglis et al., 1998). Interestingly, it has been reported that selective PDE5 inhibitors as well as the non-selective PDE inhibitor aminophylline were neuroprotective in a model of oxidative stress using motor neurons, whereas selective inhibitors of PDE1–4 did not offer protection (Nakamizo et al., 2003); this observation suggests at least that cGMP synthesis might occur in motor neurons. sGC could not be found in the motor neuron somata of the mouse spinal cord (Maihöfner et al., 2000). Nevertheless, we observed immunostaining for the β1-subunit of sGC in the motor neurons (Fig. 20). Expression of sGC in cultured motor neurons has been suggested by a number of groups (Estévez et al., 2002; Kim et al., 2002). However, we have never observed cGMP-IR in motor neurons above background levels. This is similar to the observations made with cerebellar Purkinje cells. It is known that these cells express sGC, however, we were unable to demonstrate cGMP-IR in these cells (for a detailed discussion of this topic see: De Vente and Steinbusch, 2000).

4.7. Role of NO-cGMP signaling in the spinal cord

Presently, little is known about the role of NO-cGMP signaling in the spinal cord. In view of the abundance of NO-responsive structures, it is very likely that NO-cGMP signaling will be part of neuronal information processing at many levels. NO-cGMP signaling in the spinal cord has been implicated in growth and pathfinding of dorsal root axons in the dorsal root

entry zone (Schmidt et al., 2002). cGMP levels were increased in the dorsal spinal cord after chronic constriction of the sciatic nerve in rat, implicating cGMP in thermal and mechanical hyperalgesia and tactile allodynia (Siegan et al., 1996). The role of cGMP in nociception is complicated by the fact that the site of manipulation of NO-cGMP signal transduction as well as the concentration of cGMP may give either a nociceptive or an antinociceptive response. Thus, intrathecal injection of L-arginine and NO-donor produced hyperalgesia in tail-flick, formalin injection (Kitto et al., 1992; Inoue et al., 1998), in the hot plate test (Ferreira et al., 1999), whereas administration of a low dose of 8-bromo-cGMP produced antinociception and a high dose caused hyperalgesia (Tegeder et al., 2002). In addition, cGMP has a differential effect on the activity of neurons in the different lamina, i.e. inhibition in the neurons of laminae 1 and 2, and generally excitatory in neurons in lamina 10 (Schmid and Pehl, 1996). Hyperalgesia induced by injecting formalin or zymosan in the hind paw was dependent on cGMP-dependent protein kinase I to develop (Schmidtko et al., 2003; Tegeder et al., 2004), however, thermal nociception in the hot plate test was not. This process of induction of hyperalgesia probably involves substance P, as it has been demonstrated that substance P is released upon a nociceptive stimulus, presumably from Aδ- and C-fibers, the stimulus being thermal, mechanical, or chemical (Duggan et al., 1988;). Furthermore, it was shown that the release of substance P was increased after induction of allodynia or hyperalgesia (Honoré et al., 1999). In the cGMP-dependent protein kinase I knock-out animals, where there is a reduced nociceptive behavior (see above), the
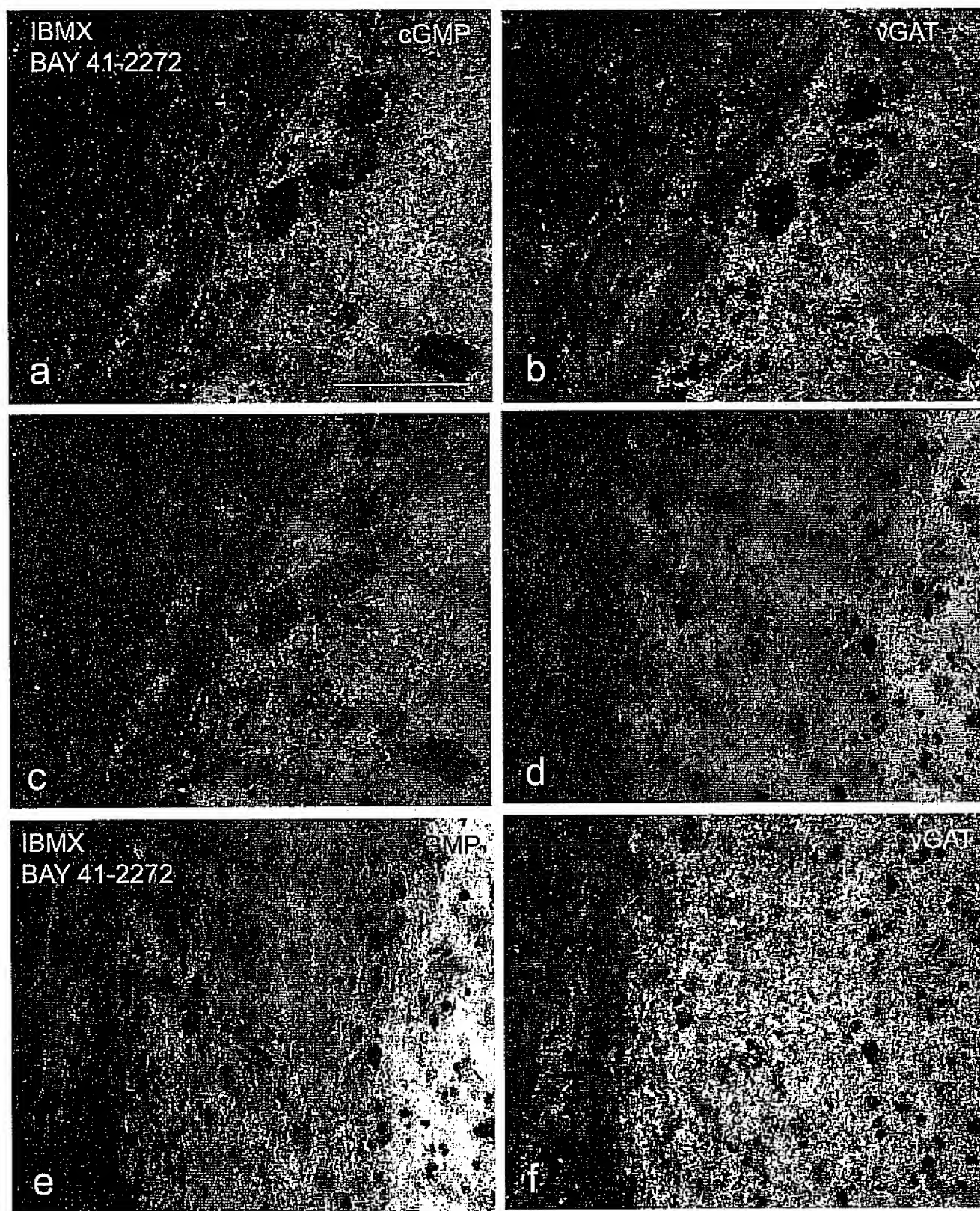
Fig. 17. Colocalization between cGMP-IR and vGAT in the cervical spinal cord. Slices was incubated in the presence of 1 mM IBMX, 1.0 μM BAY 41-2272, and 100 μM DEANO. Sections were double-immunostained for cGMP-IR and vGAT. Colocalization is partial in the ventral horn (a–c) (layers 8 and 9; transversal slice) but extensive in other layers (d–f) (dorsolateral part of a longitudinal slice). Bar represents 100 μm for all images.
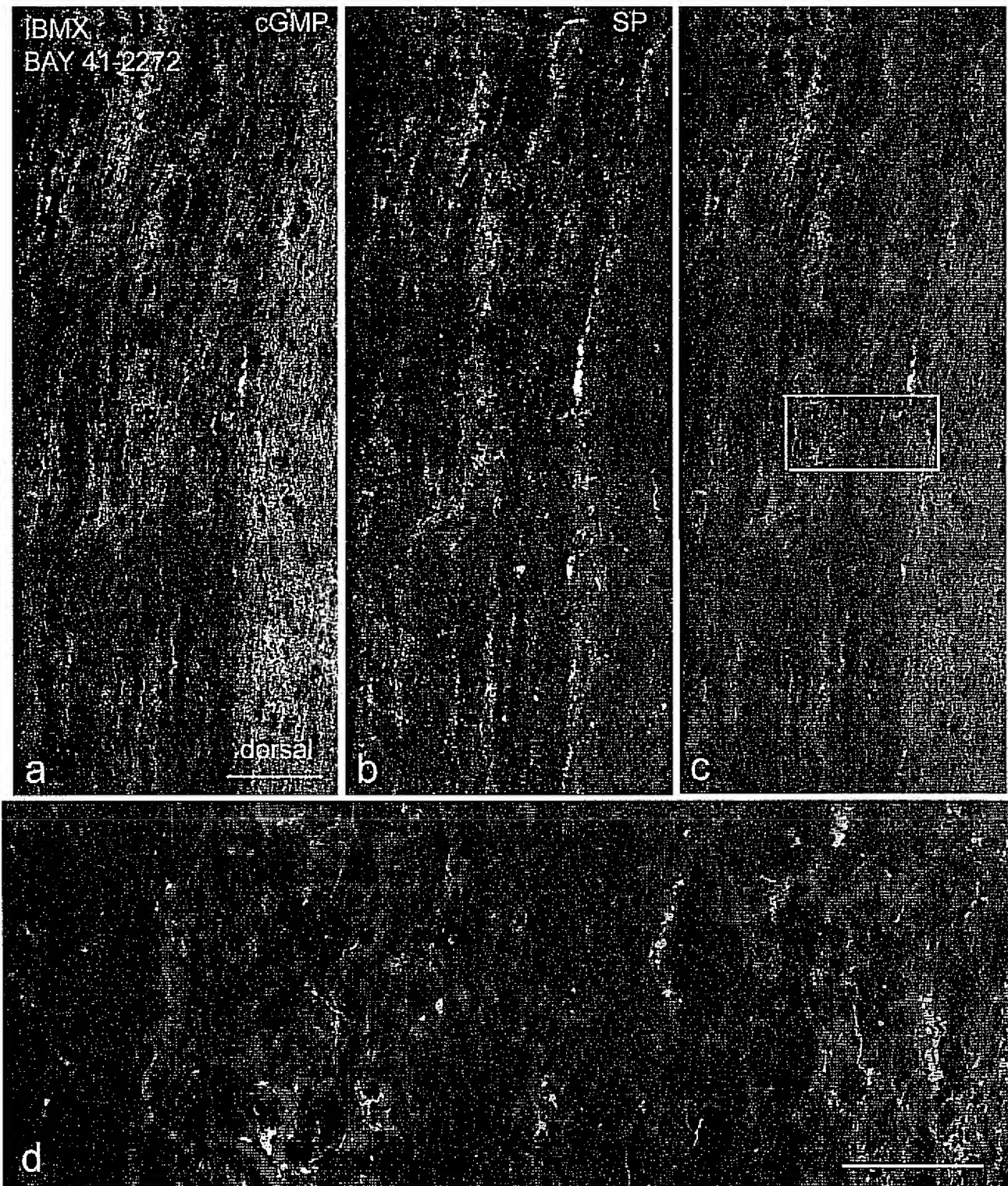
Fig. 18. Colocalization between cGMP-IR and substance P in the dorsolateral cervical spinal cord (longitudinal slice). Slice was incubated in the presence of 1 mM IBMX, 1.0 μM BAY 41-2272, and 100 μM DEANO. Section was double-immunostained for cGMP-IR and SP. Three adjacent images were aligned to obtain (a–c) using Adobe Photoshop 7.0.1. The boxed area in (c) is shown enlarged in (d) photographed with a 40× oil objective and demonstrates partial colocalization between cGMP-IR and substance P. Bar in (a) represents 100 μm for (a–c); bar in (d) represents 50 μm.
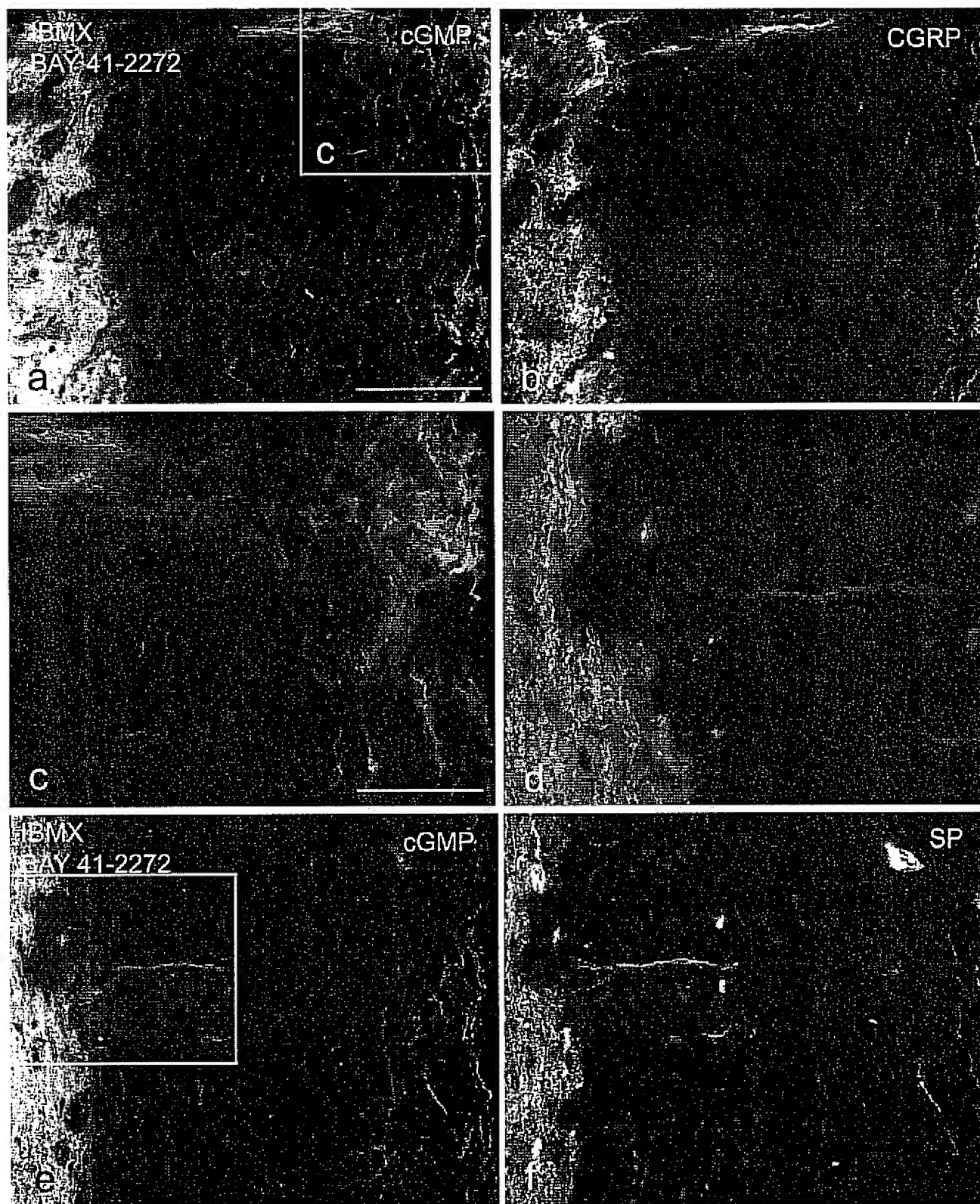
Fig. 19. Double-immunostaining of cGMP-IR with CGRP (a–c) or substance P (d–f) in a section of the dorsal cervical spinal cord. Longitudinal slices was incubated in presence of 1 mM IBMX, 1.0 μM BAY 41-2272, and 100 μM DEANO. In (c and d) enlargements are shown of the corresponding boxed areas taken with a 40× oil objective. There is no colocalization between cGMP-IR and CGRP. Partial colocalization is observed between cGMP-IR and substance P. Note that both CGRP and substance P fibers often run closely parallel to each other without actual colocalization. Bar in (a) represents 100 μm for (a, b, e, f); bar in (c) represents 50 μm for (c and d).

Table 7

Effect of incubation of slices of the rat cervical spinal cord in the presence of 10 μM SCH 51866 and 100 μM DEANO ($n = 3$) on the colocalization observed between cGMP-IR and eight neuronal marker molecules in the various laminae

	Lamina						White matter	
	1	2	3	4–7	8–9	10	dl	l
cGMP	++	++	+	±	±	+	−	−
Colocalization								
vAChT	±	±	−	−	+	−	−	−
Parvalbumin	±	±	−	−	−	−	−	−
EAAT3	±	−	−	−	−	−	−	−
Substance P	−	−	−	−	−	−	−	
CGRP	−	−	−	−	−	−	−	
vGAT	+	+	−	−	−	−	−	−
vGLUT1	−	−	−	−	−	−	−	−
vGLUT2	+	+	−	−	±	±	−	−

See Table 1 for explanation of the symbols.

density of substance P neurons in the dorsal horn is significantly reduced (Tegeder et al., 2004). It has been shown that sodium nitroprusside increases CGRP and substance P release from the dorsal horn (Garry et al., 1994), however, in these studies a very high dose of SNP was used. Our observations of NO-mediated cGMP-IR in a subpopulation of substance P-IR fibers and in fibers and boutons which bind IB4 support the hypothesis of an involvement of cGMP in the sensitization of the spinal dorsal horns neurons. Nevertheless, the small degree of colocalization of cGMP-IR in substance P-IR fibers and the absence in CGRP-IR fibers is disappointing. One reason might be that the sensitivity of the cGMP-antibody is too low to detect the cGMP

signal in SP- or CGRP-IR fibers. Although we have provided evidence that the sensitivity of the sheep-anti-formaldehyde-fixed cGMP antibody is estimated to be 0.1 μM of fixed cGMP, we cannot exclude the possibility that cGMP-IR in SP- or CGRP-IR fibers escapes detection. Another reason might be that it has been shown recently that NO binding to sGC is affected by the NO concentration, and ATP and GTP (Russwurm and Koesling, 2004; Cary et al., 2005). This complex regulation of sGC has not been studied by us, however, the fact that the stimulation of sGC by BAY 41-2272, especially in the presence of DEANO, greatly exceeds the effect of BAY 41-2272 or DEANO alone, as we have reported also for the rat

Table 8

Data from the literature on IC50 values (μM) of selective PDE inhibitors on isolated enzymes

	PDE1	PDE2	PDE4	PDE5	PDE9	PDE10
IBMX	50[f] 25[j] 14[u]	20[f] 62[j]	80[f]	30[f]	230[o] >200[p]	11[j] 2.6[k] 5[m]
8-Methoxy-IBMX	17[j,u]	111[j]	27[j]	30[q]		
BAY 60-7550	0.1[t]	0.002[t]	1.8[t]	0.583[t]	>4[t]	0.94[t]
EHNA	>100[g]	0.8[g]	100[g]	>100[r]	>100[a]	69[k] 61[m] >100[c]
Rolipram	>100[f] 143[u]	>100[f]	0.60[c] 3.2[d] 1[e]	>100[f] 407[c]	>200[p] 4.7[k]	0.71[j]
Sildenafil	0.281[i] 0.27[r]	>30[i] 43[r]	>7[l] 11[r]	0.004[h] 0.0036[r] 0.0037[s]	7[p]	>1[k]
Dipyridamole	4.2[d]			0.95[b] 1[b] 3.5[q]	>38[p]	0.72[j] 1.1[k]
SCH 51866					1.6[h] 1.55[p]	3.3[n] 1.0[k]

(a) Wunder et al. (2005); (b) Estrade et al. (1998); (c) Buele et al. (1994); (d) Yu et al. (1995); (e) Komas et al. (1991); (f) Nicholson et al. (1995); (g) Podzuweit et al. (1995); (h) Francis et al. (2001); (i) Gibson (2001); (j) Fujishige et al. (1999); (k) Soderling et al. (1999); (l) Clapham and Wilderspin (2001); (m) Loughney et al. (1999); (n) Fujishige et al. (1999); (o) Fisher et al. (1998); (p) Soderling et al. (1998); (q) McAllister et al. (1993); (r) Kotera et al. (2000); (s) Blount et al. (2004); (t) Boess et al. (2004); and (u) Yu et al. (1997).
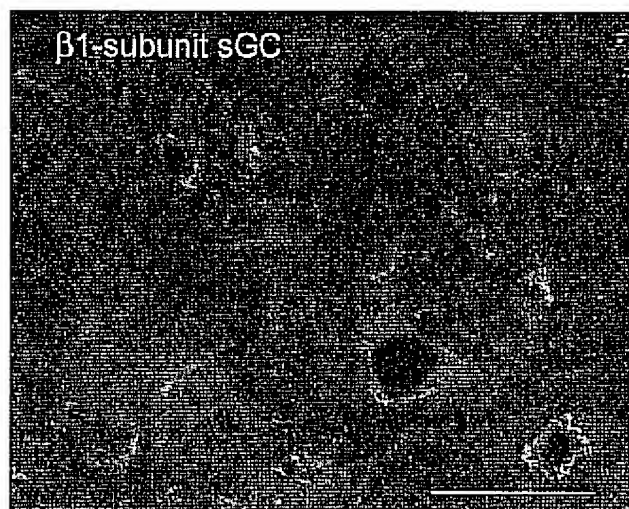
Fig. 20. Immunostaining of the β1-subunit of sGC in the ventral horn of the rat cervical spinal cord. Bar represents 50 μm.

brain (Van Staveren et al., 2005), indicates that factors beyond the control of the present experimental conditions might be of decisive importance.

Very little is known about the involvement of PDE activity in nociceptive signaling. Inthecal application of the selective PDE2 inhibitor EHNA had no effect in the formalin-induced nociception (Tegeder et al., 2002). However, recently it was reported that intrathecal zaprinast did produce an antinociceptive effect in this paradigm (Yoon et al., 2005). Sildenafil had an antinociceptive effect on hyperalgesia induced by a diabetic neuropathy (Patil et al., 2004a), and also in the writhing test and the carrageenan-induced hyperalgesia (Patil et al., 2004b). However, if this effect of sildenafil is caused by an increase in cGMP levels, the central location where sildenafil exerts this effect remains unknown (Patil et al., 2004a). Moreover, there are indications that part of this antinociceptive effect of sildenafil is caused by a peripheral accumulation of cGMP, e.g. within the cholinergic system (Patil et al., 2004b). Recently it was reported that topical superfusion of the spinal cord with blockers of cGMP or NO synthesis increased background activity of nociceptive lumbar neurons, whereas superfusion with sildenafil or 8-bromo-cGMP had no effect (Hoheisel et al., 2005), which also indicates a dual effect of cGMP on nociceptive processing.

In conclusion, the neuroanatomical data on NO-cGMP signaling in rat cervical spinal cord slices show that the second messenger function of cGMP is not restricted to vital sensory processing, but is probably also involved in propriocepsis. In addition, selective inhibition of PDE activity in the spinal cord slices and the localization of the mRNA for PDE2, 5, and 9 reveals that multiple PDE's are present in the same cellular structures, although at present it is unknown how the interplay between the different PDE's will affect cellular function.

Acknowledgements

References

Alonso, J.R., Arévalo, R., Weruaga, E., Porteros, A., Briñón, J.G., Aijón, J., 2000. Comparative and developmental neuroanatomical aspects of the NO system. In: Steinbusch, H.W.M., de Vente, J., Vincent, S.R. (Eds.), Handbook of Chemical Neuroanatomy, vol. 17: Functional Neuroanatomy of the Nitric Oxide System. Elsevier Science B.V., pp. 51–109.

Alvarez, F.J., Villalba, R.M., Zerda, R., Schneider, S.P., 2004. Vesicular glutamate transporters in the spinal cord, with special reference to sensory primary afferent synapses. J. Comp. Neurol. 472, 257–280.

Andreeva, S.G., Dikkes, P., Epstein, P.M., Rosenberg, P.A., 2001. Expression of cGMP-specific phosphodiesterase 9A mRNA in the rat brain. J. Neurosci. 21, 9068–9076.

Antal, M., Polgár, E., Chalmers, J., Minson, J.B., Llewellyn-Smith, I., Heizmann, C.W., Somogyi, P., 1991. Different populations of parvalbumin- and calbindin-D28k-immunoreactive neurons contain GABA and accumulate ^{3}H-D-aspartate in the dorsal horn of the rat spinal cord. J. Comp. Neurol. 314, 114–124.

Arvidsson, U., Riedl, M., Elde, R., Meister, B., 1997. Vesicular acetylcholine transporter (VAchT) protein: a novel and unique marker for cholinergic neurons in the central and peripheral nervous system. J. Comp. Neurol. 378, 454–467.

Beavo, J.A., 1995. Cyclic nucleotide phosphodiesterases: functional implications of multiple isoforms. Physiol. Rev. 75, 725–748.

Becker, E.M., Alonso-Alija, C., Apeler, H., Gerzer, R., Minuth, T., Pleiss, U., Schmidt, P., Schramm, M., Schröder, H., Schroeder, W., Steinke, W., Straub, A., Stasch, J.P., 2001. NO-independent regulatory site of direct sGC stimulators like YC-1 and BAY 41-2272. BMC Pharmacol. 1, 13.

Behrends, S., Kempfert, J., Mietens, A., Koglin, M., Scholz, H., Middendorff, R., 2001. Developmental changes of nitric oxide-sensitive guanylyl cyclase expression in pulmonary arteries. Biochem. Biophys. Res. Commun. 283, 883–887.

Bellamy, T.C., Garthwaite, J., 2001. cAMP-specific phosphodiesterase contributes to cGMP degradation in cerebellar cells exposed to nitric oxide. Mol. Pharmacol. 59, 54–61.

Blottner, D., Baumgarten, H.G., 1992. Nitric oxide synthetase (NOS)-containing sympathoadrenal cholinergic neurons of the rat IML-cell column: evidence from histochemistry, immunohistochemistry, and retrograde labeling. J. Comp. Neurol. 316, 45–55.

Blount, M.A., Beasley, A., Zoraghi, R., Sekhar, K.R., Bessay, E.P., Francis, S.H., Corbin, J.D., 2004. Binding of tritiated sildenafil, tadalafil, or vardenafil to the phopshodiesterase-5 catalytic site displays potency, specificity, heterogeneity, and cGMP stimulation. Mol. Pharmacol. 66, 144–152.

Boess, F.G., Hendrix, M., Van der Staay, F.J., Erb, C., Schreiber, R., Van Staveren, W., De Vente, J., Prickaerts, J., Blokland, A., Koenig, G., 2004. Inhibition of phosphodiesterase 2 increases neuronal cGMP, synaptic plasticity and memory performance. Neuropharmacology 47, 1081–1092.

Bredt, D.S., Hwang, P.M., Snyder, S.H., 1990. Localization of nitric oxide synthase indicating a neural role for nitric oxide. Nature 347, 768–770.

Cary, S.P.L., Winger, J.A., Marletta, M.A., 2005. Tonic and acute nitric oxide signaling through soluble guanylate cyclase is mediated by nonheme nitric oxide, ATP, and GTP. Proc. Natl. Acad. Sci. U.S.A. 102, 13064–13069.

Bucle, D.R., Arch, J.R.S., Connolly, B.J., Fenwick, A.E., Foster, K.A., Murray, K.J., Readshaw, S.A., Smallridge, M., Smith, D.G., 1994. Inhibition of cyclic nucleotide phosphodiesterase by derivatives of 1,3bis(cyclopropylmethyl)xanthine. Med. Chem. 37, 476–485.

Clapham, J.C., Wilderspin, A.F., 2001. Cloning of dog heart PDE1A—a first detailed characterization at the molecular level in this species. Gene 268, 165–171.

Clowry, G.J., 1993. Axotomy induces NADPH diaphorase activity in neonatal but not adult motoneurones. Neuroreport 5, 361–364.

Conti, M., Jin, S.L.C., 1999. The molecular biology of cyclic nucleotide phosphodiesterases. Prog. Nucleic Acid Res. 63, 1–38.

Denninger, J.W., Marletta, M.W., 1999. Guanylate cyclase and NO/cGMP signaling pathway. Biochim. Biophys. Acta 1411, 334–350.

De Vente, J., Steinbusch, H.W.M., Schipper, J., 1987. A new approach to immunocytochemistry of 3',5'-cyclic guanosine monophosphate: preparation, specificity, and initial application of a new antiserum against

formaldehyde-fixed 3′,5′-cyclic guanosine monophosphate. Neuroscience 22, 361–373.

De Vente, J., Hopkins, D.A., Markerink-van Ittersum, M., Emson, P.C., Schmidt, H.H.H.W., Steinbusch, H.W.M., 1998. Distribution of nitric oxide synthase and nitric oxide-receptive, cyclic GMP-producing structures in the rat brain. Neuroscience 87, 207–241.

De Vente, J., Steinbusch, H.W.M., 2000. Nitric oxide-cGMP signaling in the brain. In: Steinbusch, H.W.M., de Vente, J., Vincent, S.R. (Eds.), Handbook of Chemical Neuroanatomy, vol. 17. Elsevier, pp. 355–415.

Duggan, A.W., Hendry, I.A., Morton, C.R., Hutchinson, W.D., Zhao, Z.Q., 1988. Cutaneous stimuli releasing immunoreactive substance P in the dorsal horn of the cat. Brain Res. 451, 261–273.

Dun, N.J., Dun, S.L., Wu, S.Y., Förstermann, U., Schmidt, H.H.H.W., Tseng, L.F., 1993. Nitric oxide synthase immunoreactivity in the rat, mouse, cat and squirrel monkey spinal cord. Neuroscience 54, 845–857.

Estévez, A.G., Kamaid, A., Thompson, J.A., Cornwell, T.L., Radi, R., Barbeito, L., Beckman, J.S., 2002. Cyclic guanosine 5′ monophosphate (cGMP) prevents expression of neuronal nitric oxide synthase and apoptosis in motor neurons deprived of trophic factors in rats. Neurosci. Lett. 326, 201–205.

Estrade, M., Grondin, P., Cluzel, J., Bonhomme, B., Doly, M., 1998. Effect of a cGMP-specific phosphodiesterase inhibitor on retinal function. Eur. J. Pharmacol. 352, 157–163.

Feng-Chen, K.C., Wolpaw, J.R., 1996. Operant conditioning of H-reflex changes synaptic terminals on primate motoneurons. Proc. Natl. Acad. Sci. U.S.A. 93, 9206–9211.

Ferreira, J., Santos, A.R.S., Calixto, J.B., 1999. The role of systemic, spinal and supraspinal L-arginine-nitric oxide-cGMP pathway in thermal hyperalgesia caused by intrathecal injection of glutamate in mice. Neuropharmacology 38, 835–842.

Fisher, D.A., Smith, J.F., Pillar, J.S., St. Denis, S.H., Cheng, J.B., 1998. Isolation and characterization of PDE9A, a novel human cGMP-specific phosphodiesterase. J. Biol. Chem. 273, 15559–15564.

Francis, S.H., Turko, I.V., Corbin, J.D., 2001. Cyclic nucleotide phosphodiesterases: relating structure and function. Prog. Nucleic Acid Res. 65, 1–52.

Friebe, A., Koesling, D., 2003. Regulation of nitric oxide-sensitive guanylyl cyclase. Circ. Res. 93, 96–105.

Fujishige, K., Kotera, J., Michibata, H., Yuasa, K., Takebayashi, S., Okumura, K., Omori, K., 1999a. Cloning and characterization of a novel human phosphodiesterase that hydrolyzes both cAMP and cGMP (PDE10A). J. Biol. Chem. 274, 18438–18445.

Fujishige, K., Kotera, J., Omori, K., 1999b. Striatum- and tstis-specific phosphodiesterase PDE10A. Isolation and characterization of a rat PDE10A. Eur. J. Biochem. 266, 1118–1127.

Furuta, a., Rothstein, J.D., Martin, L.J., 1997. Glutamate transporter protein subtypes are expressed differentially during rat CNS development. J. Neurosci. 17, 8363–8375.

Garry, M.G., Durnett-Richardson, J., Hargreaves, K.M., 1994. Sodium nitroprusside evokes the release of immunoreactive calcitonin gene-related peptide and substance P from dorsal horn slices via nitric oxide-dependent and nitric oxide-independent mechanisms. J. Neurosci. 14, 4329–4337.

Gibson, A., 2001. Phosphodiesterase 5 inhibitors and nitrergic transmission—from zaprinast to sildenafil. Eur. J. Pharmacol. 411, 1–10.

Hawkins, R.D., Son, H., Arancio, O., 1998. Nitric oxide as a retrograde messenger during long-term potentiation in hippocampus. Prog. Brain Res. 118, 166–172.

He, X.H., Tay, S.S.W., Ling, E.A., 1997. Expression of NADPH-diaphorase and nitric oxide synthase in lumbosacral motoneurons after knee joint immobilisation in the guinea pig. J. Anat. 191, 603–610.

Hoheisel, U., Unger, T., Mense, S., 2005. The possible role of the NO-cGMP pathway in nociception: different spinal and supraspianl action of enzyme blockers on rat dorsal horn neurones. Pain 117, 358–367.

Honoré, P., Menning, P.M., Rogers, S.D., Nichols, M.L., Basbaum, A.I., Besson, J.M., Mantyh, P.W., 1999. Spinal substance P receptor expression and internalization in acute, short-term, and long-term inflammatory pain states. J. Neurosci. 19, 7670–7678.

Ichikawa, T., Ajiki, K., Matsuura, J., Misawa, H., 1997. Localization of two cholinergic markers, choline acetyltransferase and vesicular acetylcho-

line transporter in the central nervous system of the rat: in situ hybridization, histochemistry and immunohistochemistry. J. Chem. Neuroanat. 13, 23–39.

Inglis, F.M., Furia, F., Zuckerman, K.E., Strittmatter, S.M., Kalb, R.G., 1998. The role of nitric oxide and NMDA receptors in the development of motor neuron dendrites. J. Neurosci. 18, 10493–10501.

Inoue, T., Mashimo, T., Shibata, M., Shibuta, S., Yoshiya, I., 1998. Rapid development of nitric oxide-induced hyperalgeisa depends on an alternate to the cGMP-mediated pathway in the rat neuropathic pain model. Brain Res. 792, 263–270.

Juilfs, D.M., Fulle, H.J., Zhao, A.Z., Houslay, M.D., Garbers, D.L., Beavo, J.A., 1997. A subset of olfactory neurons that selectively express cGMP-stimulated phosphodiesterase (PDE2) and guanylyl cyclase-D define a unique olfactory signal transduction pathway. Proc. Natl. Acad. Sci. U.S.A. 94, 3388–3395.

Kawabata, A., Umeda, N., Takagi, H., 1993. L-arginine exerts a dual role in nociceptive processing in the brain: involvement of the kytorphin-met-enkephalin pathway and NO-cyclic GMP pathway. Br. J. Pharmacol. 109, 73–79.

Kim, H.J., Kim, M., Kim, S.H., Sung, J.J., Lee, K.W., 2002. Alteration in intracellular calcium homeostasis reduces motor neuronal viability expressing mutated Cu/Zn superoxide dismutase through a nitric oxide/guanylyl cyclase cGMP cascade. Neuroreport 13, 1131–1135.

Kitto, K.F., Haley, J.E., Wilcox, G.L., 1992. Involvement of nitric oxide in spinally mediated hyperalgesia in the mouse. Neurosci. Lett. 148, 1–5.

Koesling, D., Russwurm, M., Mergia, E., Mullershausen, F., Friebe, A., 2004. Nitric oxide-sensitive guanylyl cyclase: structure and regulation. Neurochem. Int. 45, 813–819.

Komas, N., Lugnier, C., Stoclet, J.C., 1991. Endothelium-dependent and independent relaxation of the rat aorta by cyclic nucleotide phospodiesterase inhibitors. Br. J. Pharmacol. 104, 495–503.

Kotera, J., Yanaka, N., Fujishige, K., Imai, Y., Akatsuka, H., Ishizuka, T., Kawashima, K., Omori, K., 1997. Expression of rat cGMP-binding cGMP-specific phosphodiesterase mRNA in Purkinje cell layers during postnatal neuronal development. Eur. J. Biochem. 249, 434–442.

Kotera, J., Fujishige, K., Michibata, H., Yuasa, K., Kubo, A., Nakamura, Y., Omori, K., 2000. Characterization and effects of methyl-2-(4-aminophenyl)-1,2-dihydro-1-oxo-7-(2-pyridinylmethoxy)-4-(3,4,5-trimethoxyphenyl)-3-isoquinoline carboxylate sulfate (T-1032), a novel potent inhibitor of cGMP-binding cGMP-specific phosphodiesterase (PDE5). Biochem. Pharmacol. 60, 1333–1341.

Loughney, K., Martins, T.J., Harris, E.A.S., Sadhu, K., Hicks, J.B., Sonnenburg, W.K., Beavo, J.A., Ferguson, K., 1996. Isolation and characterization of cDNAs corresponding to two human calcium, calmodulin-regulated, 3′,5′-cyclic nucleotide phosphodiesterases. J. Biol. Chem. 271, 796–806.

Loughney, K., Snyder, P.B., Uher, L., Rosman, G.J., Ferguson, K., Florio, V.A., 1999. Isolation and characterization of PDE10A, a novel human 3′,5′-cyclic nucleotide phosphodiesterase. Gene 234, 109–117.

Lugnier, C., Schoeffter, P., Le Bec, A., Strouthou, E., Stoclet, J.C., 1986. Selective inhibition of cyclic nucleotide phosphodiesterases of human, bovine and rat aorta. Biochem. Pharmacol. 35, 1743–1751.

Maihöfner, C., Euchenhofer, C., Tegeder, I., Beck, K.F., Pfeilschifter, J., Geisslinger, G., 2000. Regulation and immunhistochemical localization of nitric oxide synthases and soluble guanylyl cyclase in mouse spinal cord following nociceptive stimulation. Neurosci. Lett. 290, 71–75.

McAllister, L.M., Sonnenburg, W.K., Kadlecek, A., Seger, D., Le Trong, H., Colbran, J.L., Thomas, M.K., Walsh, K.A., Francis, S.H., Corbin, J.D., Beavo, J.A., 1993. The structure of a bovine lung cGMP-binding, cGMP-specific phosphodiesterase deduced from a cDNA clone. J. Biol. Chem. 268, 22863–22873.

Meller, S.T., Dykstra, C., Grzybycki, D., Murphy, S., Gebhart, G.F., 1994. The possible role of glia in nociceptive processing and hyperalgesia in the spinal cord of the rat. Neuropharmacology 33, 1471–1478.

Mullershausen, F., Russwurm, M., Friebe, A., Koesling, D., 2004. Inhibition of phosphodiesterase type 5 by the activator of nitric oxide-sensitive guanylyl cyclase BAY 41-2272. Circulation 109, 1711–1713.

Murad, F., 1994. Regulation of cytosolic guanylyl cyclase by nitric oxide: the NO-cyclic GMP signal transduction system. Adv. Pharmacol. 26, 19–33.

Nagy, J.I., Yamamoto, T., Jordan, L.M., 1993. Evidence for the cholinergic nature of C-terminals associated with subsurface cisterns in α-motoneurons of rat. Synapse 15, 17–32.

Nakamizo, T., Kawamata, J., Yoshida, K., Kawai, Y., Kanki, R., Sawada, H., Kihara, T., Yamashita, H., Shibasaki, H., Akaike, A., Shimohama, S., 2003. Phosphodiesterase inhibitors are neuroprotective to cultured spinal motor neurons. J. Neurosci. Res. 71, 485–495.

Nicholson, C.D., Shahid, M., Bruin, J., Barron, E., Spiers, I., De Boer, J., Van Amsterdam, R.G.M., Zaagsma, J., Kelly, J.J., Dent, G., Giembycz, M.A., Barnes, P.J., 1995. Characterization of ORG 20241, a combined phosphodiesterase IV/III cyclic nucleotide phosphodiesterase inhibitor for asthma. J. Pharmacol. Exp. Ther. 274, 678–687.

O'Dell, T.J., Hawkins, R.D., Kandel, E.R., Arancio, O., 1991. Tests of the roles of two diffusible substances in long-term potentiation: evidence for nitric oxide as a possible early retrograde messenger. Proc. Natl. Acad. Sci. U.S.A. 88, 11285–11289.

Ott, S.R., Delago, A., Elphick, M.R., 2004. An evolutionarily conserved mechanism for sensitization of soluble guanylyl cyclase reveals extensive nitric oxide-mediated upregulation of cyclic GMP in insect brain. Eur. J. Neurosci. 20, 1231–1244.

Panahian, N., Maines, M.D., 2001. Site of injury-directed induction of heme oxygenase-1 and -2 in experimental spinal cord injury: differential functions in neuronal defense mechanisms? J. Neurochem. 76, 539–554.

Patil, C.S., Singh, V.P., Sing, S., Kulkarni, S.K., 2004a. Modulatory effect of the PDE-5 inhibitor sildenafil in diabetic neuropathy. Pharmacology 72, 190–195.

Patil, C.S., Jain, N.K., Singh, V.P., Kulkarni, S.K., 2004b. Cholinergic-NO-cGMP mediation of sildenafil-induced antinociception. Indian J. Exp. Biol. 42, 361–367.

Pavel, J., Lukáčová, N., Maršala, J., 2000. Regional changes of cylic 3′,5′-guanosine monophosphate in the spinal cord of the rabbit following brief repeated ischemic insults. Neurochem. Res. 25, 1131–1137.

Podzuweit, T., Nennstiel, P., Müller, A., 1995. Isozyme selective inhibition of cGMP-stimulated cyclic nucleotide phosphodiesterases by erythro-9-(2-hydroxy-3-nonyl) adenine. Cell. Signal. 7, 733–738.

Repaske, D.R., Corbin, J.G., Conti, M., Goy, M.F., 1993. A cyclic GMP-stimulated cyclic nucleotide phosphodiesterase gene is highly expressed in the limbic system of the rat brain. Neuroscience 56, 673–686.

Russwurm, M., Koesling, D., 2004. NO activation of guanylyl cyclase. EMBO J. 23, 4443–4450.

Salter, M., Strijbos, P.J.L.M., Neale, S., Duffy, C., Follenfant, R.L., Garthwaite, J., 1996. The nitric oxide-cyclic GMP pathway is required for nociceptive signaling at specific loci within the somatosensory pathway. Neuroscience 73, 649–655.

Sann, H., McCarthy, P.W., Mäder, M., Schemann, M., 1995. Choline acetyltransferase-like immunoreactivity in small diameter neurones of the rat dorsal root ganglion. Neurosci. Lett. 198, 17–20.

Schmid, H.A., Pehl, U., 1996. Regional specific effects of nitric oxide donors and cGMP on the electrical activity of neurons in the rat spinal cord. J. Chem. Neuroanat. 10, 197–201.

Schmidt, H., Werner, M., Heppenstall, P.A., Henning, M., Moré, M.I., Kühbandner, S., Lewin, G.R., Hofmann, F., Feil, R., Rathjen, F.G., 2002. cGMP-mediated signaling via cGKIα is required for the guidance and connectivity of sensory axons. J. Cell Biol. 159, 489–498.

Schmidtko, A., Ruth, P., Geisslinger, G., Tegeder, I., 2003. Inhibition of cyclic guanosine 5′-monophosphate-dependent protein kinase I (PKG-I) in lumbar spinal cord reduces formalin-induced hyperalgesia and PKG upregulation. Nitric Oxide 8, 89–94.

Scholz, N.L., Truman, J.W., 2000. Invertebrate models for studying NO-mediated signaling. In: Steinbusch, H.W.M., de Vente, J., Vincent, S.R. (Eds.), Handbook of Chemical Neuroanatomy, Vol. 17: Functional Neuroanatomy of the Nitric Oxide System. Elsevier Science B.V., pp. 417–441.

Siegan, J.B., Hama, A.T., Sagen, J., 1996. Alteration in rat spinal cord cGMP by peripheral nerve injury and adrenal medullary transplantation. Neurosci. Lett. 215, 49–52.

Soderling, S.H., Bayuga, S.J., Beavo, J.A., 1998. Identification and characterization of a novel family of cyclic nucleotide phosphodiesterases. J. Biol. Chem. 273, 15552–15558.

Soderling, S.H., Bayuga, S.J., Beavo, J.A., 1999. Isolation and characterization of a dual-substrate phosphodiesterase gene family: PDE10A. Proc. Natl. Acad. Sci. U.S.A. 96, 7071–7076.

Sousa, A.M., Prado, W.A., 2001. The dual effect of a nitric oxide donor in nociception. Brain Res. 897, 9–19.

Southam, E., Garthwaite, J., 1993. The nitric oxide-cyclic GMP signalling pathway in rat brain. Neuropharmacology 32, 1267–1277.

Spike, R.C., Todd, A.J., Johnston, H.W., 1993. Coexistence of NADPH diaphorase with GABA, glycine, and acetylcholine in rat spinal cord. J. Comp. Neurol. 335, 320–333.

Stasch, J.P., Becker, E.M., Alonso-Alija, C., Apeler, H., Dembowsky, K., Feurer, A., Gerzer, R., Minuth, T., Perzborn, E., Pleiss, U., Schröder, H., Schroeder, W., Stahl, E., Steinke, W., Straub, A., Schramm, M., 1991. NO-independent regulatory site on soluble guanylate cyclase. Nature 410, 212–215.

Tamura, N., Chrisman, T.D., Garbers, D.L., 2001. The regulation and physiological roles of the guanylyl cyclase receptors. Endocr. J. 48, 611–634.

Tanaka, J., Markerink-van Ittersum, M., Steinbusch, H.W.M., De Vente, J., 1997. Nitric oxide-mediated cGMP synthesis in oligodendrocytes in the developing rat brain. Glia 19, 286–297.

Tao, Y.X., Haddad, H.E., Johns, R.A., 2000. Expression and action of cyclic GMP-dependent protein kinase Iα in inflammatory hyperalgesia in rat spinal cord. Neuroscience 95, 525–533.

Tao, Y.X., Johns, R.A., 2002. Activation and up-regulation of spinal cord nitric oxide receptor, soluble guanylate cyclase, after formalin injection into the rat hind paw. Neuroscience 11, 439–446.

Tegeder, I., Schmidtko, A., Niederberger, E., Ruth, P., Geisslinger, G., 2002. Dual effects of spinally delivered 8-bromo-cyclic guanosine monophosphate (8-bromo-cGMP) in formalin-induced nociception in rats. Neurosci. Lett. 332, 146–150.

Tegeder, I., Del Turco, D., Schmidtko, A., Sausbier, M., Feil, R., Hofmann, F., Deller, T., Ruth, P., Geisslinger, G., 2004. Reduced inflammatory hyperalgesia with preservation of acute thermal nociception in mice lacking cGMP-dependent protein kinase I. Proc. Natl. Acad. Sci. U.S.A. 101, 3253–3257.

Thompson, W.J., 1991. Cyclic nucleotide phosphodiesterases: pharmacology, biochemistry and function. Pharmacol. Ther. 51, 13–33.

Urushitani, M., Shimahama, S., Kihara, T., Sawada, H., Akaike, A., Ibi, M., Inoue, R., Kitamura, Y., Taniguchi, T., Kimura, J., 1998. Mechanism of selective motor neuronal death after exposure of spinal cord to glutamate: involvement of glutamate-induced nitric oxide in motor neuron toxicity and nonmotor neuron protection. Ann. Neurol. 44, 796–807.

Valtschanoff, J.G., Weinberg, R.J., Rustioni, A., 1992. NADPH diaphorase in the spinal cord of rats. J. Comp. Neurol. 321, 209–222.

Van Staveren, W.C.G., Glick, J., Markerink-van Ittersum, M., Shimizu, M., Beavo, J.A., Steinbusch, H.W.M., De Vente, J., 2002. Cloning and localization of the cGMP-specific phosphodiesterase type 9 in the rat brain. J. Neurocytol. 31, 729–741.

Van Staveren, W.C.G., Steinbusch, H.W.M., Markerink-van Ittersum, M., Repaske, D.R., Goy, M.F., Kotera, J., Omori, K., Beavo, J.A., De Vente, J., 2003. mRNA expression patterns of the cGMP-hydrolyzing phosphodiesterases types 2, 5, and 9 during development of the rat brain. J. Comp. Neurol. 467, 566–580.

Van Staveren, W.C.G., Markerink-van Ittersum, M., Steinbusch, H.W.M., Behrends, S., De Vente, J., 2005. Localization and characterization of cGMP-immunoreactive structures in rat brain slices after NO-dependent and NO-independent stimulation of soluble guanylyl cyclase. Brain Res. 1036, 77–89.

Vincent, S.R., Kimura, H., 1992. Histochemical mapping of nitric oxide synthase in the rat brain. Neuroscience 46, 755–784.

Vles, J.S.H., De Louw, A.J., Steinbusch, H., Markerink-van Ittersum, M., Steinbusch, H.W.M., Blanco, C.E., Axer, H., Troost, J., De Vente, J., 2000. Localization and age-related changes of nitric oxide- and ANP-mediated cyclic-GMP synthesis in rat cervical spinal cord: an immunocytochemical study. Brain Res. 857, 219–234.

Wang, H.G., Lu, F.M., Jin, I., Udo, H., Kandel, E.R., De Vente, J., Walter, U., Lohmann, S.M., Hawkins, R.D., Antonova, I., 2005. Presynaptic roles of NO, cGK, and RhoA in long-lasting potentiation and aggregation of synaptic proteins. Neuron 45, 389–403.

Weruaga, E., Alonso, J.R., Porteros, A., Crespo, C., Arevalo, R., Briñón, Velasco, A., Aijón, J., 1998. Nonspecific labeling of myelin with secondary antisera and high concentrations of Triton X-100. J. Histochem. Cytochem. 46, 109–117.

Wilson, J.M., Rempel, J., Brownstone, R.M., 2004. Postnatal development of cholinergic synapses on mouse spinal motoneurons. J. Comp. Neurol. 474, 13–23.

Wu, C.C., Ko, F.N., Kuo, S.C., Lee, F.Y., Teng, C.M., 1995a. YC-1 inhibited human platelet aggregation through NO-independent activation of soluble guanylate cyclase. Br. J. Pharmacol. 116, 1973–1978.

Wu, J., Lin, Q., Lu, Y., Willis, W.D., Westlund, K.N., 1998. Changes in nitric oxide synthase isoforms in the spinal cord of rat following induction of chronic arthritis. Exp. Brain Res. 118, 457–465.

Wu, Y., Li, Y., Liu, H., Wu, W., 1995b. Induction of nitric oxide synthase and motoneuron death in newborn and early postnatal rats following spinal root avulsion. Neurosci. Lett. 194, 109–112.

Wunder, F., Tersteegen, A., Rebmann, Erb, C., Fahrig, T., Mendrix, M., 2005. Characterization of the first potent and selective PDE9 inhibitor using a cGMP reporter cell line. Mol. Pharmacol. 68, 1775–1781.

Yoon, M.H., Choi, J.I., Bae, H.B., Jeong, S.W., Chung, S.S., Yoo, K.Y., Jeong, C.Y., Kim, S.J., Chung, S.T., Kim, C.M., 2005. Lack of the nitric oxide-cyclic GMP-potassium channel pathway for the antinociceptive effect of intrathecal zaprinast in a rat formalin test. Neurosci. Lett. 390, 114–117.

Yu, S.M., Cheng, Z.J., Kuo, S.C., 1995. Endothelium-dependent relaxation of rat aorta by butein, a novel cyclic AMP-specific phosphodiesterase inhibitor. Eur. J. Pharmacol. 280, 69–77.

Yu, J., Wolda, S.L., Frazier, A.L.B., Florio, V.A., Martins, T.J., Snyder, P.B., Harris, E.A.S., McCaw, K.N., Farrell, C.A., Steiner, B., Bentley, J.K., Beavo, J.A., Ferguson, K., Gelinas, R., 1997. Identification and characterisation of a human calmodulin-stimulated phosphodiesterase PDE1B1. Cell. Signal. 9, 519–529.

Zhang, X., Verge, V., Wiesenfeld-Hallin, Z., Ju, G., Bredt, D., Snyder, S.H., Hökfelt, T., 1993. Nitric oxide synthase-like immunoreactivity in lumbar dorsal root ganglia and spinal cord of rat and monkey and effect of peripheral axotomy. J. Comp. Neurol. 335, 563–575.